

THE APPLICATION OF ENERGY CONCEPTS TO PAVEMENTS

NOVEMBER 1972 — NUMBER 38



BY

W. H. HIGHTER

JHRP

JOINT HIGHWAY RESEARCH PROJECT
PURDUE UNIVERSITY AND
INDIANA STATE HIGHWAY COMMISSION

Informational Report

THE APPLICATION OF ENERGY CONCEPTS TO PAVEMENTS

TO: J. F. McLaughlin, Director
Joint Highway Research Project

November 9, 1972

FROM: H. L. Michael, Associate Director
Joint Highway Research Project

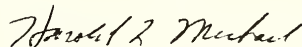
File: 9-7

Attached is an Informational Report titled "The Application of Energy Concepts to Pavements" by William H. Hightner, a Graduate Instructor in Research in Civil Engineering. The research was directed by Professor M. E. Harr of our staff and was financed by the United States Air Force Weapons Laboratory. Mr. Hightner also used the Report for his Ph.D. thesis requirement.

The objective of the research was to verify the hypothesis that there is a functional relationship between the cumulative energy as measured by cumulative peak deflections imparted to a given pavement system and the condition of that system. One of the conclusions of the research was that performance trends in airfield and highway pavements can be predicted from knowledge of cumulative total peak deflections.

The Report is presented to the Board as information of possible value to it.

Respectfully submitted,



Harold L. Michael
Associate Director

HLM:ms

cc:	W. L. Dolch	M. L. Hayes	C. F. Scholer
	R. L. Eskew	C. W. Lovell	M. B. Scott
	W. H. Goetz	G. W. Marks	J. A. Spooner
	M. J. Gutzwiller	R. D. Miles	N. W. Steinkamp
	G. K. Hallock	J. W. Miller	H. R. J. Walsh
	R. H. Harrell	G. T. Satterly	E. J. Yoder

Informational Report
THE APPLICATION OF ENERGY CONCEPTS TO PAVEMENTS

by
William H. Hightner
Graduate Instructor in Research

This Copy of This Report Provided By

Joint Highway Research Project

File No.: 9-7

Purdue University
West Lafayette, Indiana
November 9, 1972

ACKNOWLEDGEMENTS

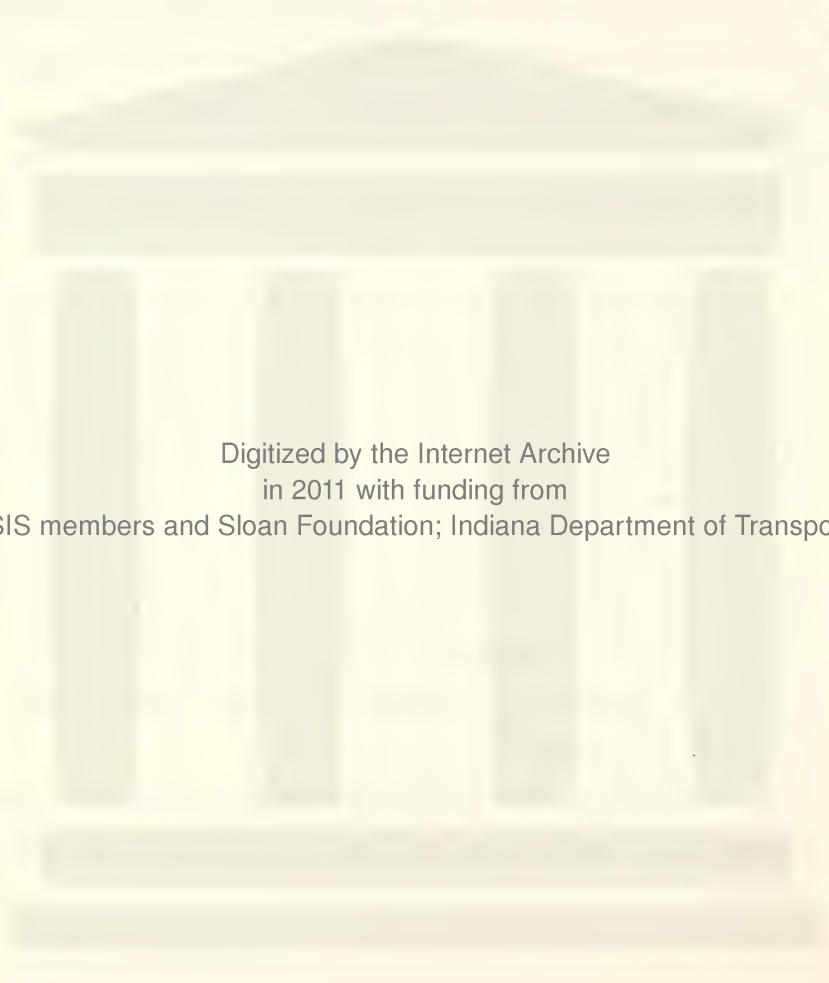
The author wishes to express his appreciation to his advisor, Dr. M. E. Harr for suggesting the research topic, for his encouragement and guidance throughout the course of the study and for his many contributions to the author's professional development.

The interest expressed by the other members of the graduate committee, Professors V. L. Anderson, W. H. Goetz, and E. O. Stitz, is gratefully acknowledged.

The author is also deeply grateful to the United States Air Force Weapons Laboratory for the financial support which made this thesis possible and in particular to Mr. L. M. Womack, who as project officer never hesitated with his assistance and was especially helpful during the field test phase of the research.

Thanks are also due Mr. W. L. DeGroff of the Purdue staff for his competent and conscientious assistance in the design and operation of the field test instrumentation. The author also wishes to acknowledge the many useful dialogues concerning pavement behavior held with Major R. E. Boyer.

To his wife, Carolyn, whose encouragement and patience were major factors in the completion of this thesis, the author expresses his gratitude.



Digitized by the Internet Archive
in 2011 with funding from
LYRASIS members and Sloan Foundation; Indiana Department of Transportation

TABLE OF CONTENTS

	Page
LIST OF TABLES	v
LIST OF FIGURES	vi
ABBREVIATIONS AND SYMBOLS	xi
ABSTRACT	xiii
INTRODUCTION	1
REVIEW OF THE LITERATURE	5
Introduction	5
The Winkler Hypothesis	6
Elastic Models	10
Viscoelastic Theory	13
Transfer Function Theory	17
Energy Concepts and Methods	18
Failure Criteria	19
THEORY	23
Presentation and Formulation of the Working Hypothesis	23
Procedure Used to Test the Working Hypothesis	37
VALIDATION OF THE WORKING HYPOTHESIS BY AASHO ROAD TEST DATA	40
ANALYSIS OF AIR FORCE BASE DATA	47
GENERAL DESCRIPTION OF THE KIRTLAND FIELD TEST	58
Introduction	58
Background	58
Objectives of the 1972 Field Test	59
Type of Data Collected	59
Description of Test Sites	60
Prime Movers	60
Statistical Design of the Overlay Experiment	64
PRESENTATION AND DISCUSSION OF THE KIRTLAND FIELD TEST	69
Introduction	69
Fire Truck Velocity Tests	69
Load Cart Tests on Overlays	76
The Determination of Pavement Deflection Basins	83

TABLE OF CONTENTS (cont'd)

	Page
Pavement System Reaction Coefficient	87
A CASE HISTORY AND A CASE FOR THE FUTURE	95
Introduction	95
Case History-Highway Overlays	95
The Future--Transfer Functions and Energy Concepts	103
SUMMARY	108
CONCLUSIONS	111
RECOMMENDATIONS FOR FUTURE RESEARCH	113
BIBLIOGRAPHY	114
APPENDICES:	
Appendix I: Traffic and Construction Histories of Selected Air Force Bases	121
Appendix II: Description of the Field Test Installation . .	129
VITA	159

LIST OF TABLES

Table	Page
I Comparison of Highway and Airport Pavement Load Characteristics	24
II The Activities of an Aircraft In Its Airport Operational Cycle	26
III Layer Properties of Test Sites	62
IV P-2 Fire Truck Data	66
V Fire Truck Velocity Test Data	73
VI Results of Data Analysis when Temperature Effects were not Considered	79
VII Maximum Deflection Data for Overlays	81
VIII Abbreviated Construction History, Pease Air Force Base, New Hampshire	123
IX Abbreviated Construction History, Castle Air Force Base, California	124
X Traffic Data for Pease Air Force Base, New Hampshire	125
XI Traffic Data for Castle Air Force Base, California	126
XII Traffic Data for Dyess Air Force Base, Texas	127
XIII Traffic Data for Minot Air Force Base, North Dakota	128
XIV Description of Instruments Used in Field Test	131

LIST OF FIGURES

Figure		Page
1	Aircraft Gross Weight Trend	2
2	Trend of Airfield Length Required for Takeoff	4
3	Aircraft Ground Operational Cycle	27
4	Schematic Representations of a Deflection Basin and a Deflection Trough	30
5	Theoretical Model of Elastic Pavement on a Winkler Foundation	33
6	Expressions for the Deflection and Moment at the Midpoint of a Symmetrically Loaded Elastic Beam Supported by a Winkler Foundation	35
7	Schematic Representation of the Procedure Used to Verify and Apply the Working Hypothesis	38
8	The Effect of Surface Course Thickness on the Condition of a Pavement as a Function of Its Cumulative Total Deflection	42
9	Predicted vs. Observed Present Serviceability Index for AASHO Road Test Data	44
10	The Predicted Effect of Surface Course Thickness on the Condition of a Pavement as a Function of Its Cumulative Total Deflection	46
11	Observed and Predicted Deflections for Load Cart at Taxiways 2 and 6	49
12	Assumed Annual Pavement Temperature Data for Castle and Pease Air Force Bases	51
13	Total Peak Deflection Trend for Pease Air Force Base, New Hampshire	53
14	Total Peak Deflection Trend for Castle Air Force Base, California	54
15	Cumulative Total Peak Deflection by Year, Pease Air Force Base, New Hampshire	55

LIST OF FIGURES (cont'd)

Figure		Page
16	Cumulative Total Peak Deflection by Year, Castle Air Force Base, California	56
17	Test Site Locations	61
18	The Containers Hold Lead Shot Which Put 23,120 lbs on the Load Wheel	63
19	Front View of Load Cart	63
20	Schematic of Load Cart Showing Track and Wheel Base Dimensions	65
21	The P-2 Fire Truck Used In Velocity Tests	66
22	Normal Distribution and Distribution of Passes of the Prime Mover for 10, 50 and 100 Coverages	67
23	The Effect of the B Parameter in the Equation $D(x) = Ae^{-Bx}$	72
24	Maximum Pavement Deflection vs. Horizontal Velocity for P-2 Fire Truck	74
25	Vertical Velocity of Pavement as a Function of Vehicle Velocity	77
26	Vertical Velocity of Pavement as a Function of Load Cart Velocity	78
27	Maximum Deflection vs. Pavement Temperature	82
28	Maximum Deflection vs. Asphalt Thickness	84
29	Maximum Deflection vs. Asphalt Thickness	85
30	A and B Parameters vs. Asphalt Thickness	86
31	Deflection Basin for C-130 Aircraft on Taxiway 2. Asphalt Thickness - 5.5 Inches	88
32	Deflection Basin for C-135 Aircraft on Taxiway 2. Asphalt Thickness - 5.5 Inches	89
33	Deflection Basin for Load Cart on Taxiway 2. Asphalt Thickness 11.5 Inches	90

LIST OF FIGURES (cont'd)

Figure		Page
34	Deflection Basin for Load Cart on Taxiway 2. Asphalt Thickness 13.5 Inches	91
35	Pavement System Reaction Coefficient as a Function of Asphalt Thickness and Temperature for the Same Subgrade Conditions	94
36	The Effect of Surface Thickness on Surface Deflection	96
37	The Effect of Surface Course Thickness on the Service Life of a Highway Pavement	99
38	The Effect of Overlays (Upper Bound, 100% Rejuvenation)	100
39	The Effect of Overlays (Lower Bound, 0% Rejuvenation)	102
40	The Effect of Overlays (50% Rejuvenation)	104
41	Sample Calculations for the Service Life of Overlays	105
42	Location of Selected Air Force Bases at which Traffic Data Were Analyzed	122
43	Schematic Representation of the Transient Deflection Measuring System	130
44	Instrumentation Layout Using the Load Cart as the Prime Mover	132
45	In-Hole LVDT Installation, Prime Movers can Run Directly Over this Installation	133
46	Linear Variable Differential Transformer Beam Installation	134
47	Detail of Beam Support Installation	135
48	In-Hole LVDT Installation with Overlay Holder Mount Extension	136

LIST OF FIGURES (cont'd)

Figure		Page
49	Pre-assembled View of Components Required to Epoxy Holder Mount Extension. Bushing Aligns Holder Mount Extension (Knurled) with Previously Epoxied Holder Mount	138
50	Holder Mount Extension in Position for Epoxying. Bar Keeps Top of Mount Flush with Pavement Surface	138
51	Pre-assembled View of In-Hole LVDT Installation	139
52	Assembled View of In-Hole LVDT Installation	139
53	Pre-assembled View of Beam Support Components. This Configuration Lacked Lateral Stability	140
54	View of Installed Beam Support. Nylon Bushing in Cap Provides Lateral Support	140
55	Placing Asphalt Before Hand Spreading	142
56	Raking and Rolling Two Inch Asphalt Lift	142
57	Locating Reference Rod Holes After Overlay has been Compacted	143
58	A Cylinder of Asphalt About One Inch Greater in Diameter than the Holder Cap is Ready for Removal	143
59	Removing Asphalt to Expose Cap	144
60	Loose Asphalt was Removed and Holder Mount Cap from Previous Overlay is Exposed	144
61	Heating Epoxy and Asphalt to Accelerate Curing	146
62	Styrofoam Disc is Visible Between Holder Mount Extensions	148
63	Reference Rod Extension and Connector are First Screwed on to 17.5 Foot Reference Rod	148
64	Reference Rod Extension in Place. Note Spanner Wrench Holes in Connector	149
65	The LVDT is then Fastened to the Reference Rod Extension	149

LIST OF FIGURES (cont'd)

Figure		Page
66	LVDT Wires Extend Through Slot in Holder Mount	150
67	Installing the LVDT Core Holder. LVDT Core is Visible in the Foreground	150
68	LVDT Lead Wires are Protected by a Shallow Trench Cut into the Pavement	151
69	Installing LVDT's on the Aluminum Beam	151
70	Calibrating an LVDT. Note Intercom for Communicating with Instrumentation Van	153
71	The Calibration Apparatus Allowed an Accuracy of 0.5 ⁰	153
72	Load Wheel Passing Directly Over LVDT Installation . . .	154
73	Tread Markings of Load Wheel can be Seen on the Tape . .	154
74	The Center Grooves of the Load Wheel were Painted so that Its Lateral Position could be Controlled	156
75	Another View of the Load Cart Showing the Beam LVDT Installation	156
76	View of the Overlay Showing Pressure Switches Used to Measure the Velocity of the Load Cart	157
77	The Interior of the Instrumentation Van	157

ABBREVIATIONS AND SYMBOLS

A	Normal distribution model parameter, maximum deflection, inches
AASHO	American Association of State Highway Officials
AFB	Air Force Base
B	Normal distribution model parameter, a measure of the spatial rate at which energy is dissipated by the pavement.
CBR	California Bearing Ratio
D	Deflection, inches
E	Young's modulus, pounds per square inch
E_r	Resilient modulus, ratio of deviator stress and resilient strain, pounds per square inch
F	Force
I	Moment of inertia, inches ⁴
K	Kips
L	Length
LVDT	Linear variable differential transformer
MPH	Miles per hour
OL	Overlay
PSI	Present Serviceability Index
R^2	Multiple correlation coefficient
R/W	Runway
S	Pavement system reaction coefficient, Pounds per cubic inch
T	Taxiway
V_v	Vertical velocity, feet per second
W	Weight
WASHO	Western Association of State Highway Officials

d	Deflection, inches
e	Constant equal to 2.71828...
ft	Feet
g	Acceleration of gravity, 32.2 feet per second per second
k	Modulus of subgrade reaction, pounds per cubic inch
lbs	Pounds
p	Pressure exerted on the subgrade
pci	Pounds per cubic inch
psi	Pounds per square inch
q	Load intensity, pounds per square foot
sec	Second
W	Deflection of subgrade surface, inches
λ	Parameter equal to $\sqrt[4]{\frac{k}{4EI}}$

ABSTRACT

Highter, William H., Ph.D., Purdue University, December, 1972.
The Application of Energy Concepts to Pavements. Major Professor:
M. E. Harr.

Pavement engineers have not been able to predict the performance of pavement systems prior to their actual construction and operational utilization. A solution to this problem was obtained by verifying the following hypothesis developed from energy concepts:

There is a functional relationship between the cumulative energy as measured by cumulative peak deflections imparted to a given pavement system and the condition of that system.

The hypothesis was tested by applying it to load-deflection and performance trend data gathered in the AASHO Road Test. Regression analysis was performed to find a relationship that predicted the level of the Present Serviceability Index (PSI) as a function of the pavement profile and a measure of the cumulative energy imparted to the pavement.

Because of the paucity of airfield condition and deflection data, indirect means had to be used to test the working hypothesis for airfield pavements. Traffic records and construction histories for two Air Force Bases were analyzed. The analysis indicated there is a threshold cumulative total peak deflection at which cracking develops in airfield pavements.

Field testing provided insight into the effect of the thickness of overlays on the energy imparted to a pavement and led to the development of a procedure to provide the thickness of an overlay so that the pavement will perform satisfactorily under an anticipated traffic volume.

It was concluded that, in the future, performance trends in airfield and highway pavements can be predicted from knowledge of cumulative total

peak deflections. It is suggested that transfer function theory be applied so that these deflections can be obtained easily and with a minimum of interruption to operational traffic.

SECTION I

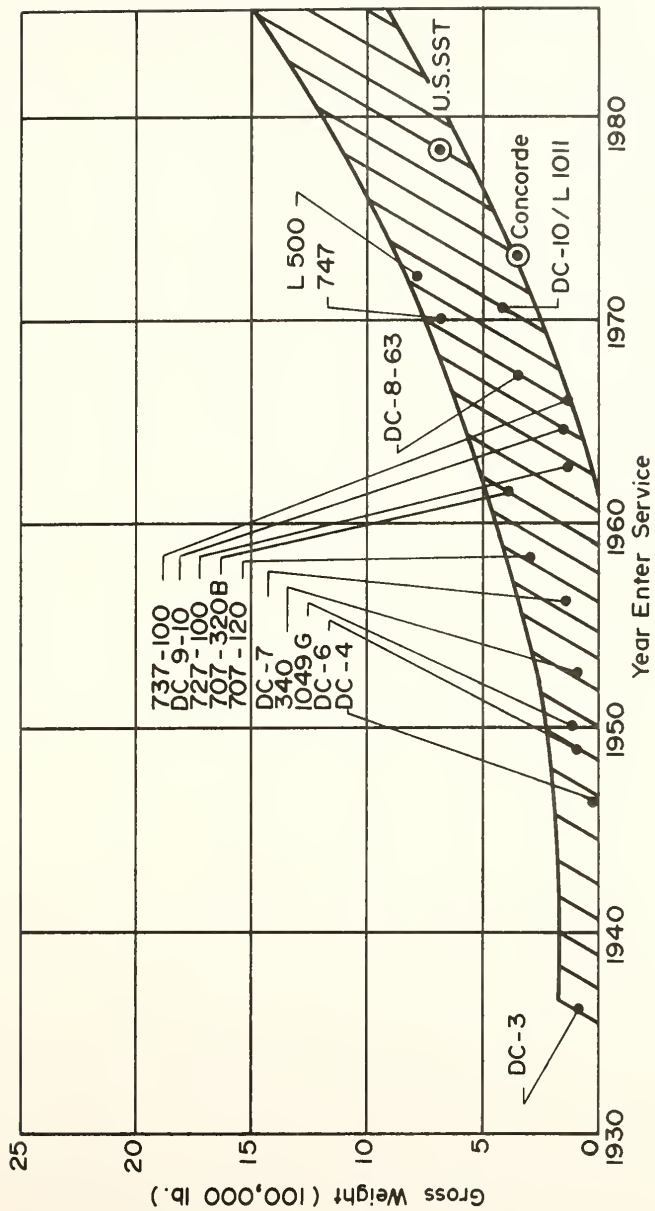
INTRODUCTION

At the present time no rational method of structural pavement design is available. Most design methods are empirical and are based upon correlations with in-service performance. These procedures have enabled the engineer to design with some degree of confidence but do not allow him to predict the performance of the structure.

The increase in gross weight of aircraft entering service is illustrated in Figure 1. Individual wheel loads are also increasing: the Boeing 747 has a wheel load of 41,600 lbs.; a DC-10 model scheduled to enter service in a few years will have an individual wheel loading of 52,600 lbs. When these trends are extended into the future, the need for a procedure which allows the designer to predict the performance of future aircraft when operated on existing pavements becomes apparent.

The effect of the Boeing 747 on existing pavements could not be fully anticipated; increased deterioration due to this aircraft has been documented (Ref. 2) but the ultimate effect is still not known.

Rough pavements also have an economic impact on aircraft landing gear. Parsons (Ref. 3) has estimated that the average cost for landing gear maintenance during the expected 12 year life of a single aircraft is one million dollars. In comparison, the cost of rehabilitating a World War II runway at Tampa International Airport was about three million dollars.



After Robinson (Ref. 1)

FIGURE 1 AIRCRAFT GROSS WEIGHT TREND.

The emphasis of future airport construction projects will be on upgrading existing pavements so that new aircraft can be accommodated as they enter service. Figure 2 indicates that the required length of runways increased as new aircraft were introduced into service.

The design of pavement overlays, both rigid and flexible, is presently based on the same precepts stated earlier for the design of pavements and therefore the same inherent limitations in regard to the prediction of their performance apply. Thus a method is also needed whereby the performance of overlays can be predicted.

This research effort uses energy principles to correlate the performance of airport pavements with the volume of mixed aircraft traffic applied. In addition, the effects of pavement overlays with respect to increased pavement service life are quantified.

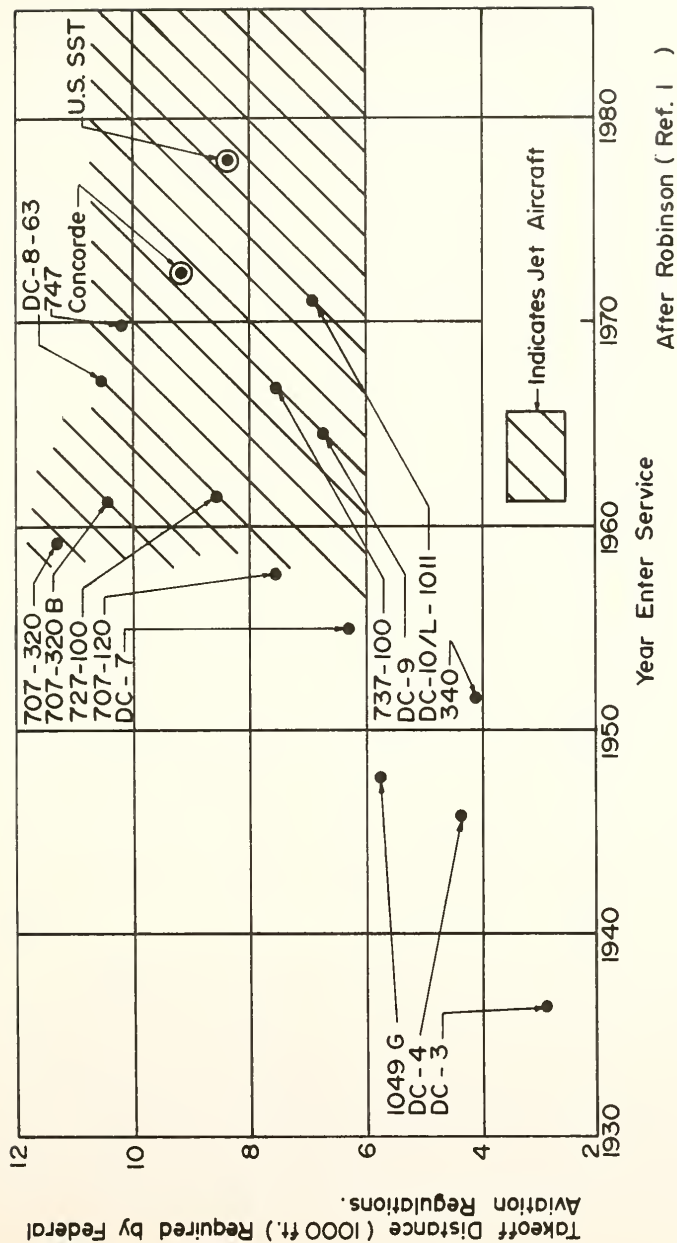


FIGURE 2 TREND OF AIRFIELD LENGTH REQUIRED FOR TAKEOFF.

SECTION II

REVIEW OF THE LITERATURE

Introduction

The failure criteria applied in the evaluation of existing pavement systems can be classified within two independent concepts of pavement failure -- structural and functional failure. Structural failure occurs when the pavement can no longer sustain the imposed loads; functional failure occurs when normal operating speeds of the vehicle traversing the pavement result in intolerable passenger discomfort and/or the inability of the vehicle operator to control the vehicle safely.

Although the two classifications of failure criteria are independent, they have a common basis in the shape of the deflection basin which results from imposed vehicular loads. Structural failure occurs when the strains in the total deflection basin result in stresses which exceed the strength of any component of the pavement system; functional failure occurs when the permanent deflections of the pavement make it too rough to be traversed safely at operating speeds.

Compressive and tensile strains in a pavement are created by the curvature of the pavement as it deflects under imposed loads. A method of predicting this curvature has not yet been developed although the use of transfer functions as proposed by Harr and Boyer (Ref. 4) and Boyer (Ref. 5) shows great promise. As a first step toward a solution

of the problem of preventing fatigue failures in pavements, methods of predicting deflections are valuable and a summary of important contributions in this area is presented here.

This section is a critical and historical review of four theories that have been developed in the literature to predict vertical surface deflections of pavements subjected to repeated loads. The Winkler, elastic, and viscoelastic theories offer models to predict the behavior of the pavement system; transfer function theory provides a relationship between a response of a pavement system and an operational input to that system.

The Winkler Hypothesis

Winkler (Ref. 6) was among the first to consider the transfer of load between surface materials and the underlying subgrade. He introduced the concept of the subgrade acting as a dense fluid or a system of independent, linear, closely-spaced springs. This is essentially a representation of a discontinuous type of foundation. The reaction at any point was proportional to the deflection at that point, or

$$p = kw \quad (1)$$

where

w is the deflection of the subgrade surface

k is a proportionality constant

p is the pressure exerted on the subgrade.

However, Winkler neither published values of k nor did he indicate what characteristics it might depend upon.

Zimmermann (Ref. 7) applied the Winkler hypothesis to the analysis of railroad tracks and concluded that the value of k depended on the type of subgrade material.

Hayashi (Ref. 8) used the Winkler hypothesis to solve the problem of beams supported by soil. His analysis included the interfacial shear which exists between the beam and the soil. However, Florin (Ref. 9) concluded that this shear had an insignificant effect on the vertical pressure exerted by the foundation.

Westergaard (Ref. 10) used the Winkler concept to find the stresses in rigid highway pavements. Although he recognized that the modulus of subgrade reaction k was dependent on the dimensions of the loaded area, he assumed that k had the same value at all points within the area under consideration. He defended this assumption by noting that a fourfold increase in the subgrade modulus k (from 50 pci to 200 pci) yielded only minor changes in the pavement stresses. He suggested that a standard procedure be adopted to determine the values of k . He later (Ref. 11) extended the analysis to include airport pavements.

Yoder (Ref. 12) noted that for typical truck wheel loads the pavement thickness required for a subgrade with $k = 100$ pci was only one inch more than that required for a subgrade with $k = 500$ pci. Both Yoder and Westergaard (Ref. 10) concluded that small errors in determining k would not appreciably affect the design of a pavement.

Timoshenko (Ref. 13) used the Winkler hypothesis to solve for the bending of a rail produced by the wheel pressures of a locomotive.

He noted that the fourth root of k appeared in both the solution for the stresses in the rail and the pressures on the ties and concluded that an error in the determination of k would introduce a much smaller error in the magnitude of the stresses and pressures.

Hetenyi (Ref. 14) offered solutions for beams of infinite and finite length supported by Winkler foundations and subject to various combinations of moments and concentrated and distributed loads. He neither gave values for the subgrade modulus nor discussed what factors might affect it.

Harr and Leonards (Ref. 15) showed that temperature and moisture gradients across the depth of a concrete slab could produce significant deflections in a Winkler foundation.

Terzaghi (Ref. 16) critically examined the concept of a subgrade modulus. He pointed out that the modulus was dependent upon the elastic properties of the subgrade material as well as the dimensions of the loaded area. He further noted that the Winkler hypothesis could be used with some confidence to predict stresses and bending moments but was unreliable as a predictor of settlements or deflections.

Vesic and Saxena (Ref. 17), working with AASHTO Road Test rigid pavement data, concluded that no single value of k yielded perfect agreement between statically induced bending moments, contact pressures, and deflections. However, they derived a relationship which correlated the coefficient of subgrade reaction that gave good agreement of bending moments with deformation characteristics of the subgrade and the slab material. Vesic and Saxena suggested that k , in addition to being a function of subgrade soil types and condition, is inversely

proportional to the slab thickness.

There does exist a reasonable approximate relationship between the coefficient of subgrade reaction of a soil and its CBR (California Bearing Ratio) value (e.g. Ref. 12). Finn (Ref. 18) using AASHO Road Test data presented a figure that showed that the CBR (and k) value of an embankment soil increased as the soil was subjected to more and more cycles of load. However, as test sections in the Road Test failed they were removed from the experiment. It is reasonable to assume that some of these sections experiencing failure had low CBR values initially. Finn noted it was not clear that the CBR (k) value increased with load cycles and that such a conclusion was tenuous.

It was reported (Ref. 19) that the CBR values of subbase and base material tested in the summer months were double those of the same soil tested in the spring. These changes in CBR (k) values were attributed to seasonal moisture changes rather than to increases in density as a result of an increasing number of load cycles.

Sebastyan (Ref. 20) presented evidence indicating that the modulus of subgrade reaction depended on the load intensity to which the soil was subjected.

In summary, the modulus of subgrade reaction is dependent on the type and condition of the soil, the dimensions of the loaded area, and the load intensity. Theories using the Winkler hypothesis have predicted values of stresses and bending moments reasonably well but have not been nearly as successful in predicting deflections or settlements. Permanent deflections cannot be predicted because of the linear elastic nature of the model. No single value of k can predict

perfect agreement between bending moments, contact pressures, and deflections.

Elastic Models

Westergaard (Ref. 10) was the first to apply elastic theory to pavements. He assumed the concrete pavement slab was homogeneous and isotropic and that the subgrade reaction was vertical and was proportional to the deflections of the slab i.e. a Winkler foundation. However, the validity of the Winkler hypothesis was questioned as early as the 1930's. Researchers sought models that could yield agreement of all statical influences such as bending moments, shearing forces, contact pressures, and deflections.

Biot (Ref. 21) solved for the contact pressures of an infinite elastic beam supported by a semi-infinite elastic solid. With the contact pressures known, a determination of the equivalent modulus of subgrade reaction could then be made through a back-calculation. Biot concluded that k was a function of the rigidity of the beam as well as the elastic properties of the subgrade. Thus no unique value of the subgrade modulus could be assigned to a given subgrade.

Hogg (Ref. 22) solved the problem of a thin plate of infinite size supported by a semi-infinite elastic solid. Expressions were obtained for the vertical deflection and curvature of the plate for a concentrated load and for a circular uniformly distributed load. In his analysis he neglected axial stresses perpendicular to the plate and shearing stresses parallel to the plate.

Burmister (Refs. 23 and 24) solved the problem of a multilayered elastic system subjected to a uniform circular load. His solution included an equation for the settlement at the surface of the uppermost layer. In his analysis he assumed that each layer was homogeneous, isotropic, and infinite in two dimensions, each layer was continuously supported by the layer beneath, the contact between layers was either perfectly rough (no slip and Poisson's ratio $\nu = 0$) or perfectly smooth (no interfacial shear stresses), deformations within each layer were small, and mass inertia of the system was negligible i.e. the second derivative of the displacements with respect to time within the layers vanished. Burmister's assumptions allowed each layer to be characterized by two parameters - Young's modulus and Poisson's ratio. These assumptions are nearly universally applied in elastic layered theory and simplify mathematical manipulations greatly.

Tables and charts of influence values to aid in determining stresses and deflections have been prepared by Burmister (Refs. 23, 24, and 25) and Fox (Ref. 26) for two layer elastic systems and by Acum and Fox (Ref. 27), Jones (Ref. 28), and Peattie (Ref. 29) for 3 layer systems. The influence values given by all these investigators were for stresses and displacements under the center of a uniformly loaded circular area. In all cases Poisson's ratio was equal to 0.5 (constant volume) for each layer in the system and the interface between layers was assumed to be perfectly rough. Fox also gave results for a perfectly smooth interface condition.

Barksdale and Leonards (Ref. 30) extended elastic layer theory to four-layer systems, each layer having arbitrary values of Young's Modulus and Poisson's ratio.

Vesic and Saxena (Ref. 17) found that the load response of the AASHO Road Test subgrade could be adequately described by the response of a homogeneous, isotropic, elastic solid with two characteristics - the deformation modulus and Poisson's ratio.

Dehlen and Monismith (Ref. 31) applied an approximate nonlinear elastic analysis to a section consisting of full-depth asphalt overlaying a sandy clay. Their results showed that, for engineering purposes, linear elastic theory could be used with some confidence for full-depth asphalt concrete but not for pavement systems which have non-cohesive soils close to the surface.

Burmister (Ref. 25) using data from in-service observations at the Western Association of State Highway Officials (WASHO) Road Test applied elastic layered theory to evaluate the strength properties of the various layers in the pavement system.

There exists evidence that indicates that the influence of Poisson's ratio varies with depth in an asphalt layer and that Young's modulus of soils subject to traffic loadings is not constant. Klomp and Niesman (Ref. 32) noted that the influence of Poisson's ratio of the calculated strain in an asphalt layer was stronger in the upper half than in the lower half of the pavement. Furthermore, they found that for the calculation of strains at the bottom interface of an asphalt layer, the influence of ν was relatively small. Nijboer and Delcours (Ref. 33) used wave theory and observed a stiffening of a

granular base under repeated traffic loads.

Seed, Chan, and Lee (Ref. 34) and Larew and Leonards (Ref. 35) working with fine-grained soils showed that resilient (recoverable or elastic) and total deformations were influenced by confining pressure, applied stress level, and number of stress applications. Therefore, the resilient modulus, E_r (the deviator stress divided by the resilient strain), of even a homogeneous subgrade subjected to repeated loads varies with both depth and horizontal position. Since the resilient modulus was found to increase with decreasing deviator stress, it would then increase with depth below a pavement surface. Therefore, the contribution of the upper portion of a subgrade to the elastic deflection would be greater than predicted by elastic theory if the resilient modulus were held constant throughout each layer.

Geldmacher et al. (Ref. 36) measured field deflections of rigid pavements subjected to moving loads and found that the load deflection measurements were linear over a single axle load range of 9,000 to 20,000 pounds.

Viscoelastic Theory

The response of all real materials to loads is influenced to some degree by time and the rate of loading. Viscoelastic theory was developed to accommodate the time dependent nature of materials. To simplify analysis, viscoelastic pavement models are usually assumed to be linearly viscoelastic; the validity of this assumption must be determined experimentally for each material (Ref. 37). It is usually further assumed that the pavement system is homogeneous and isotropic

although attempts have been made to predict anisotropic behavior (e.g. Ref. 38).

Many investigators have verified the viscoelastic nature of bitumen for small deformations e. g. Van der Poel (Ref. 39), Brown and Sparks (Ref. 40), Kuhn and Rigden (Ref. 41), and Brodnyan (Ref. 42). Mack (Refs. 43 and 44), Wood and Goetz (Ref. 45), and Pister and Monismith (Ref. 46) are among those who have verified the viscoelastic nature of asphalt concrete for small deformations.

For the calculation of the stresses imposed in a pavement by moving traffic loads, Klomp and Niesman (Ref. 32) noted that the properties of the construction material could not be adequately defined by a modulus of elasticity but that the effects of mass and damping had to be considered also.

The influence of temperature and vehicle velocity (rate of loading) were well documented in the AASHO Road Test (Ref. 19). For rigid pavements deflection and strain data were found to be affected significantly by daily temperature changes. A study of the effect of the temperature of the asphalt concrete surfacing on load-induced deflections revealed that the effect was negligible for temperatures in the 80°-120°F. range. At about 80°F. deflections decreased as the temperature decreased. The extent of the decrease was a function of the age or traffic history of the pavement, the speed of the vehicle, the pavement design, and the season of the year.

For both rigid and flexible pavements a pronounced reduction in deflection accompanied an increase in vehicle speed. For asphalt pavements increasing the speed from 2 to 35 mph reduced the deflection

38%; a reduction of deflection of nearly 30% was noted when the vehicle speed was increased from 2 to 60 mph on a portland cement concrete pavement. These results substantiated those earlier reported by Geldmacher et al. (Ref. 36) who found under the same environmental conditions a 10.8% decrease in deflection at the center of the driving lane of a rigid pavement as the vehicle speed was increased from creep speed to 20MPH - a 23.1% decrease was noted at the edge of the pavement.

Harr (Ref. 47) used a viscoelastic model to show the influence of vehicle speed on the resulting pavement deflections.

Monismith and Secor (Ref. 48) determined that at least a four element viscoelastic model was needed to simulate instantaneous and retarded elastic deformation and viscous flow in asphalt concrete triaxial tests. They used triaxial test data as solution parameters for a statically loaded viscoelastic plate supported by an elastic layer and compared theoretical predictions of deflections to deflections measured in the lab at the surface of an asphalt layer supported by closely spaced springs. Wide discrepancies were found but the comparison of theoretical and experimental deflections was improved, except at high temperatures, when differences in tensile and compressive properties of the asphalt were incorporated in the analysis.

Pister and Westmann (Ref. 49) used a viscoelastic beam supported by a Winkler foundation to demonstrate the effects of the velocity of a point load on the deflection and curvature of an asphaltic pavement. They showed that loads moving with low velocities are most critical; at high velocity the behavior of the system was elastic. The authors

applied a bilinear elastic model to investigate the effects of different moduli in tension and compression of an infinite elastic beam supported by a Winkler foundation. They noted that deflections and stresses obtained by the bilinear model differed only slightly from those predicted by the usual methods. However, the curvature and hence the maximum strains obtained by the two methods were considerably different. The maximum tensile strains obtained in the bilinear analysis were double those predicted by the theory which considered equal tensile and compressive moduli of elasticity. Since curvature is fundamental to pavement evaluation, the results indicated by Pister and Westmann are extremely important.

Barksdale and Leonards (Ref. 30) used a layered viscoelastic model to investigate the effects of repeated stationary loads. Permanent deformations were calculated using experimentally determined material properties and compared favorably with the AASHO Road Test data.

Perloff and Moavenzadeh (Ref. 50) solved for the deflections caused by a point load moving over a semi-infinite, homogeneous, linear viscoelastic medium.

Viscoelastic theory has an advantage over elastic theory in that the time dependent nature of the material is taken into account. However, the classical assumptions inherent in elastic theory are usually also invoked to simplify viscoelastic analysis. Both elastic and viscoelastic theory compel the engineer to assume a model to characterize the behavior of the system. In addition, the parameters inherent in these models must be determined "a priori".

Transfer Function Theory

Although transfer function theory has been applied for some time by mechanical and electrical engineers (e.g., Tsien (Ref. 51); Crafton (Ref. 52); Raven (Ref. 53); and Senaut (Ref. 54)), Swami, Goetz, and Harr (Ref. 55) were the first to use transfer functions to characterize the time-dependent behavior of asphalt concrete. A sinusoidal loading was applied and the transfer function was derived from the frequency response of the material. By treating a static loading as a step function of time, the transfer function obtained from dynamic tests was used successfully to predict the response of the material when it was subjected to static loading. It was shown that the transfer function represented a material properties that were independent of the type of load input and that the temperature of the test specimen had the greatest single effect on the transfer function.

Ali (Ref. 56) developed a technique for generating a reproducible impulse loading in the laboratory. This was an important contribution because the Laplace transform of an impulse loading is unity, and therefore the response to the impulse loading in the Laplace plane is the transfer function itself. He also tested the adequacy of the transfer function thus obtained by predicting the pavement response to step loading.

Boyer (Ref. 5) was the first to determine transfer functions for an in-service pavement system by relating time dependent responses at different points on the surface of the pavement.

The advantage of this "a posteriori" modeling technique is that it is capable of accommodating more material descriptors than are

normally included in elastic or viscoelastic theory, and a theoretical model which may or may not be representative of the pavement system need not be assumed. Furthermore, the transfer functions itself provides an instantaneous measure of relevant pavement parameters.

Energy Concepts and Methods

Lord Rayleigh was among the first to apply energy methods to physical systems. For conservative systems (no energy losses) with simple harmonic motion, he recognized that at a principal mode or natural frequency the maximum kinetic energy was equal to the maximum potential energy. In order to evaluate the energy quantities it is necessary to estimate the deflection of the system under dynamic conditions. It has been demonstrated (Tse et al., Ref. 57) that if the assumed deflection curve is a reasonable approximation, then the calculated natural frequency will be very close to, but slightly higher than, the actual fundamental frequency.

Methods which apply the conservation of energy to complex structural systems have seen wide application. For example, the concept that the external work done to a system is equal to the increase in internal strain energy has been used frequently to solve for deflections in indeterminate structures (Ref. 58). The principle of virtual work has been used to find the reactions in complex structures (e.g. Ref. 58).

Although energy methods have not yet been applied to in-service asphalt concrete pavements, laboratory testing has indicated that energy is fundamental to fatigue failure in asphalt concrete. Moore

and Kennedy (Ref. 59) using indirect tension tests noted a linear trend in the stress-fatigue life relationship. Pell and Brown (Ref. 60) noted a similar relationship between tensile strain and fatigue life. Van Dijk et al. (Ref. 61) noted that the total energy dissipated in constant stress and constant strain fatigue tests on asphalt concrete specimens was practically the same. Chomton and Valayer (Ref. 62) performed tests that indicated absorbed energy was the sole independent factor in predicting the life of bituminous mixes in fatigue tests.

Failure Criteria

There are essentially four different modes of pavement failure; lack of stability in the wearing course; excessive deflections in the base material due to compaction by vehicular loads; cumulative shear deformations in the subgrade; and temporary rebound in the subgrade and base materials (Larew and Leonards, Ref. 35). These failure modes are manifested by an uneven surface and a pavement can be considered to have failed functionally when deformations of its components are sufficiently large to cause an unacceptably uneven riding surface or to cause cracking of the surface material (Seed, Chan, and Lee (Ref. 34)).

Cracking is usually associated with large deflections because strains in the pavement usually increase with increase in deflections. Cracking will hasten the onset of failure because the protection given by the surface layer to the underlying materials from the effects of both wheel loads and the penetration of water is lost whenever cracking occurs, resulting in an increased rate of deterioration (Kasianchuk,

Ref. 63).

Sebastyan (Ref. 64) reported that tests undertaken by the Canadian Department of Transport on pavement rebound due to aircraft loadings indicated that a well designed asphalt pavement has a rebound deflection value between 0.06 and 0.10 inches (the corresponding figures for a highway are 0.03 - 0.05 inches).

Bulman (Ref. 65) discussed deflection techniques for pavement evaluation and indicated how deflection data can be used for overlay design. The Asphalt Institute (Ref. 66) presented a method whereby the structural adequacy of a pavement can be evaluated using deflection data.

Ahlvin (Ref. 67) noted that there is a strong relationship between surface deflections of a pavement under a given loading and repetitions to failure of the pavement under that loading. He asserted that "the best behavior - indicating parameter found for pavements, so far (1971), has been deflection."

Other investigations have used vehicle vertical acceleration as a criterion. Houbolt (Ref. 68) recommended that when the acceleration response experienced in an aircraft exceeds 0.3g remedial measures be taken. The Port of New York Authority (Ref. 69) found the maximum level of aircraft vibration before (passenger) discomfort was noted was 0.12g. in the normal operation area and 0.3g. in infrequently trafficked areas. Hall and Kopelson (Ref. 70) also used a roughness criterion based on accelerations and indicated that a runway was undesirable when the acceleration at either the pilot's compartment or the aircraft's center of gravity exceeded 0.5g.

Acceleration response of aircraft is felt to be a superior roughness criterion because aircraft response motion continues for some time after a particular input. The aircraft response to one section of a runway, then, is dependent on the proceeding sections of the runway (Hall and Kopelson, Ref. 70).

Although only qualitative data exist with respect to aircraft performance on rough runways, pilots' opinions seem to indicate a degradation in aircraft acceleration in the takeoff run. Even more serious is the effect of rough runways on the readability of cockpit instruments (Foxworth and Marthinsen, Ref. 71).

A unique functional failure criterion which may have application in airport pavements was developed in the AASHO Road Test (Carey and Irick, Ref. 72). A Present Serviceability Index (PSI) rating on a scale of 0 to 5 (very poor to very good) was assigned to sections of pavement by personnel trafficking the section at normal operating speeds. It was found that replication or the ability of the panel to be consistent in its ratings was excellent. Although the Present Serviceability Index concept is subjective, an equation was derived by regression analysis that allowed the PSI to be predicted by the objective measurement of pertinent pavement variables. The variables used in the formula were longitudinal profile variations, the amount of cracking and patching, and additionally for flexible pavements, transverse profile variations (rutting). Pavement performance analyses were then based on the trend of the serviceability index as more and more cycles of moving vehicular loads were applied to the given pavement section.

In the present investigation, energy concepts are applied to asphalt pavement systems in order to anticipate impending pavement distress. The application of energy theory is not dependent on the type of failure criterion used and thus can be applied in conjunction with any criterion selected.

SECTION III

THEORY

Presentation and Formulation of the Working Hypothesis

The general hypothesis which served as the basis of this research effort was:

There is a functional relationship between the cumulative energy as measured by cumulative peak deflections imparted to a given pavement system and the condition of that system.

Energy methods have seen wide application in mechanical engineering and form the basis of the formulation of the Lagrange and Hamilton equations of motion. Although they have been used to some degree in civil engineering, most notably in structural analysis and vibration theory, and in the derivation of dynamic pile driving formulas, they have never before been applied "per se" to pavement systems. However, the very nature of the loading and response of pavement systems suggest that the external loading-response behavior can be described within the philosophy inherent to energy methods.

Pavements can be conveniently categorized into highway or airport systems, depending on the characteristics of the prime movers (vehicles) which traffic them. Table I points out some of the basic differences between the load characteristics of highway and airport pavements. The table indicates that airport pavements are subject to more severe wheel loads and higher speeds than highway pavements, but their total volume of traffic is much less than highways. The combined effects of heavy loads and higher speeds indicate that dynamic effects may be much more important for airport pavements than for highways.

Table I

COMPARISON OF HIGHWAY AND AIRPORT PAVEMENT

LOAD CHARACTERISTICS

	Highway	Airport
A. magnitude of load	normal load $\approx 10,000$ lb tire pressure ≤ 70 psi	normal load $\approx 40,000$ lb tire pressure ≤ 200 psi
B. traffic volume	high	low
C. distribution of loading	more nearly uniform than airport pavements	many parts of runway areas are seldom loaded
D. speed of prime mover	maximum 75 MPH	up to 240 MPH (see Figure 3 for variability in speed)
E. shear (horiz.) loads due to braking and accelerating	moderate or negligible	can be very severe
F. prime mover load pattern	single or dual wheels	many types of gear configuration

Because this research is devoted primarily to airport pavements where the imposed loads are more severe than highways, the underlying theory will first be developed in the context of airfield pavements. Highway pavements will be treated later in this section.

Table II presents a list of the activities of an aircraft in its arrival and departure operations at an airport. Figure 3 illustrates these operations schematically in chronological order. It is seen that most of the loads imparted to the pavement by aircraft are dynamic in nature - static loads exist only when the aircraft is parked at the apron. Both horizontal and vertical loads are in evidence; however, horizontal loads are primarily induced when the aircraft brakes or turns sharply. The latter loads are especially critical during the centrifugal maneuver of taxiing around fast runway turnoffs which transfer loads to the outer undercarriage aircraft gear. Whereas the lateral and longitudinal dimensions of airfield pavements are much greater than the thickness, detrimental effects due to horizontal shear are usually prevalent only at the boundaries of the pavement where no lateral support is available. This research is concerned with effects that predominate in airport pavements such as the load induced vertical deflections which occur on runways and primary taxiways; edge effects are not included in the scope of the present work.

The dynamic loads imposed by aircraft in their landing and takeoff operations are governed by a complex interaction between the aircraft and the pavement. Among the aircraft characteristics which enter this interaction are weight, location of the center of gravity, aerodynamic

Table II
THE ACTIVITIES OF AN AIRCRAFT IN
ITS AIRPORT OPERATIONAL CYCLE

Departure	Arrival
Static (parked)	Landing Impact
Low speed taxiing	High speed braking
Turning	Decelerated roll-out
Low speed braking	Low speed braking
Accelerated takeoff roll	Turning
Aborted takeoff roll (emergency operation, used infrequently)	Low speed taxi
Takeoff rotation	Static (parked)

After Reference 73

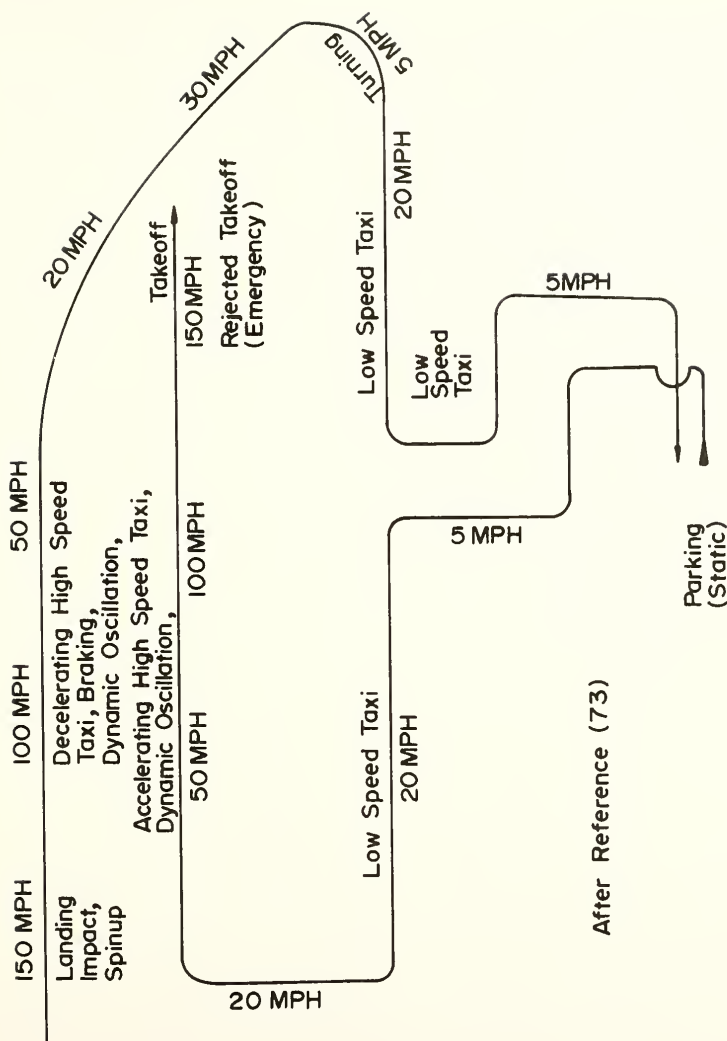


FIGURE 3 AIRCRAFT GROUND OPERATIONAL CYCLE.

lift, landing gear configuration, the spacing, size, and air pressure of the tires (Ref. 73).

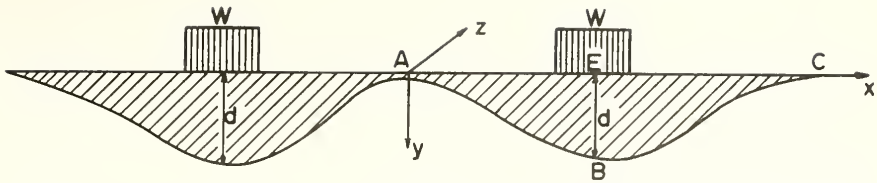
In addition, the variability and degree of pavement roughness also influences the dynamic loading. This is particularly true because aircraft response motion continues for some time after its initiation and the passage of the aircraft (Ref. 70). It is not surprising then that the actual loads imposed on pavements by aircraft defy anything more than qualitative description. It would thus seem that methods of pavement analysis which require more or less precise knowledge of induced loads have a small probability of success in predicting performance. Unfortunately, in spite of this deficiency, the existence of a unique and reproducible load-deflection (or stress-strain) relationship is central to most methods of pavement design and analysis in use today.

Present day methods of pavement analysis (such as elastic models) are based on theories which were developed from the consideration of a single (statistical) point in the material and are therefore local in nature. Thus, even if the loads which are required as input data to such analyses were known, the developed procedures would provide a quantitative evaluation of only isolated points in the pavement system. The overall behavior of a pavement may demonstrate considerable deviation from these predictions. In other words, such methods might provide knowledge of the condition of individual statistical points in a runway but would not indicate the variation between these points, which in effect, is what is really needed - information

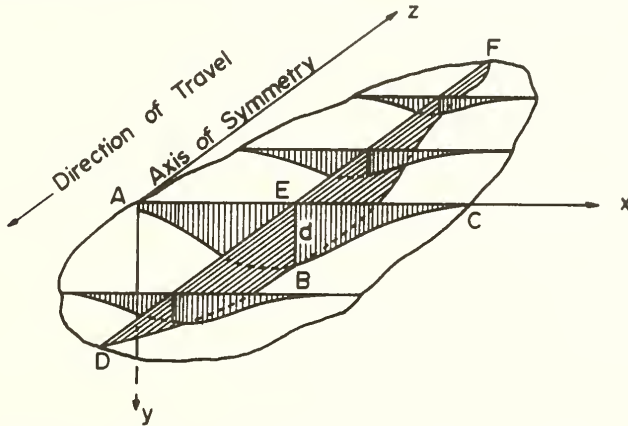
pertaining to the condition of the whole runway.

Energy concepts are global; that is, they provide a quantitative spatial evaluation rather than one limited to the very near vicinity of a point. Methods evolving from energy concepts, by their very nature, lend themselves to the evaluation of large sections of airport and highway pavements. If load-induced deflections of a pavement are immediately recoverable upon removal of the load, the system would be said to be elastic and the energy imparted to the pavement system by the prime mover would be conserved. After many passes real pavement systems cannot accommodate all the energy transferred to them by prime movers and some of the energy is expended in creating permanent deformations and/or cracks. Cracks are new surfaces formed as manifestations of an excess of energy that is not released by the pavement system upon release of the load. Systems which behave in this manner are said to be nonconservative. The fact that pavements respond differently at different times to the same increment of load may be a partial explanation for the failure of elastic pavement models to predict the performance of real pavements reliably.

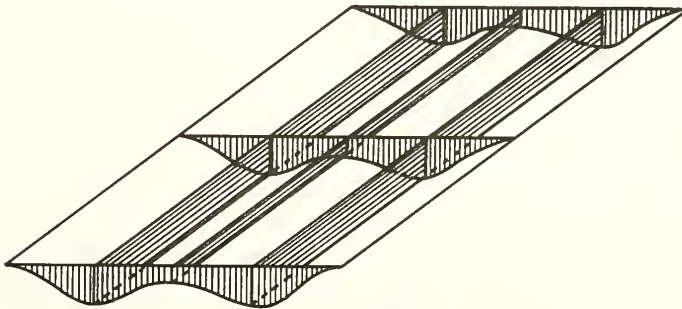
Consider what happens when a prime mover traverses a pavement. Figure 4 -A is a schematic stop-motion representation of the deflection basin created by a moving vehicle. The shape of the deflection basin reflects the weight and wheel configuration of the prime mover as well as properties of the pavement system and its support. The maximum deflections are seen to occur directly under the wheels. In this regard it might be said that the pavement system acts as a filter which attenuates the input energy out from under the wheels and in doing so



A - 2Dimensional View of the Plane Containing the Peak Deflections.



B - 3Dimensional Illustration of Half of the Symmetrical Deflection Basin.



C - 3Dimensional Deflection Trough

Not to Scale

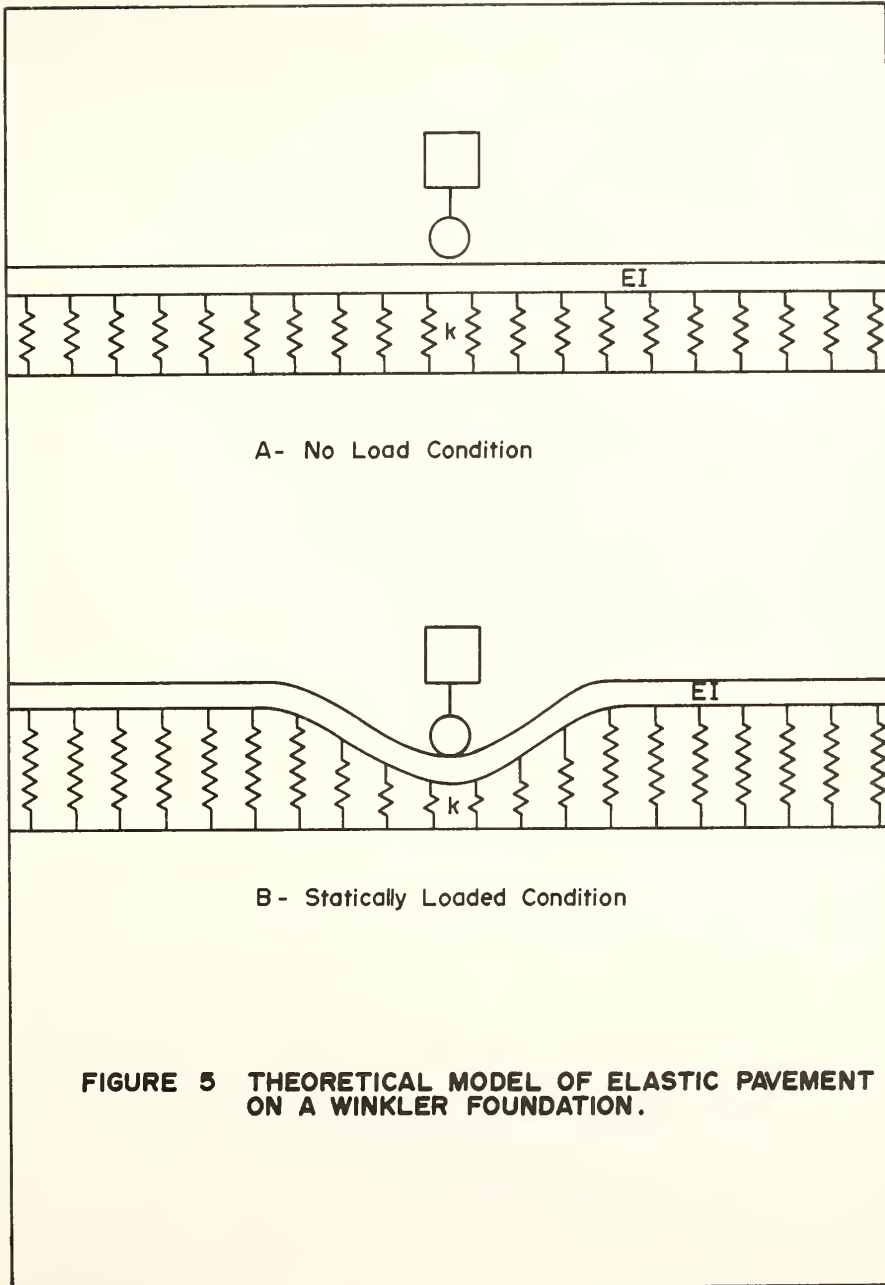
FIGURE 4 SCHEMATIC REPRESENTATIONS OF A DEFLECTION BASIN AND A DEFLECTION TROUGH.

creates a three dimensional deflection basin. Figure 4-B is a three dimensional illustration of half of the symmetrical deflection basin. Point D in this figure is on the outer boundary of the deflection basin and is in the wheel path of the load shown located at point E in this representation. As the load moves in the negative z direction (out of the page) point D is deflected downward, eventually reaching its peak deflection (at a time slightly after the passage of the vehicle) designated on the figure as d. With the continuance of the prime mover, the deflection decreases and the pavement returns to its initial position, point F.

Therefore, in concept, the plane paralleling the z axis in the figure, containing the points D, B, and F, can be thought of as the deflection-time response of a single point lying in the wheel path of a moving prime mover. Thus, conceptually, the prime mover can be thought of as creating a "trough" of deflections (like a standing wave) represented by the plane containing the points A, B, and C as it traverses the pavement. Figure 4-C is a three dimensional representation of the deflection trough created by a prime mover as it traverses the pavement. This, in effect, reduces the 3 dimensional problem (the deflection basin) to a 2 dimensional problem in a plane. The analytical system, then, can be modeled as a beam whose length represents the width of the pavement. In this regard, the beam can be thought of as being infinitely long because the width of airport pavements are many times larger than the width of the peak deflection basin; that is, edge effects can be ignored.

In order to gain some insight into the application of energy methods to pavement systems, a simple but important model will be considered. Figure 5 shows an airport runway modelled as an infinitely long elastic beam supported by a series of individual elastic springs (Winkler foundation), where the length of the beam represents the width of the runway. The beam has a unit width in the longitudinal direction of the runway. An elastic system is not an unreasonable model, for illustrative purposes, because real pavements act nearly elastically for single coverages - it is only after many prime mover passes that non-elastic characteristics become manifest. The change in energy in such a system when it is loaded statically consists of the sum of the strain energy imparted to the elastic springs supporting the beam and the strain energy in the beam itself. The total strain energy of the elastic beam, when in its deflected shape, can be taken as the sum of four components:

- (1) Strain energy due to axial loads. This component of the strain energy considers movements in the plane of the pavement. As the induced loads (represented as the steady-state trough) are normal to this surface, there will be little longitudinal displacement, elongation or contraction, of the pavement when compared to the bending mode; hence, this strain energy component may be assumed to be negligible.
- (2) Strain energy due to shear forces. For beams with length to depth ratios of 10 or more the contribution of the shear forces to the total strain energy is negligible (Rogers and Causey, Ref. 58). For an airport runway this ratio would be



greater than 33 (a minimum of 100 feet wide and a maximum of 3 feet deep), and hence the strain energy due to shear forces can also be neglected.

- (3) Strain energy due to twisting. As pointed out above, the steady-state trough has reduced the problem to a 2 dimensional or "plane deflection" consideration. Hence, there is no tendency for the beam to twist and this component of the strain energy is zero.
- (4) Strain energy due to bending. This component is the prime contributor of strain energy to the beam. The strain energy due to bending can be related to the curvature or change in slope of the deflected structure; or, expressed symbolically,

$$U_{\text{bending}} = \int_{-\infty}^{+\infty} EI \left(\frac{d^2 D}{dx^2} \right)^2 dx \quad (2)$$

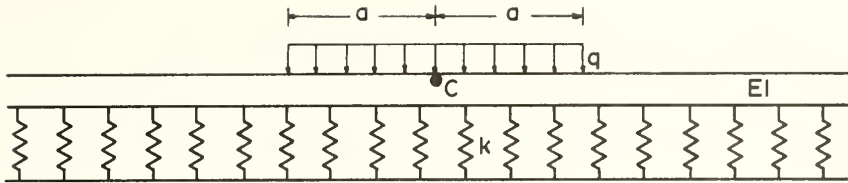
where D = the normal deflection

E = Young's modulus

I = moment of inertia

Experimental results from field tests on actual airfield pavements to be described in a following Section, indicate that the curvature of the surface under loading, $d^2 D/dx^2$, is very small except within the close proximity of the aircraft wheels. Within this region, it is related to the deflection directly under the aircraft wheel. On Figure 6 is shown the relationship between maximum deflection and curvature for an elastic beam on a Winkler foundation.

The strain energy in the base, modelled as a series of elastic springs, is a function of both the beam deflection and the spring



Elastic Beam Supported by a Winkler Foundation

The Maximum Deflection Occurs at Point C.

$$D_c = \frac{q}{k} (1 - e^{-\lambda a} \cos \lambda a) \quad \text{where } \lambda = \sqrt[4]{\frac{k}{4EI}}$$

The Moment at C is Given by

$$EI \frac{d^2 D}{dy^2} = \frac{q}{2\lambda^2} e^{-\lambda a} \sin \lambda a$$

Substituting

$$D_c = \frac{q}{k} \left(1 - \frac{2\lambda^2 EI}{q} \frac{d^2 D}{dx^2} \cot \lambda a \right)$$

FIGURE 6 EXPRESSIONS FOR THE DEFLECTION AND MOMENT AT THE MIDPOINT OF A SYMMETRICALLY LOADED ELASTIC BEAM SUPPORTED BY A WINKLER FOUNDATION.

(Ref. 57), or

$$U_{\text{foundation}} = k \int_{-\infty}^{+\infty} (W(x))^2 dx \quad (3)$$

where k is the stiffness of the springs and W is the deflection of the subgrade. The total strain energy of the system can be taken as

$$U_{\text{total}} = U_{\text{bending}} + U_{\text{foundation}} \quad (4)$$

$$= \frac{EI}{2} \int_{-\infty}^{+\infty} \frac{d^2 D}{dx^2}^2 dx + k \int_{-\infty}^{+\infty} (W(x))^2 dx \quad (5)$$

Both terms in the equation are seen to be related to the load induced deflections of the beam and are independent of the rate and the path by which these deflections are attained.

As stated previously, the pavement system acts as a filter which attenuates the peak deflection under the load (wheel of the prime mover). With this characterization, the peak deflection becomes a measure of the load induced energy available to do work to the structure. Consequently, the magnitude of the maximum peak pavement deflection (d in Figure 4) provides both a measure of the induced loads and the characteristics of the pavement system. Stated another way the maximum deflected shape of the pavement provides a measure of the net energy introduced into a pavement system by a prime mover. Of considerable importance in this regard is the recent development of transfer functions (Harr and Boyer, Ref. 4) which provides directly the deflected response of a pavement due to any prime mover. Thus pavement engineers will be able to quantify and compile the cumulative peak deflection data needed to predict the performance trends of air-field and highway pavement by a non-destructive method with a minimum

of interruption to operational traffic.

Procedure Used To Test The Working Hypothesis

To test the working hypothesis, data from which cumulative peak pavement deflections could be determined and a measure of the condition of the pavement associated with these deflections were required. Because this research is oriented toward airfield pavements, condition and deflection data were sought for such pavements. However, the necessary data could not be found for any airfield - military or civilian - and the paucity of such data would enable only a qualitative check of the working hypothesis to be made with airfield data and another data source had to be found in order to test the hypothesis quantitatively.

Pavement deflection and condition information that satisfied the needs of this research were found in data collected at the AASHO Road Test (Ref. 19). Figure 7-A is a schematic representation of the procedure which will be used subsequently to test the working hypothesis using results from the AASHO Road Test. Cumulative pavement deflections associated with a given pavement condition will be determined for many test sections having varying pavement profiles. Regression analysis will then be used to find an equation which predicts the performance of the pavement from surface, base, and subbase thicknesses and cumulative total pavement deflection input data. Expressed symbolically, a functional relationship will be sought in the form of

$$PSI = f \left[\begin{array}{cccc} \text{surface} & \text{base} & \text{subbase} & \text{cumulative} \\ \text{thickness,} & \text{thickness,} & \text{thickness,} & \text{total peak pavement} \\ & & & \text{deflection} \end{array} \right] \quad (6)$$

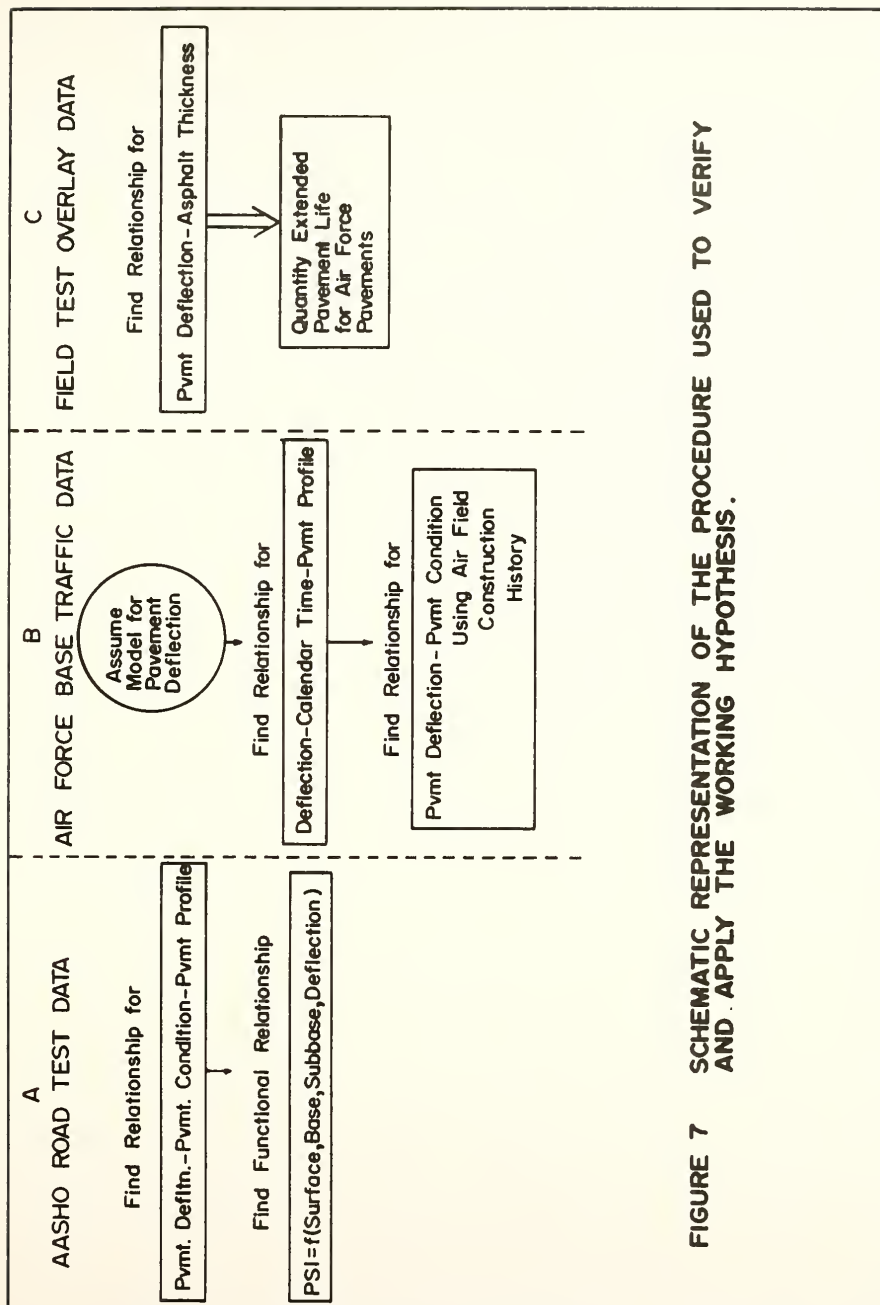


FIGURE 7 SCHEMATIC REPRESENTATION OF THE PROCEDURE USED TO VERIFY AND APPLY THE WORKING HYPOTHESIS.

Figure 7-B indicates how the working hypothesis will be tested for actual airfield pavements. Generally, the U. S. Air Force does not collect or compile deflection data for any of its air bases. However, air base traffic records were obtained for two Air Force bases. The traffic data will be used in conjunction with a mathematical pavement model to yield cumulative deflections. A comparison will then be made between this measure of the energy imparted to the pavements and the maintenance history of the airfields.

Figure 7-C illustrates schematically how some of the data obtained in the Kirtland Field Test will be used to define the effectiveness of overlays from a performance point of view. A case history will be generated to illustrate a developed procedure which can provide the thickness of an overlay so that a pavement will perform satisfactorily under an anticipated traffic volume.

SECTION IV

VALIDATION OF THE WORKING HYPOTHESIS BY
AASHO ROAD TEST DATA

Pavement deflection and condition information that satisfied the needs of this research were found in data collected at the AASHO Road Test. The pavement study phase of the Road Test consisted of trafficking test sections arranged continuously in a loop until failure occurred. The test sections differed from one another by having varying surface, base, and subbase thicknesses. The data included periodic Benkelman beam deflection measurements, periodic surveys that measured the performance of the pavement in terms of the Present Serviceability Index (PSI) as well as a listing of the number of load applications corresponding to a given PSI.

The load vehicle which was used for the periodic Benkelman beam deflections was not the same as those used to traffic the test sections so these data had to be scaled to account for the heavier vehicles used for trafficking. It was assumed that the load-deflection relationship for the test sections was linear over the range of load for the two types of trucks. This assumption seems to be justified by the literature findings (Refs. 5 and 36). Assuming that the bi-weekly Benkelman beam deflection measurements were representative of those that would have been obtained by daily measurements (had they been taken) and having knowledge of the pavement profile, the number of load

applications corresponding to a given PSI enabled a correspondence to be found between the cumulative total pavement deflection of a given test section (pavement profile) and the condition of the pavement.

Figure 8 shows this correspondence for three of the sixty test sections analyzed. Each test section yielded five cumulative deflection - PSI data points. The curves are typical of all the test sections analyzed and are presented here to illustrate the effect of surface course thickness on the condition of a pavement as a function of its cumulative total deflection. The shape of these curves is characteristic of all test sections analyzed: they become asymptotic to limiting cumulative deflection as failure is approached. The amount of cumulative deflection a pavement can attain for a corresponding PSI value was found to increase as the thickness of any of its components (either the surface, base, or subbase) increases.

Cumulative deflection - PSI data sets such as those illustrated in Figure 8 but where the base and subbase thicknesses were varied were applied to regression analysis and a functional relationship of the following form was obtained:

$$\text{PSI} = f(\text{surface thickness, base thickness, subbase thickness, cumulative total peak deflection}). \quad (7)$$

The criterion followed for acceptance of a regression model was one whose mean residual (the mean difference between the PSI predicted by the model and that observed) was less than 0.3. This criterion was chosen because:

- (1) It was found during the road test that panels which rated a given section on two different occasions could replicate

6-9-8 Surface Course 6 inches Thick
 Base Course 9 inches Thick
 Subbase Course 8 inches Thick

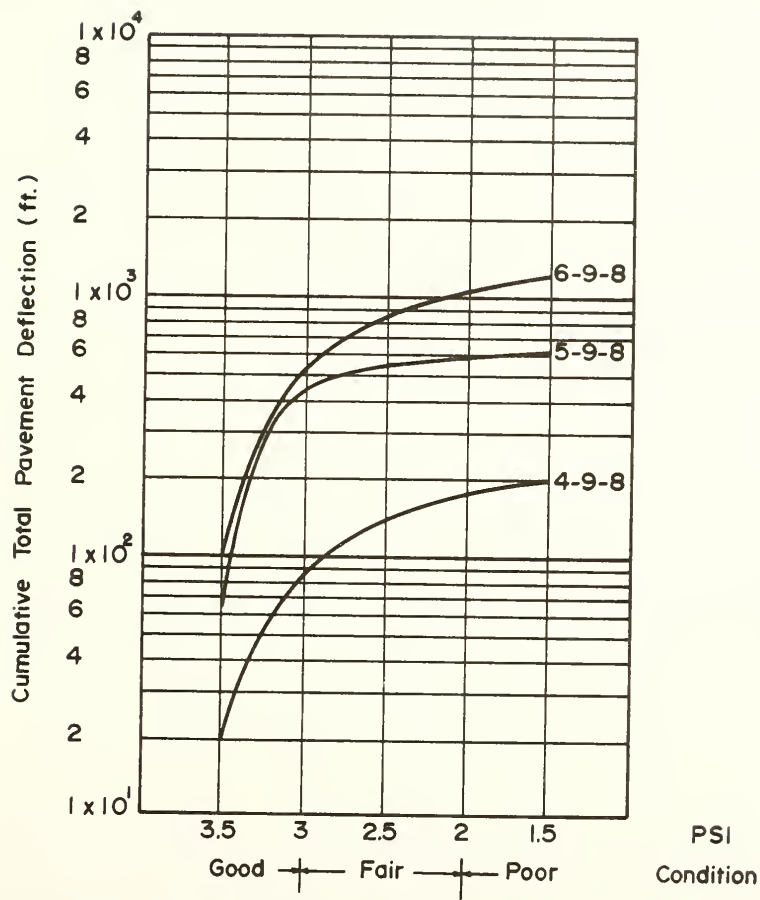


FIGURE 8 THE EFFECT OF SURFACE COURSE THICKNESS ON THE CONDITION OF A PAVEMENT AS A FUNCTION OF ITS CUMULATIVE TOTAL DEFLECTION.

their earlier rating within a mean difference of about 0.2 with a range of from 0 to 0.5.

- (2) The assumption that a single bi-weekly Benkelman beam deflection measurement was representative of the deflections over a two week period was not unreasonable, but probably did involve some error in the analysis.

For these reasons it was felt that a regression model which fitted the data too closely was unrealistic and misleading.

The regression equation which satisfied this stated criterion was;

$$PSI = .031 + .383S + .077B + .071SB - .0022D + 5.56 \times 10^{-7} D^2 \quad (8)$$

where

PSI = Present Serviceability Index

S = Asphaltic surface thickness, inches

B = base course thickness, inches

SB = subbase thickness, inches

D = cumulative total pavement deflection, feet.

The average error in the predictive equation was 0.288. Figure 9 illustrates the scatter in the Present Serviceability Index as predicted by equation 8. The dashed lines in the figure indicate the mean difference within which the original AASHO panels were able to replicate their PSI ratings.

An examination of equation 8 indicates that 1 inch of asphaltic concrete is equivalent to 5 inches of base material and 5.4 inches of subbase in the AASHO Road Test. Should one chose to do so, the cost-

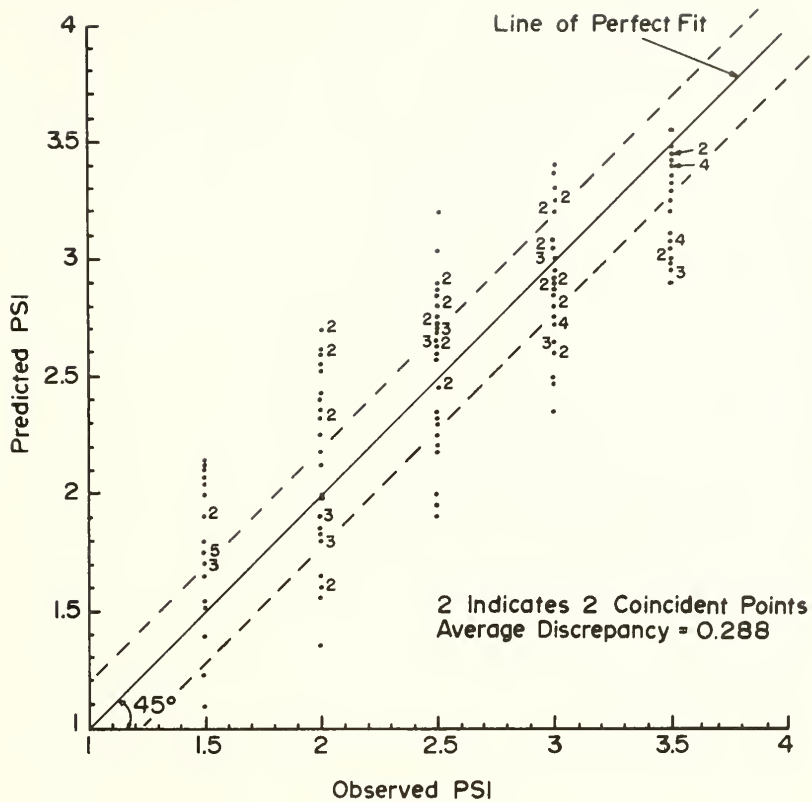


FIGURE 9 PREDICTED VS. OBSERVED PRESENT SERVICEABILITY INDEX FOR AASHO ROAD TEST DATA.

effectiveness of the various elements of the pavement profile could be quantified from this type of information.

Figure 10 is a plot of equation 8 for three pavement profiles. The thicknesses were chosen only to indicate the effectiveness of asphalt surface thickness as predicted by this equation. The horizontal dashed line in the figure ($D = 1200$ ft.) indicates that, at this cumulative total deflection, the pavement with 6 inches of asphaltic concrete would be in fair condition; that the one with 5 inches of surface would be at the fair-poor interface, and that the 4 inches course would be in poor condition, nearly failed. Comparing the cumulative total deflections at failure for the three pavements, it is seen that the pavement with 6 inches of surfacing would accommodate over 100% more deflection than the pavement with 4 inches.

It should be noted that equation 8 cannot be applied to all asphalt concrete pavements. In a statistical sense it can be applied with confidence only to pavement profiles that are similar to those trafficked at the AASHO Road Test and which are subject to environmental conditions which are similar to those encountered at the Road Test. The equation is presented here for the purpose of validating the working hypothesis for a condition where reliable data are available.

S - B - SB

6 - 9 - 16

Surface Course 6 inches Thick

Base Course 9 inches Thick

Subbase Course 16 inches Thick

Predictive Equation:

$$PSI = .031 + .383S + .077B + .071SB - .0022D + 5.56 \times 10^{-7} D^2$$

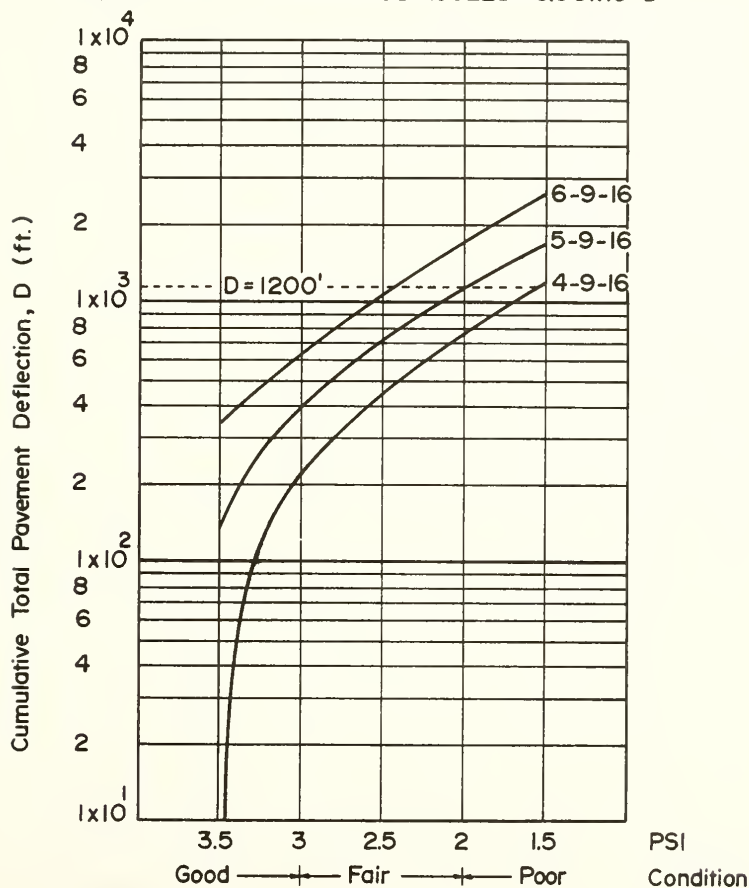


FIGURE 10 THE PREDICTED EFFECT OF SURFACE COURSE THICKNESS ON THE CONDITION OF A PAVEMENT AS A FUNCTION OF ITS CUMULATIVE TOTAL DEFLECTION.

SECTION V

ANALYSIS OF AIR FORCE BASE DATA

Equation 8 presented a functional relationship, obtained from AASHO Road Test data, which correlated the condition of an asphalt pavement with its component thicknesses and the cumulative total deflection which it had experienced. The next step in this research (see Figure 7-B) is to examine the validity of the working hypothesis for airport pavements. To do this, pavement deflection and condition data had to be obtained for air bases.

The data record for airport pavement condition is not as complete as that for the AASHO Road Test. In the absence of periodic condition survey reports, condition data were obtained from the construction histories of Pease Air Force Base, New Hampshire and Castle Air Force Base, California; condition survey reports that were available; and direct communication with the pavement engineers at the two bases involved. These data are presented in Appendix I.

The Air Force does not collect or compile deflection data for its air bases at the present time. However, reliable air base traffic records (presented in Appendix I) were obtained for Pease and Castle Air Force Bases.

In the absence of actual deflection data, which may in the future be obtained by the methods proposed by Harr and Boyer (Ref. 4), an analytical model was employed. Following the assumptions developed in the section dealing with Theory, the model used was that of a stationary load supported by a three layer elastic system. A computer

routine written by Barksdale (Ref. 74) which determines the surface deflections of such a system was used. The input data required for the elastic layer computer program were the thickness, Young's modulus, and Poisson's ratio for each layer and the aircraft loading. The assumptions involved in the program are those assumed by Burmister (Refs. 23 and 24) which were listed in the Review of the Literature section.

Analytical procedures which predict deflections rather well have been available for some time. For example, Wiseman, Harr, and Leonards (Ref. 75) modelled a pavement as a slab on a Winkler foundation and found close agreement between the computed deflections and those measured in a controlled test. However, the curvature of the deflected slab varied significantly from that predicted by the model. Similar results were found when deflections actually measured in the Kirtland Field Test (see Section VII) were compared with those predicted by the three layer elastic analysis. Figure 11 compares deflections measured in the field test to those computed by the model. The parameters used in the layer analysis are those listed in Table III which were measured by personnel from the Civil Engineering Research Facility, University of New Mexico. The figure shows good agreement between predicted and observed deflections up to about 40 inches from the point of loading but the curvature of the predicted and measured deflected surfaces are much different. It is important to note that the working hypothesis is concerned only with the peak deflection and the shape of the deflection curve is not of consequence. For this reason it is felt that the layer analysis will yield a reasonable estimate of

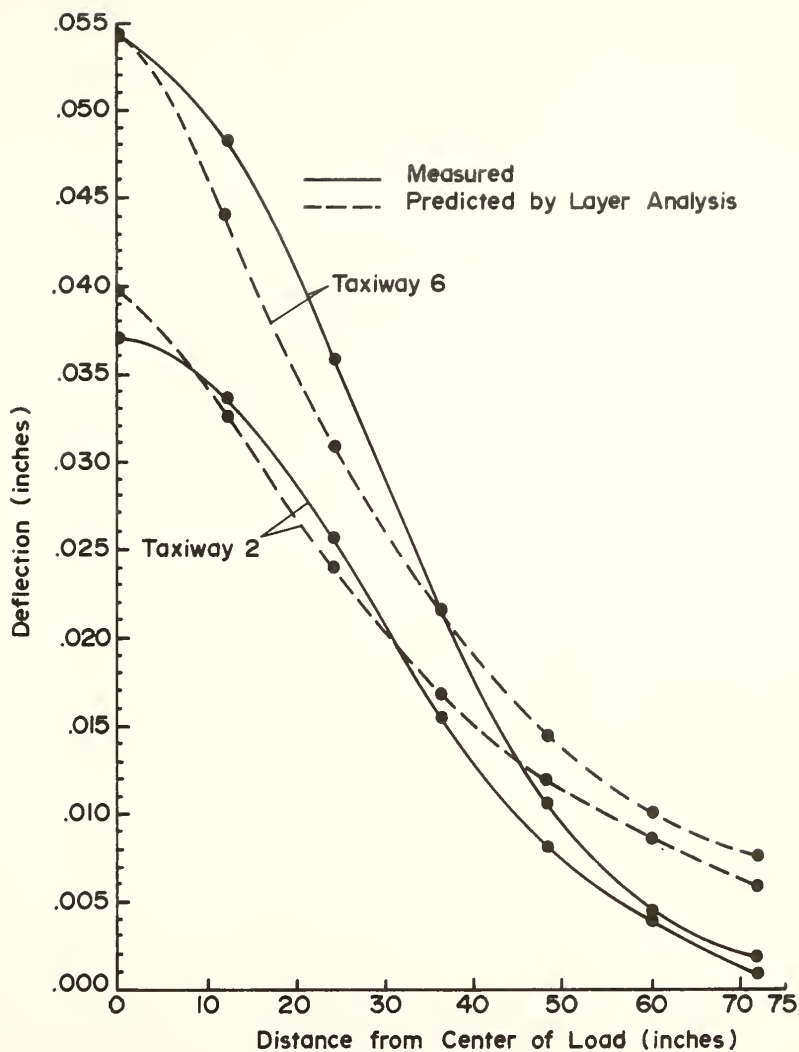


FIGURE II OBSERVED AND PREDICTED DEFLECTIONS FOR LOAD CART AT TAXIWAYS 2 AND 6 .

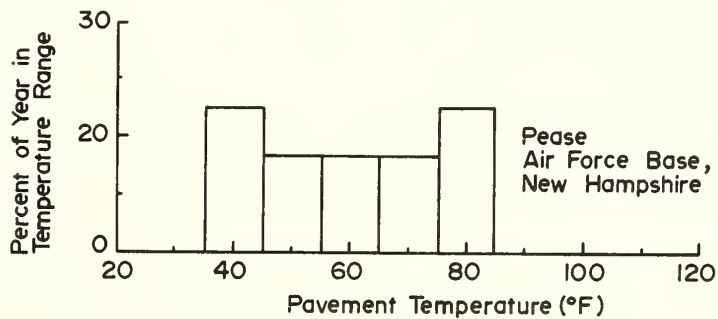
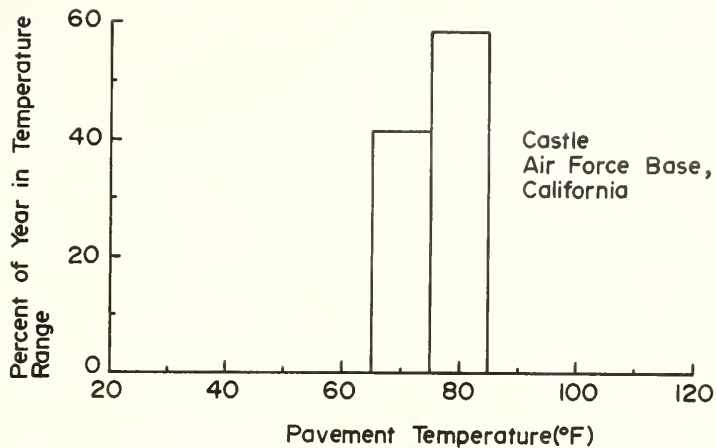
the energy imparted to pavements as measured by peak pavement deflections.

The value of Young's modulus used for the asphalt layer for the two air bases was that measured at Taxiway 2 in the Kirtland Field Test. This decision seems justified because:

- (1) the age and thickness of the pavement at Kirtland is similar to those at Pease and Castle Air Force Bases.
- (2) a "ball park" estimate was felt to be sufficient because it was found that all other parameters being equal doubling Young's modulus resulted in only an eleven percent decrease in the computed peak deflection.

The moduli used for the base and subbase layers were determined from plate load tests.

The procedure used to find the cumulative peak pavement deflections for Pease and Castle Air Force Bases was as follows. The deflections under each wheel of an aircraft that was operational in a given year at an air base were calculated and added together. This deflection was then multiplied by the number of annual operations of the aircraft which yielded the total deflection for each aircraft by year. The total deflections thus obtained for each type of aircraft operating at the given base were summed giving the total peak deflection on an annual basis. Because the load induced deflections for asphalt pavements are temperature dependent, it was then necessary to make a temperature correction for the annual total peak deflections. It was found that the pavement temperatures during the Kirtland Field Test were about 15°F. higher than ambient and this is reflected in the temperature data illustrated in Figure 12. Deflections were computed for a temperature of 60°F. and then reduced or increased according to



DATA FROM REFERENCE (76)

FIGURE 12 ASSUMED ANNUAL PAVEMENT TEMPERATURE DATA FOR CASTLE AND PEASE AIR FORCE BASES.

Figure 27. For temperatures beyond the range of this figure, data from Ref. 19 were used. In making the temperature correction, it was assumed that the distribution of deflections (traffic) was evenly distributed throughout each year.

Figures 13 and 14 illustrate trends in the total peak deflection per year for the Pease and Castle Air Force Bases, respectively. The bars in solid lines were obtained from traffic data by the method described above. These data established the trends in the yearly total peak deflections for which traffic data were available. These trends were then extrapolated back to the year of original construction so that cumulative total peak deflections from the time the bases became operational could be obtained. The extrapolated data are indicated by the bars in broken lines in the two figures.

Figure 15 shows the cumulative total peak deflections by year for Pease Air Force Base. Construction milestones and condition information are also indicated in the figure. The pavement was in good condition in 1964 after experiencing 2040 feet of cumulative deflection but by 1970, when the cumulative total peak deflection had reached 2852 feet, extensive cracking had developed.

Figure 16 illustrates the cumulative total peak deflection by year for Castle Air Force Base. The figure indicates that after only 1400 feet of cumulative total peak deflection (1954) an overlay was required and that after an additional 2625 feet of total deflection (1963) cracks had begun to develop. This latter figure is within the range of cumulative deflection at which cracking was also noted at Pease.

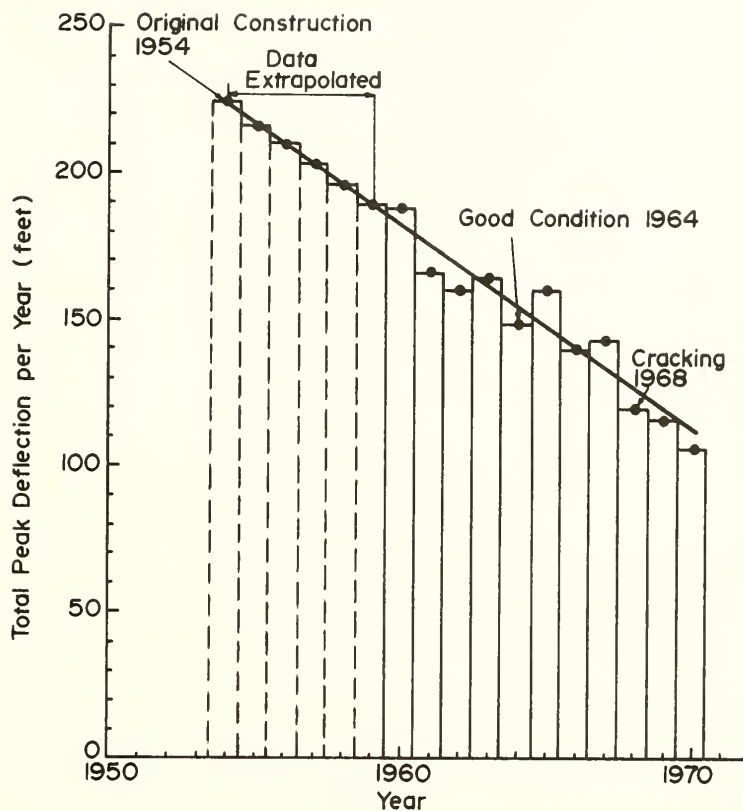


FIGURE 13 TOTAL PEAK DEFLECTION TREND FOR PEASE AIR FORCE BASE, NEW HAMPSHIRE

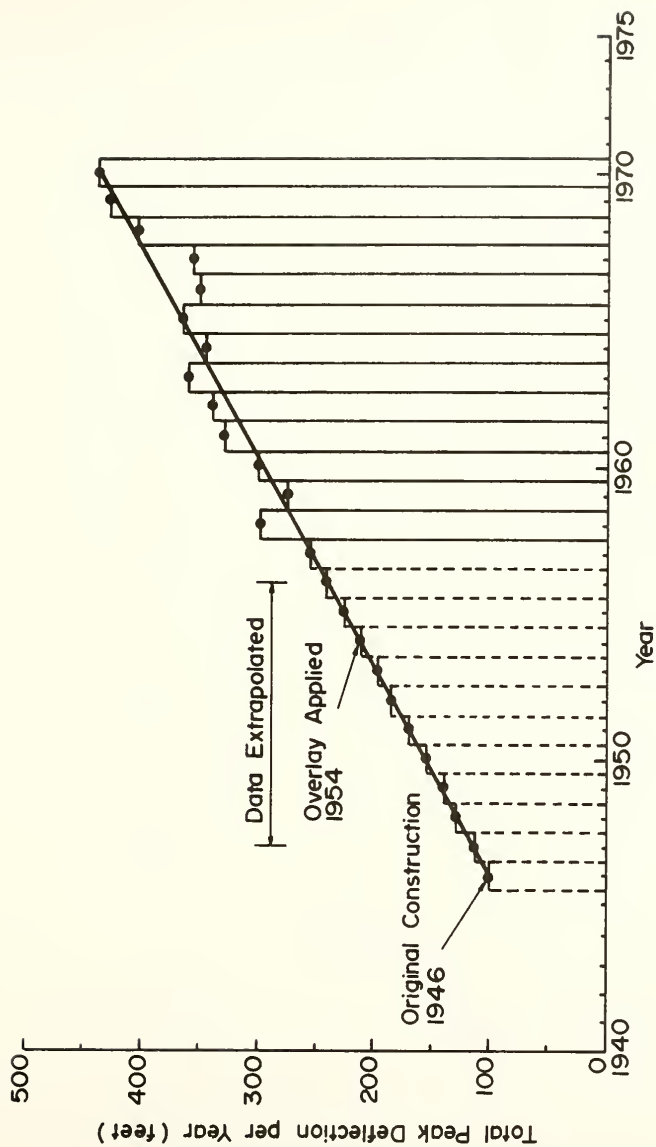


FIGURE 14 TOTAL PEAK DEFLECTION TREND FOR CASTLE AIR FORCE BASE, CALIFORNIA .

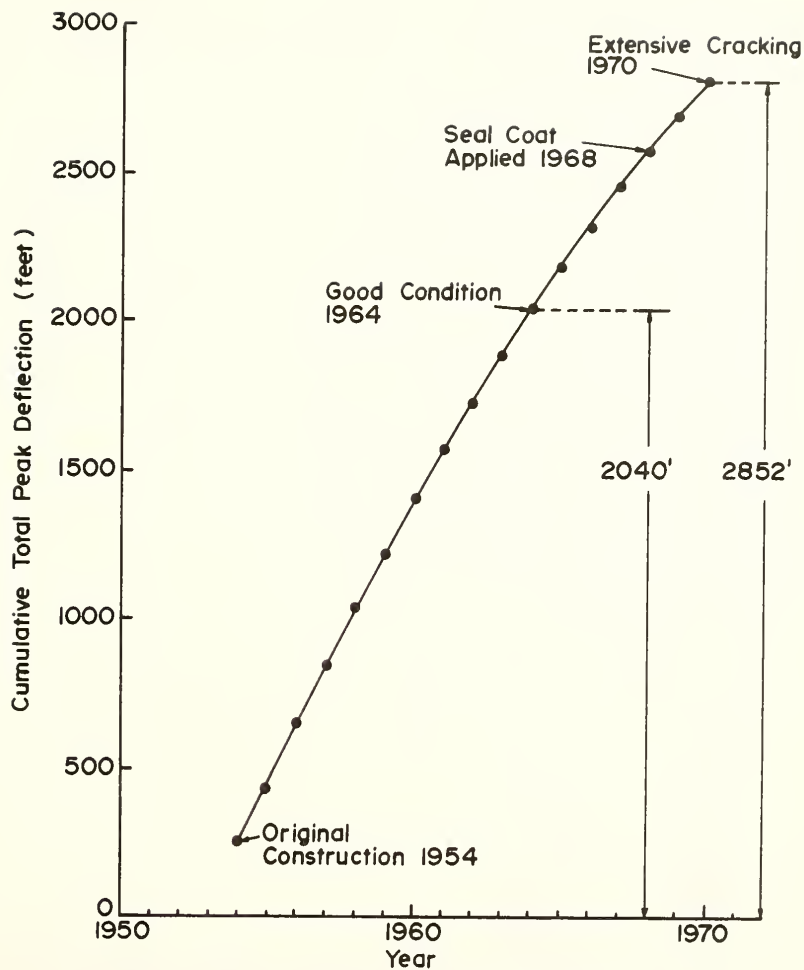


FIGURE 15 CUMULATIVE TOTAL PEAK DEFLECTION BY YEAR, PEASE AIR FORCE BASE, NEW HAMPSHIRE.

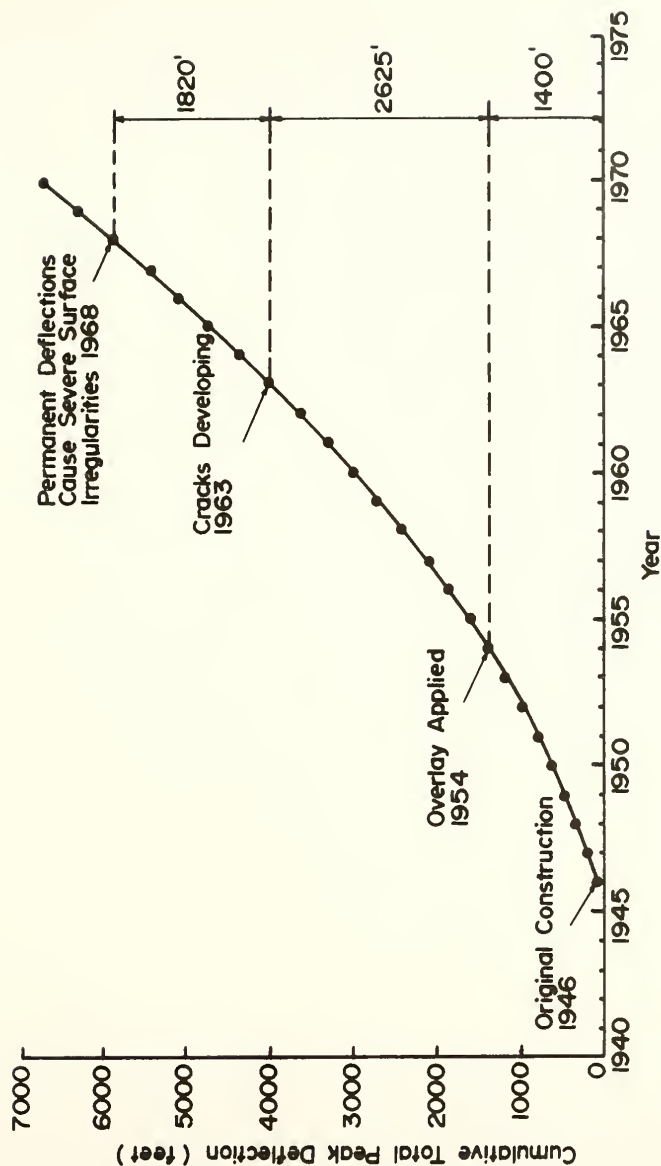


FIGURE 16 CUMULATIVE TOTAL PEAK DEFLECTION BY YEAR, CASTLE AIR FORCE BASE, CALIFORNIA.

The cumulative deflection of 1400 feet at which an overlay was applied at Castle is considerably less than the cumulative deflection at which cracking was noted at both Pease and Castle Air Force Bases. A possible explanation for this discrepancy is that the data for Castle had to be extrapolated back 11 years while that from Pease was extrapolated 6 years. Such a long extrapolation may not be legitimate because jet aircraft were introduced during this 11 year period. Figure 1 indicates that the gross weights of aircraft introduced into service at this time increased substantially.

If the year 1954 is selected as a base date for both air bases then it appears that both air base pavements began to deteriorate when they experienced a cumulative total peak deflection of about 2500 feet. In any case, the Air Force Base data lend themselves to qualitative support of the working hypothesis in that there seems to be a **threshold** cumulative deflection at which pavement deterioration at both Pease and Castle Air Force Bases was noted.

SECTION VI

GENERAL DESCRIPTION OF THE KIRTLAND FIELD TEST

Introduction

The purpose of this Section is to elucidate the objectives of the Kirtland Field Test, describe the pavement sections used and the type of data obtained, and to provide a brief description of the test procedure. A detailed account of the instrumentation used and its installation is presented in Appendix II.

Background

In June and July 1971 an extensive preliminary instrumentation test was undertaken at Kirtland Air Force Base, New Mexico in order to provide information regarding the suitability of various commercially available deflection devices for measuring vertical pavement deflections created by moving aircraft. Among the devices tested were accelerometers, velocity transducers, and linear variable differential transformers (LVDTs). A requirement of the type of instrument selected was that its configuration during testing was such that an aircraft wheel could pass directly over it without damage to either the tire or the instrument itself. In addition, the instrument had to be sensitive and accurate over a rather wide range of deflections.

Only LVDTs (linear variable differential transformers) were found to satisfy the criteria and were chosen as the instrument for a more extensive field test to be carried out at Kirtland AFB in 1972. The

LVDTs had a particular advantage in that they measured deflections directly and the data obtained from them did not require integration with respect to time as was the case for the accelerometers and velocity transducers. Harr and Boyer (Ref. 4) discussed the instrumentation test in detail.

Objectives of the 1972 Field Test

The actual field test consisted of two parts whose purposes were:

Part I. Overlays

- a. To provide data so that the effect of overlay thickness on the energy transfer between prime mover and pavement system could be ascertained.
- b. To secure the data necessary for the prediction of the performance of overlays yet to be constructed.

Part II. Pavement Sections

- a. To provide data so that the energy transfer between prime mover and pavement system could be evaluated on three different pavement profiles.
- b. To provide data so that the effect of prime mover horizontal velocities on subsequent pavement deflections and vertical velocities could be assessed.

Type of Data Collected

A single data set consisted of the time dependent deflections recorded by six LVDTs arranged in a line which was perpendicular

to the direction of travel of the prime mover. This provided the data required to determine the entire deflection basin created by the prime mover.

Description of Test Sites

The overlay test site was located on Taxiway (T-2) which parallels the main runway (see Figure 17). This site was selected because aircraft traffic could conveniently be diverted to a parallel taxiway (T-8) for the duration of the test (approximately four weeks) and because the pavement profile and condition indicated that remedial measures might have to be taken on this taxiway in the future if the pavement were expected to accommodate all aircraft in the Air Force inventory. A total of 8 inches of overlays were constructed in 2 inch lifts by personnel from the Base Engineer's Office. Deflection data were also collected on T-2 before the overlays were applied.

Taxiways T-6 and T-8 were used as test sites so that the effect of different pavement profiles on the prime mover - pavement energy transfer could be investigated.

Thus a total of 7 different pavement sections were tested with the load cart at three test sites. Table III gives descriptive profiles of the test sites along with measured layer properties.

Prime Movers

The prime mover used in the field test was the load cart shown in Figures 18 and 19. By raising the outer rear wheels, a 23,120 lb. load could be applied to the load wheel whose footprint was approximately

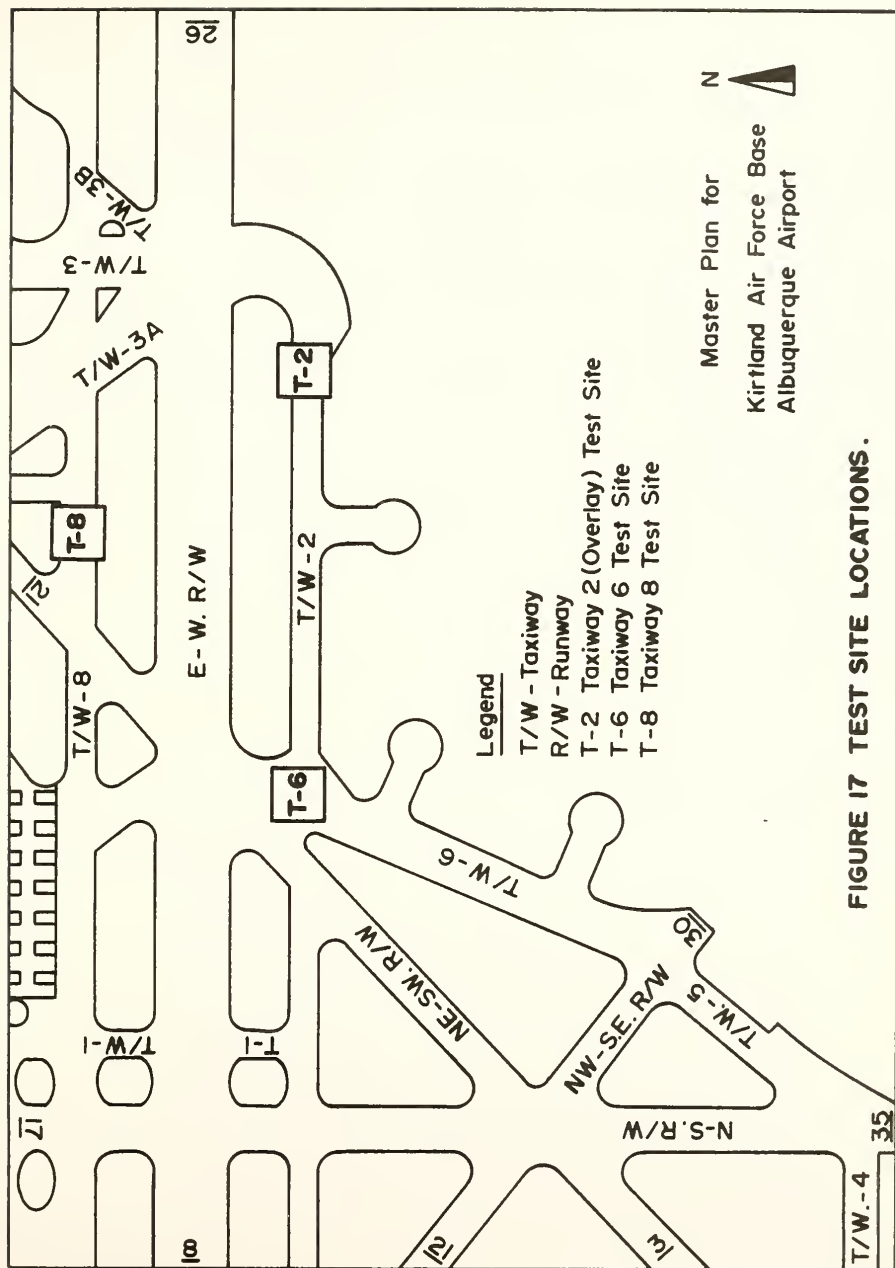


Table III

LAYER PROPERTIES OF TEST SITES

Layer	Test Site			
	Taxiway 6	Taxiway 8 (Modulus is average of two tests)	Taxiway 2	Taxiway 2 with 8" overlay
Surface Course				
Thickness	3 inches	10 inches	6 inches	14 inches
Modulus	$1.62 \times 10^6 \text{ psi}$	$2.5 \times 10^6 \text{ psi}$	$1.4 \times 10^6 \text{ psi}$	$2.46 \times 10^6 \text{ psi}$
Base Course				
Thickness	9 inches	6 inches	10 inches	10 inches
Classification	GP	SW	GP	GP
CBR	42.5%	127%	80%	80%
Modulus	$1.4 \times 10^5 \text{ psi}$	$3.1 \times 10^5 \text{ psi}$	$3.9 \times 10^4 \text{ psi}$	$1.05 \times 10^5 \text{ psi}$
Subgrade				
Classification	SP	SW-SM	SP-SM	SP-SM
CBR	19%	84%	32.7%	32.7%
Modulus	$5.94 \times 10^3 \text{ psi}$	$2.31 \times 10^4 \text{ psi}$	$9.8 \times 10^3 \text{ psi}$	$2.28 \times 10^4 \text{ psi}$

Data courtesy of Dr. H. A. B. Rao of the Eric H. Wang Civil Engineering Research Facility, University of New Mexico. The moduli were measured by frequency vibration tests.



Figure 18 The containers hold lead shot which put 23,120 lbs. on the load wheel.



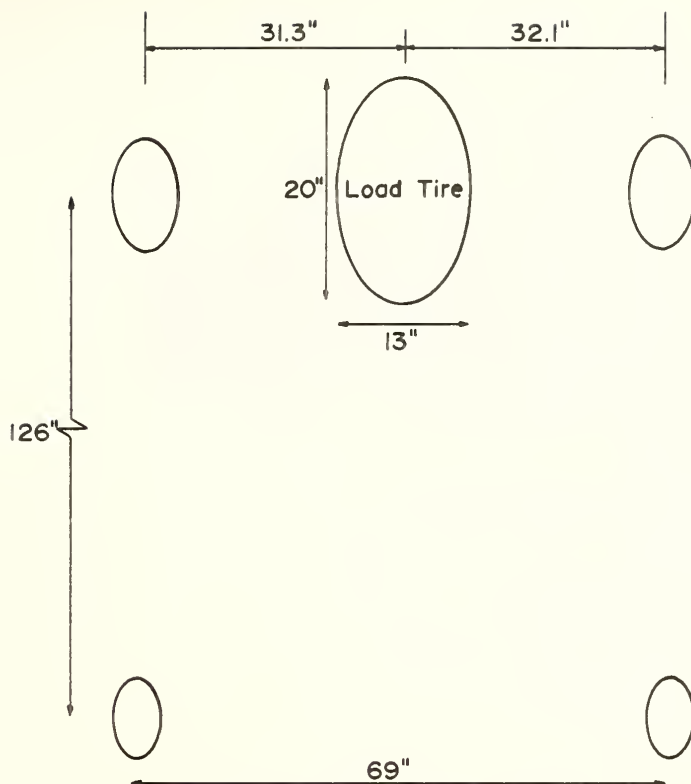
Figure 19 Front view of load cart.

246 square inches. A 20' x 20' areal dimension of the overlays was employed. This was governed by the wheel base and track (see Figure 20) of the self-propelled load cart. The load cart performed satisfactorily at slow speeds (less than about 12 ft./sec.) but at higher speeds there was a tendency for the cart to tip and distribute more load on the outer rear wheels. When this effect was noted in a particular data set, it was removed from the analysis.

The effect of horizontal vehicle velocity on the resulting deflections and the vertical velocity of the pavement was investigated at test site T-6 by an Air Force P-2 type fire truck. The truck is shown in Figure 21 and pertinent characteristics are presented in Table IV.

Statistical Design of the Overlay Experiment

The Corps of Engineers in a study of aircraft channelized traffic reported (Ref. 77) that 75% of the wheels of heavy jet aircraft travel within a strip 7.5 feet in width as a result of steerable landing gear. It seems likely that on a taxiway where the aircraft speeds are less than those on a runway, aircraft traffic would be channelized to an even greater extent. In addition, histograms have been presented (Ref. 78) that indicate the pattern of traffic across heavily travelled parts of the pavement is nearly normally distributed. With these facts as a basis, the center five feet of the overlays was trafficked as shown in Figure 22. Random number tables (Ref. 79) were consulted so that the order of the passes of the prime mover could be randomized consistent with the normal distribution. Lines of tape were placed



Not to Scale

Load Tire Characteristics-B.F. Goodrich
Type III Tubeless Aircraft Tire, Size 20.00-20
26 Ply Rating
Measured Footprint 246 sq.inches

FIGURE 20 SCHEMATIC OF LOAD CART SHOWING TRACK AND WHEEL BASE DIMENSIONS.



Figure 21 The P-2 fire truck used in velocity tests.

Table IV

P-2 FIRE TRUCK DATA

Wheel Base		Length (inches)
between first (front) and second axle		83.5
between second and third axle		129
between third and fourth axle		66.75
Axle		weight (pounds)
first (front)		16,400
second		16,520
third		16,120
fourth		15,240
Total		64,280
Tires - 16.00 - 25; 24 ply		

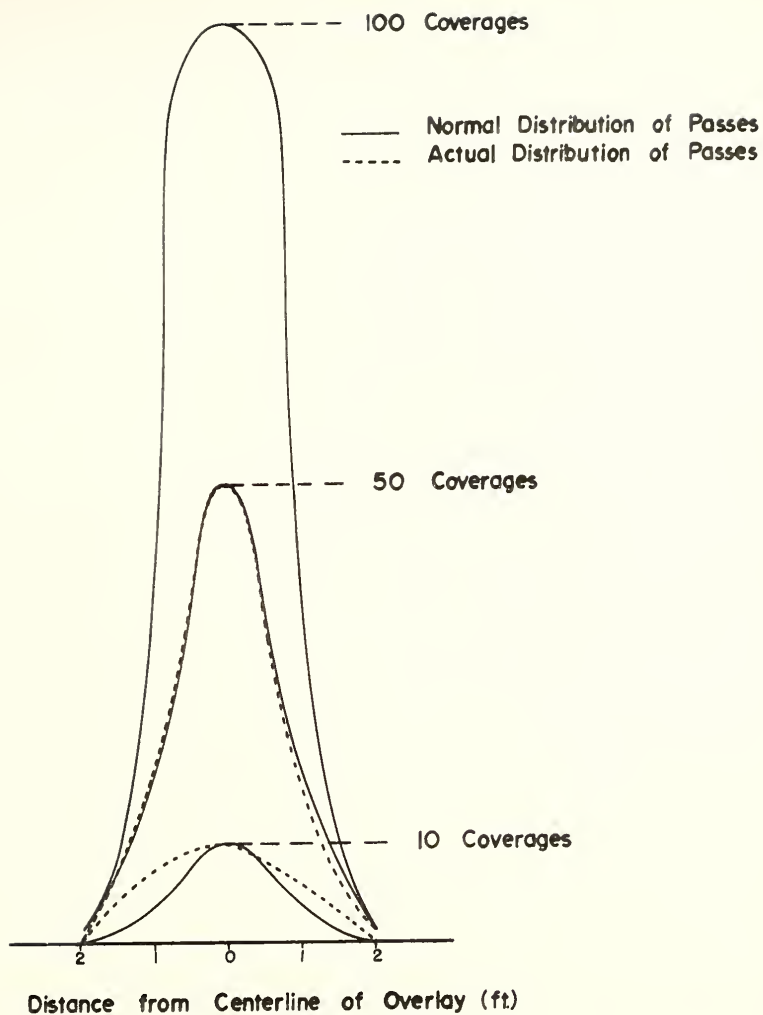


FIGURE 22 NORMAL DISTRIBUTION AND DISTRIBUTION OF PASSES OF THE PRIME MOVER FOR 10,50 AND 100 COVERAGES.

on the surface so that the load cart operator could maneuver the vehicle in order to get the desired distribution.

SECTION VII

PRESENTATION AND DISCUSSION OF THE KIRTLAND FIELD TEST

Introduction

The results and analysis of the fire truck velocity tests are presented first in this section and are followed by the overlay test results. Some illustrations of pavement deflection basins created by aircraft and the load cart are presented. Finally, the concept of a pavement system reaction coefficient is discussed.

Fire Truck Velocity Tests

In order to document the effect of the horizontal velocity of a prime mover on the maximum deflection and maximum vertical velocity of a pavement, deflection-time records produced by a P-2 fire truck travelling at a range of speed of 8.8 to 51 feet per second were obtained. The data were analyzed by the following procedure. For each such data record the time corresponding to the maximum deflection for the instrument closest to the vehicle wheels was observed. The deflections corresponding to this time for the other LVDT's were then noted and regression analysis was used to define a functional relationship. The regression equation had to satisfy the following restrictions:

1. The maximum deflection occurs at $x = 0$; where x is measured from the point of maximum deflection.
2. From (1) it follows that the slope or first derivative of

the deflection equation at $x = 0$ must be zero.

3. A satisfactory "fit" of the data had to be obtained.

The multiple-correlation coefficient, R^2 , which measures the proportion of total variation about the mean explained by the regression equation was used to judge satisfactory fit. R^2 cannot exceed 1 and is equal to unity only if the fit is exact. An R^2 of .7144 (or 71.44%) indicates that a given regression equation explains 71.44% of the total variation.

Three different models were investigated:

$$1. D(X) = Ae^{-BX} \cos BX \quad (9)$$

$$2. D(X) = Ae^{-BX^2} \quad (10)$$

$$3. D(X) = Ae^{-BX^2} \cos BX \quad (11)$$

where A is the deflection at $X = 0$ and has dimensions of length (L)

B is a parameter having dimensions of L^{-1} in equation 9

and L^{-2} in equations 10 and 11, and $D(X)$ is the deflection

X inches from the point of maximum deflection.

Equation 9 was selected because it is the form of the equation for the deflection of a beam supported by a Winkler foundation. Equation 10 was chosen because it describes the distribution of stress in a body having discrete particles. Because strain and hence deflection is related to stress, it was felt that this was a viable model to examine. Equation 11 was selected after it was found that both equations 9 and 10 fitted the data well; it was an attempt to combine the two equations to see if the fit would be improved.

Data sets in which a prime mover wheel had passed directly over an instrument were used to test the three models so that the "best" model could be selected. The multiple correlation coefficients for these trial runs were all between .900 and .999 and little difference was noted between the R^2 values for any one of the models. However, the "A" parameter of equation 10 was closer to the observed deflection under the wheels of the prime movers. This feature is important because the maximum pavement deflection is central to the working hypothesis of this research and for this reason equation 10 was selected to determine the maximum deflection for data sets where the prime mover did not pass directly over an LVDT.

The "A" parameter in equation 10 represents the maximum deflection (the deflection under a prime mover wheel). The term e^{-BX^2} indicates how the pavement acts to filter this deflection at points laterally away from the wheel. Figure 23 is a plot of equation 10 for $A = 1$ and various values of B. For low values of B the deflection basin is wider than for higher values indicating that the pavement exhibits more beam-like action. For high values of B the deflection basin is seen to be localized.

The results of tests of the variation in prime mover speeds on maximum deflections of the pavement are tabularized in Table V. The results indicate that maximum deflection decreases with increasing speed and that the B values also generally decrease with increasing speed, which indicates the deflection basins are narrower at higher velocities. Maximum deflections vs. vehicle speed are plotted in Figure 24. Results indicate that a nearly linear relationship exists

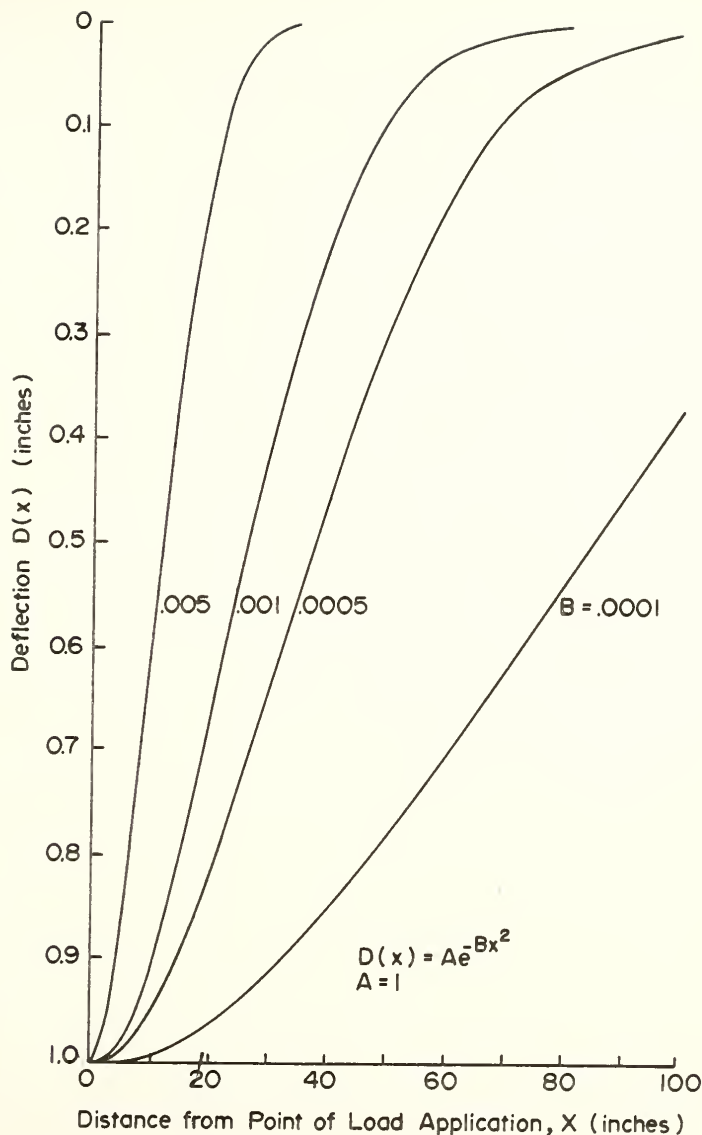


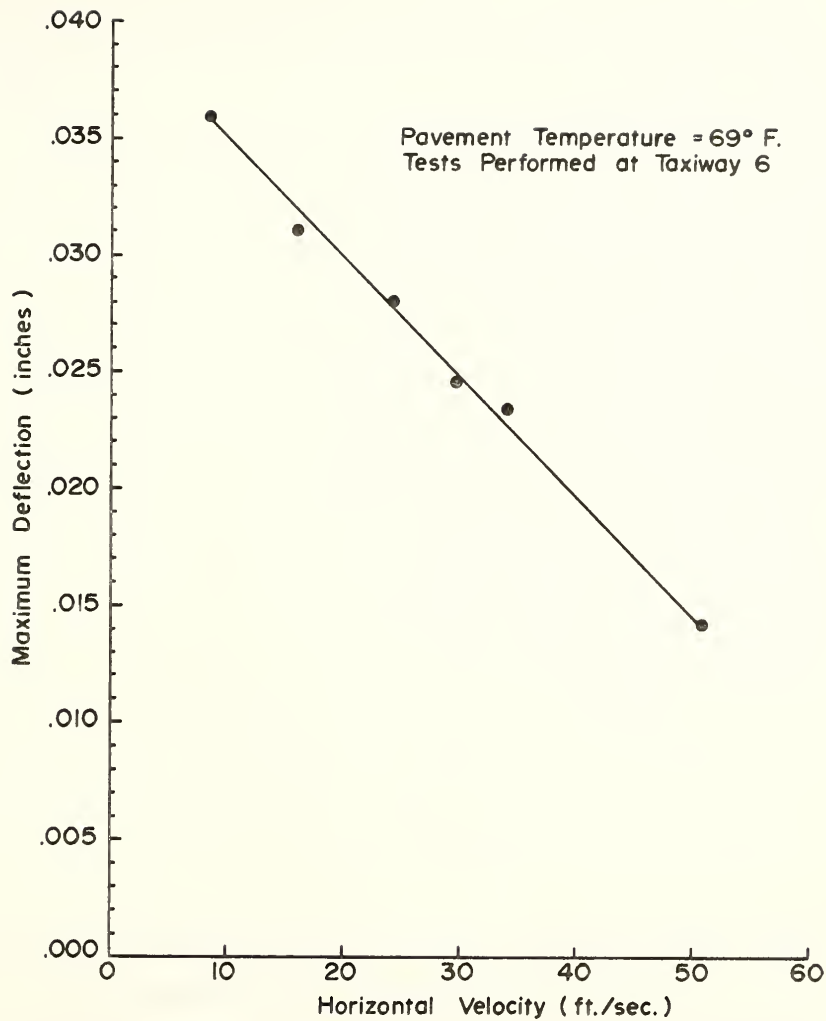
FIGURE 23 THE EFFECT OF THE B PARAMETER IN THE EQUATION $D(X) = Ae^{-Bx^2}$

Table V

FIRE TRUCK VELOCITY TEST DATA

Horiz. Velocity (FPS)	"A" (inches)	"B" $\frac{1}{\text{inches}^2}$	R ² *	Number of Tests
8.8	.03611	.003974	.9845	3
16	.03115	.004021	.9988	1
24	.02826	.004087	.9981	1
30	.02473	.002705	.9567	2
34	.02354	.003480	.9977	1
51	.01442	.002613	.9970	1

*Model Fitted was $D(X) = Ae^{-BX^2}$



**FIGURE 24 MAXIMUM PAVEMENT DEFLECTION VS.
HORIZONTAL VELOCITY FOR P-2 FIRE TRUCK.**

over the range of speeds tested. It is expected that the curve would approach a horizontal asymptote at higher velocities but this effect apparently occurs beyond the maximum speed of the P-2 fire truck (about 35 MPH).

The procedure followed for finding the maximum vertical velocity of the pavement consisted of smoothing the deflection-time data records by a second degree polynomial to eliminate sudden jumps in the data and then taking the first derivative with respect to time of the smoothed deflection-time data records. The maximum vertical velocity invariably occurred between 50 and 150 milliseconds before the pavement reached its maximum deflection. The maximum vertical velocity determined from each deflection-time record was noted and regression analysis was used to find an equation of the form

$$\text{Vertical Velocity} = f(X) \quad (12)$$

where X is measured from the point of maximum deflection.

By the same process described earlier for the deflection regression equation, it was found that the equation

$$V_v(X) = Ae^{-BX^2} \quad (13)$$

where A is the vertical velocity at $x = 0$ and has dimensions of LT^{-1} ,

B is a parameter having dimensions of L^{-2} ,

and $V_v(X)$ is the vertical velocity x inches from the point of maximum vertical velocity

provided the best fit of the data sets. Typical R^2 values varied from 0.9356 to 0.9947.

The results of the analysis for both the load cart and the fire truck at taxiway T-6 are presented in Figure 25. An examination of the figure indicates that the maximum vertical velocity of the pavement is independent of the prime mover horizontal velocity and of the prime movers themselves. This seems to indicate that the vertical velocity is solely a pavement parameter independent of magnitude and mode of loading. To check this, the load cart data for taxiways T-2 and T-8 were also analyzed and are presented along with those data for taxiway T-6 in Figure 26. The figure shows that there is very little difference in the results between taxiways T-2 and T-8 but the mean vertical velocity of taxiway T-6 is definitely greater than those of T-2 or T-8. The results seem to indicate the likelihood that vertical pavement velocity is a invariant pavement parameter. Further studies should be undertaken to examine this.

Load Cart Tests on Overlays

The same procedure used to find an equation to describe the deflections caused by the fire truck on T-6 was applied to the load cart/overlay data on T-2. The data were first separated according to overlay thicknesses and regression analysis was performed on equation 10. The results of these analyses are displayed in Table VI.

The multiple correlation coefficients in the table were judged to be unsatisfactory for the 6 and 8 inch overlays. Furthermore, there is an aberration in the A values (maximum pavement deflection); the maximum deflection for the 8 inch overlay is greater than that for the 6 inch overlays. This is contrary to all deflection theories and

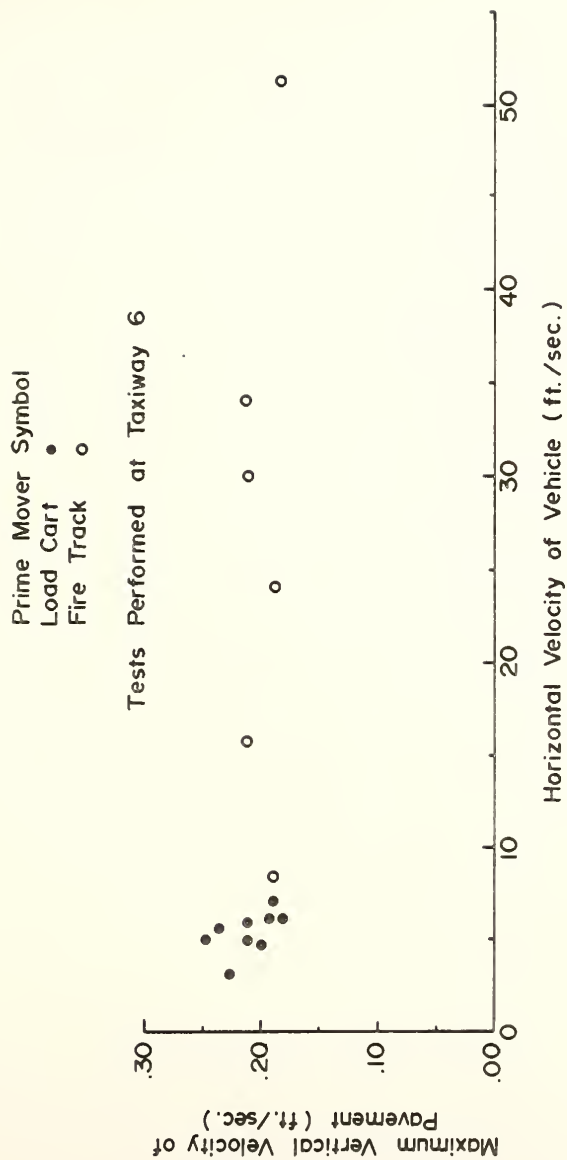


FIGURE 25 VERTICAL VELOCITY OF PAVEMENT AS A FUNCTION OF VEHICLE VELOCITY.

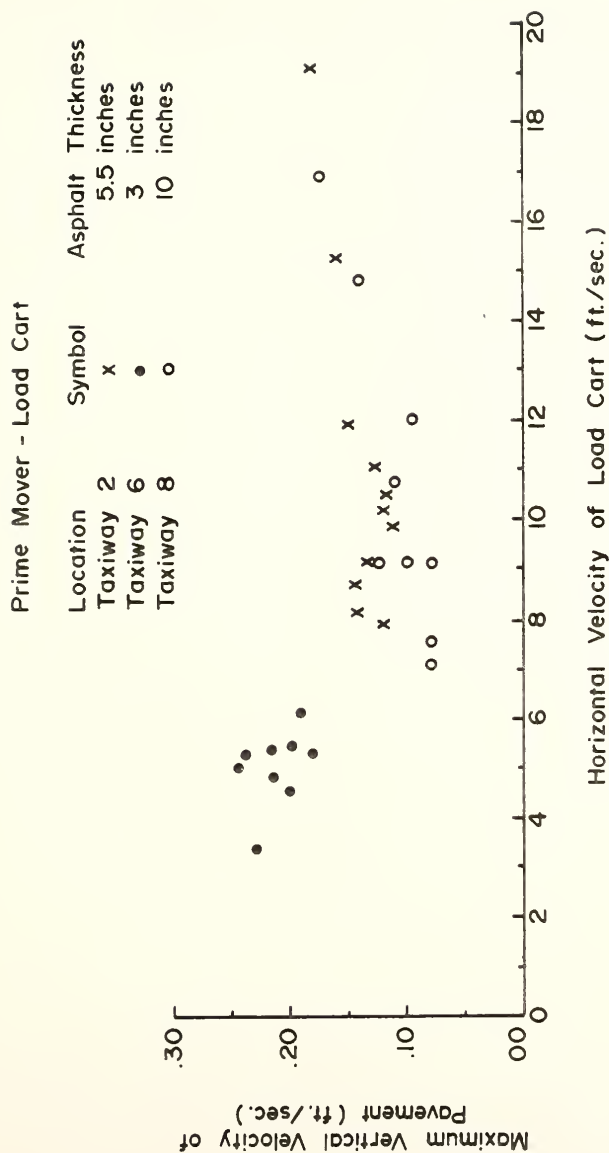


FIGURE 26 VERTICAL VELOCITY OF PAVEMENT AS A FUNCTION OF LOAD CART VELOCITY.

Table VI

RESULTS OF DATA ANALYSIS WHEN TEMPERATURE EFFECTS
WERE NOT CONSIDERED

Overlay Thickness (inches)	"A" Parameter (inches)	"B" Parameter (1/inches)	R^2	Temp. Range (°F)	Number of Data Sets
2	.03174	.001046	.9405	44°-59°	14
4	.02844	.000704	.9085	59°-70°	10
6	.02569	.000722	.8777	54°-70°	14
8	.02693	.000831	.7354	69°-79°	14

previous field observations. These results indicate that either the pavement was performing abnormally, undetected instrumentation failure occurred, or that a factor other than pavement thickness influenced the deflection measurements. The third possibility was investigated first. The pavement temperature ranges over which data for each overlay were collected are indicated in Table VI. Throughout the duration of the field test it was felt that as long as the tests were performed when the temperature of the pavement was above freezing and below 70°F, temperature would have an insignificant effect on load induced deflections. This belief was based on AASHO Road Test data (Reference 19). However, the likelihood that temperature did influence the test data was not discounted without first investigating the possibility. The data for each overlay were grouped according to temperatures and regression analysis was performed again. The results, tabularized in Table VII, show a marked increase in R^2 values and indicated that for a given temperature deflections decrease with increasing asphalt thickness. The R^2 values are understood to be only qualitative for such small sample sizes, but they are indicators of goodness of fit. The improvement of the fit of the model again indicates the common belief that temperature is an important variable even for fairly small temperature ranges.

Figure 27 shows graphically the effect of temperature on deflection for several asphalt thicknesses consistent with the aforementioned procedure for making these determinations. The curves indicate that temperature does not significantly influence load induced deflections between 45 and 60°F but that the range from 60 to at least 80°F is critical. The curve for the asphalt thickness of 13.5 inches appear to

Table VII

MAXIMUM DEFLECTION DATA FOR OVERLAYS

Overlay Thickness (inches)	Asphalt Thickness (inches)	Temperature of	Maximum Deflection(A) (inches)	B (1/inches ²)	R ² *	Number of Tests
0	5.5	59	.03705	.00088	.9498	28
2	7.5	44	.02824	.00112	.9637	2
2	7.5	57	.03166	.00087	.9385	6
2	7.5	60.5	.03251	.00010	.9466	6
4	9.5	59	.02753	.00055	.9742	2
4	9.5	65	.02924	.00075	.9216	4
4	9.5	70	.03428	.00030	.9048	4
6	11.5	54	.02239	.00046	.9454	2
6	11.5	58	.02328	.00053	.9394	2
6	11.5	60	.02418	.00059	.9344	4
6	11.5	69.5	.02963	.00062	.8882	6
8	13.5	69	.02358	.00071	.8542	6
8	13.5	76	.03703	.00500	.9561	2
8	13.5	78.5	.04044	.00535	.8591	6

*Model Fitted was $D(X) = Ae^{-BX^2}$

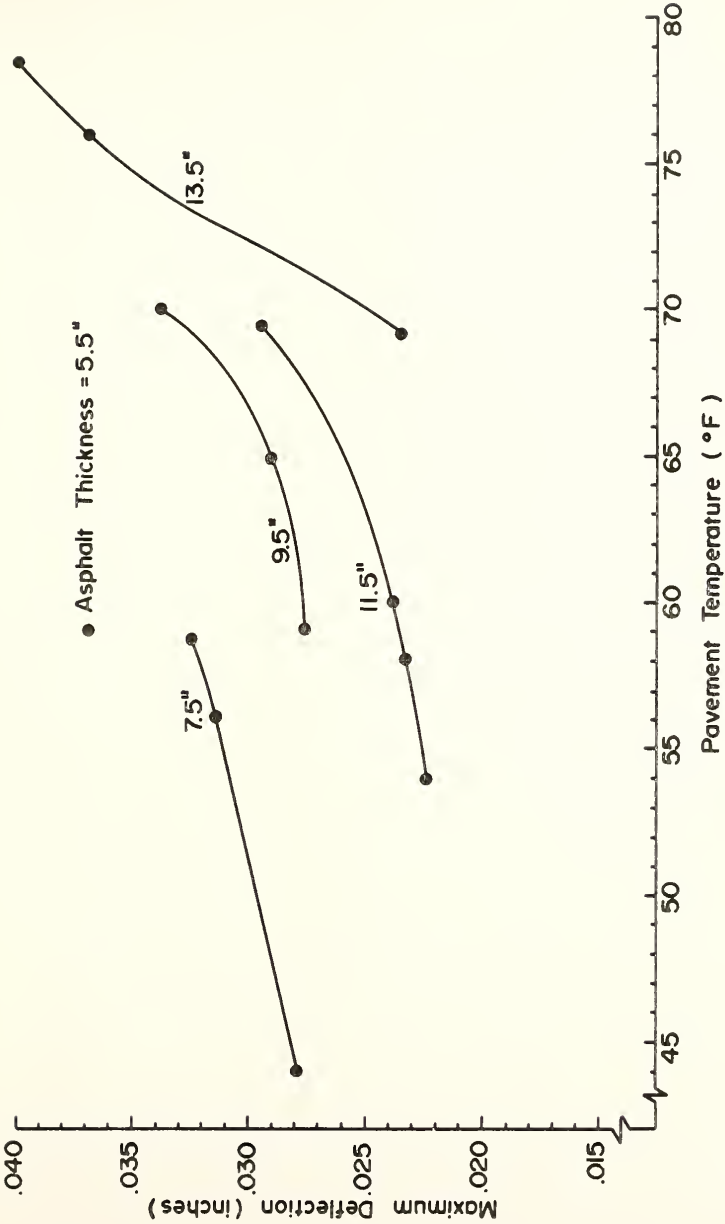


FIGURE 27 MAXIMUM DEFLECTION VS. PAVEMENT TEMPERATURE.

be leveling off at 80° indicating that the temperature effect is beginning to stabilize with respect to deflection.

Figure 28 was obtained from Figure 27 and shows that deflections vary nearly linearly with asphalt thickness over the range of asphalt thicknesses studied and for the same subgrade. Figure 29 is a similar plot but all three tests sites are included. Except for taxiway T-6 the data follow a linear relationship. Cracking is quite prevalent at T-6 and problems have been encountered at this location with the subgrade drainage. These reasons may account for the large deflections registered on this relatively thin (three inch asphalt thickness) taxiway.

The variation of the A and B parameters of the regression model (equation 10) with asphalt thickness is illustrated in Figure 30. B decreases with increasing asphalt thickness which indicates that the deflection basin tends to be wider for thicker pavements.

The Determination of Pavement Deflection Basins

Three dimensional deflection basins were obtained from deflection-time records by noting the position of the prime mover with respect to the LVDT's. This was accomplished by knowing the velocity of the prime mover and the time when it was directly adjacent to the line of instruments. For example, if the prime mover velocity were 5 ft./sec. and the time on the data record corresponding to the maximum deflection was 23 seconds, then the deflections of the instruments at 18 seconds were taken as the deflections of the pavement at a point 25 feet ahead of the moving prime mover. The deflections measured at 26 seconds were those 15 feet behind the prime mover. The only assumption involved in

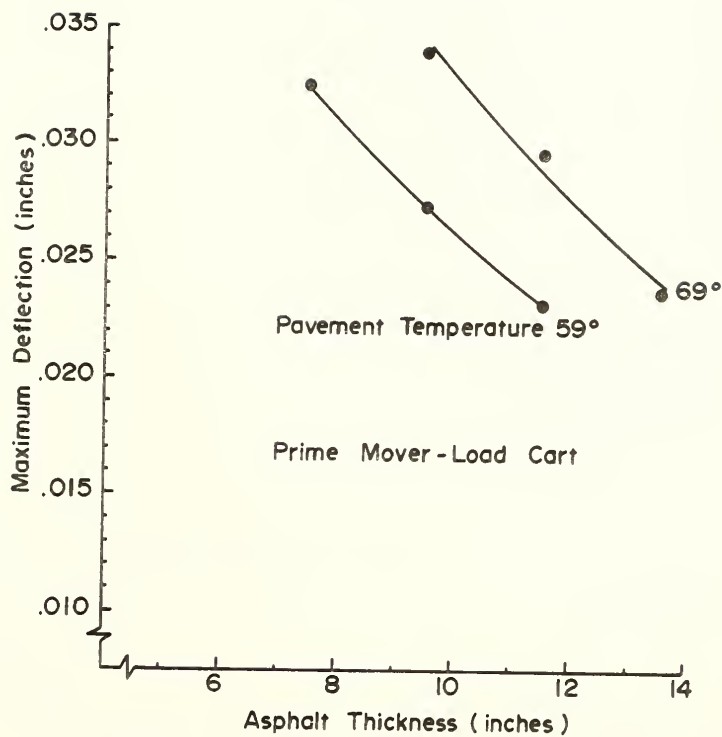


FIGURE 28 MAXIMUM DEFLECTION VS. ASPHALT THICKNESS.

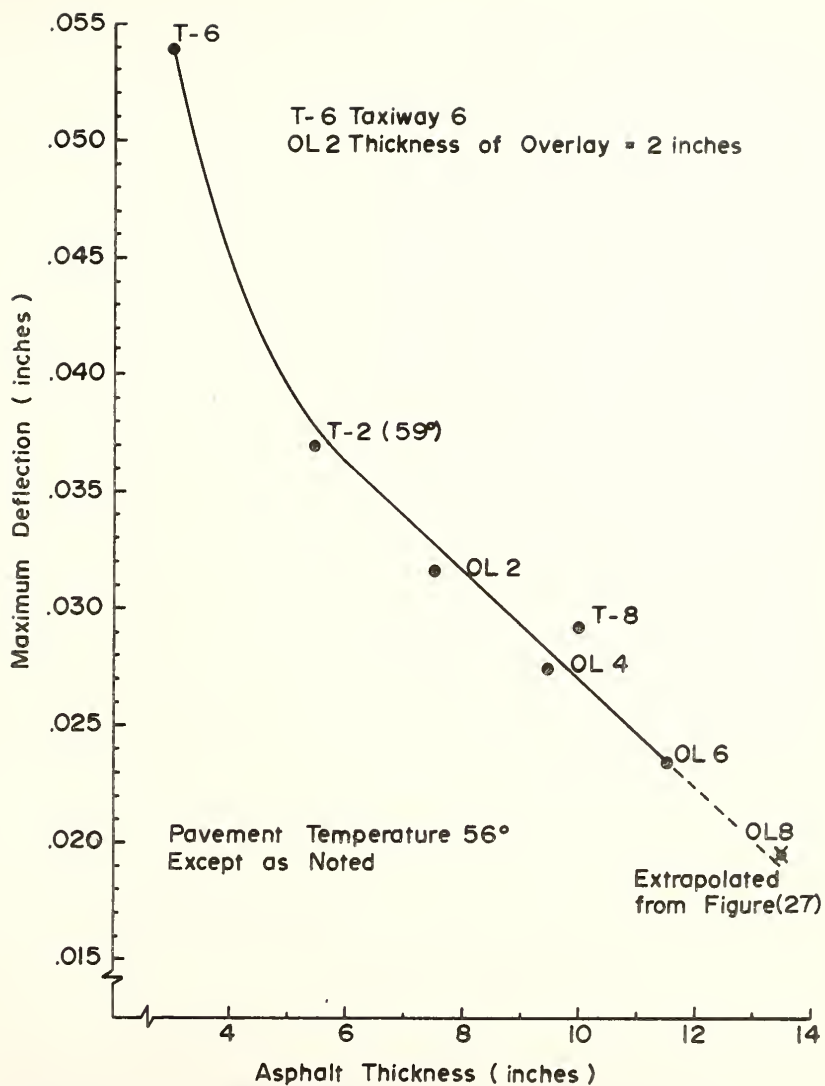


FIGURE 29 MAXIMUM DEFLECTION VS ASPHALT THICKNESS.

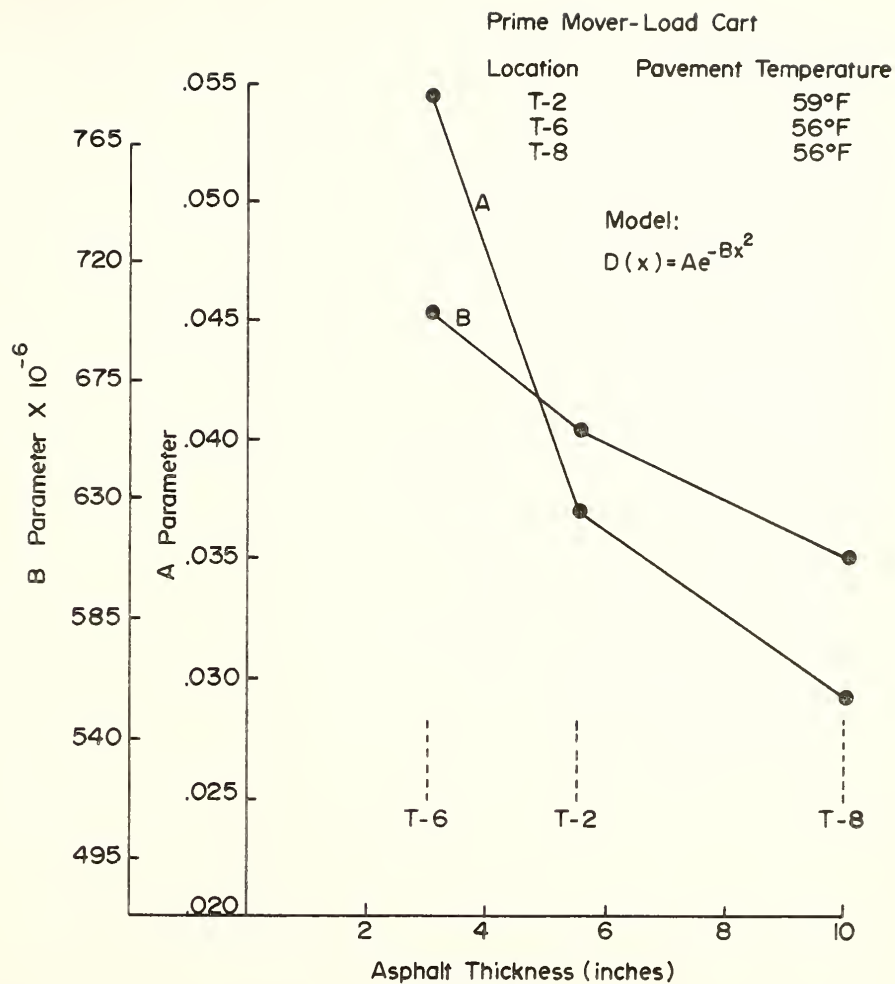


FIGURE 30 A AND B PARAMETERS VS. ASPHALT THICKNESS.

this method of determining the deflection basin was that the pavement system was homogeneous over the length and width of the deflection basin.

Program CONTUR (Ref. 80) in conjunction with a CALCOMP plotter was used to plot contour lines of the deflection basins displayed in Figures 31, 32, 33, and 34. Because the deflection basins are symmetrical about the points of load application, only half of each basin is illustrated in the figures. Examination of these figures indicates that:

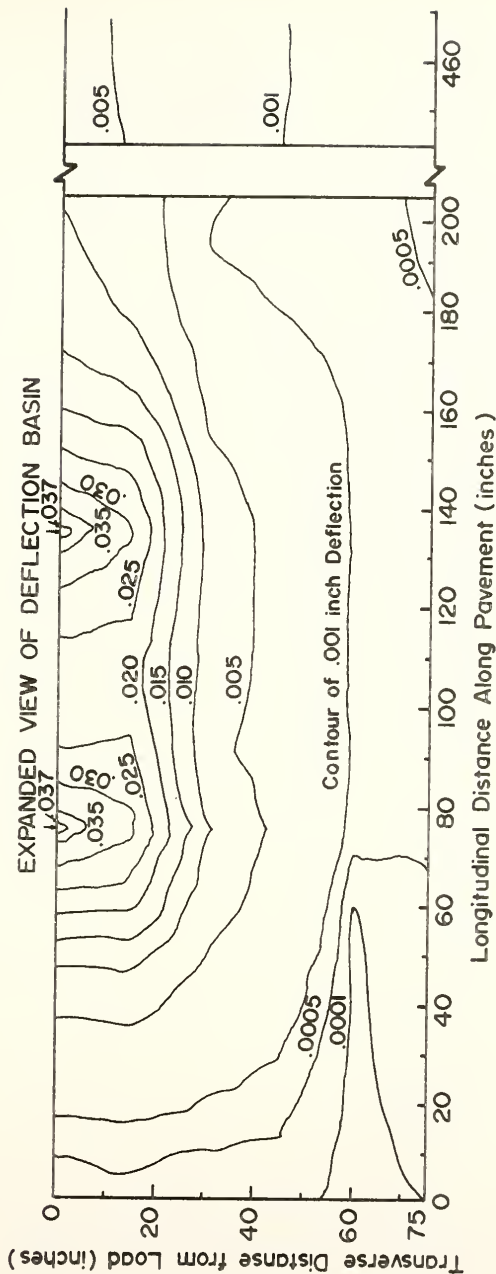
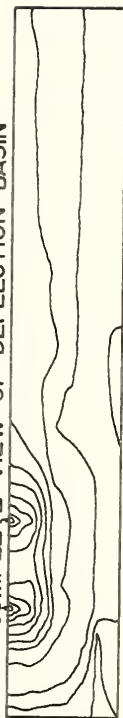
- (1) The deflection basin extends much farther behind the prime mover than it does in the direction of travel of the prime mover;
- (2) The pavement does not return to its original position immediately after the load has passed; the time lapse seems to be related to the magnitude of the deflection;
- (3) The curvature of the basin is highest in the vicinity of the load;
- (4) The width of the deflection basin is much smaller than its length.

Pavement System Reaction Coefficient

An attempt was made to define a parameter that would be independent of the magnitude and mode of loading and which would be representative of pertinent characteristics of the pavement system.

The pavement system was modelled as a series of springs, with spring constant S , which were connected by a thin membrane. The strain or potential energy in the linear elastic springs is then proportional to the square of the deflection at each point in the deflection basin. The energy basin is defined as the square of the deflection basin and has exactly the same shape as the deflection basins illustrated in

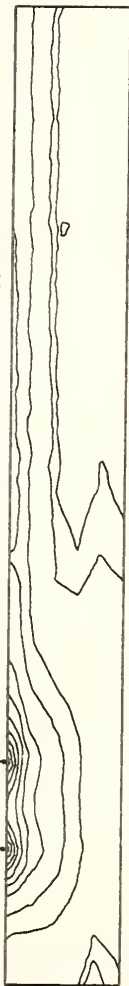
COMPLETE VIEW OF DEFLECTION BASIN



DIRECTION OF TRAVEL WAS RIGHT TO LEFT. PAVEMENT TEMPERATURE WAS 61°F. ARROWS INDICATE POINTS OF LOAD APPLICATION.

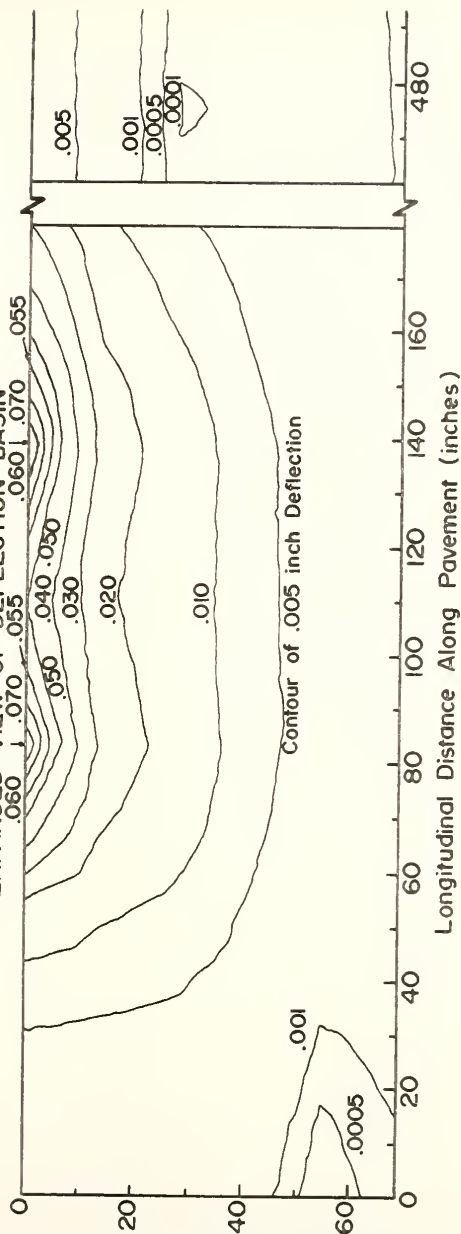
FIGURE 31 DEFLECTION BASIN FOR C-130 AIRCRAFT ON TAXIWAY 2. ASPHALT THICKNESS - 5.5 INCHES.

COMPLETE VIEW OF DEFLECTION BASIN



Transverse Distance from Load (inches)

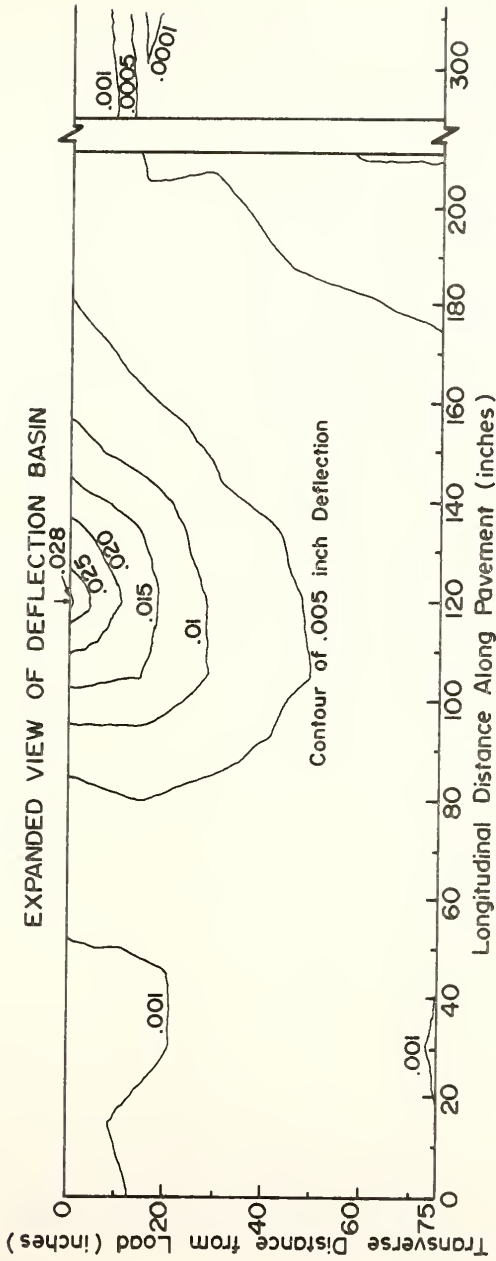
EXPANDED VIEW OF DEFLECTION BASIN



DIRECTION OF TRAVEL WAS RIGHT TO LEFT. PAVEMENT TEMPERATURE WAS 61°F. ARROWS INDICATE POINTS OF LOAD APPLICATION.

FIGURE 32 DEFLECTION BASIN FOR C-135 AIRCRAFT ON TAXIWAY 2. ASPHALT THICKNESS - 5.5 INCHES.

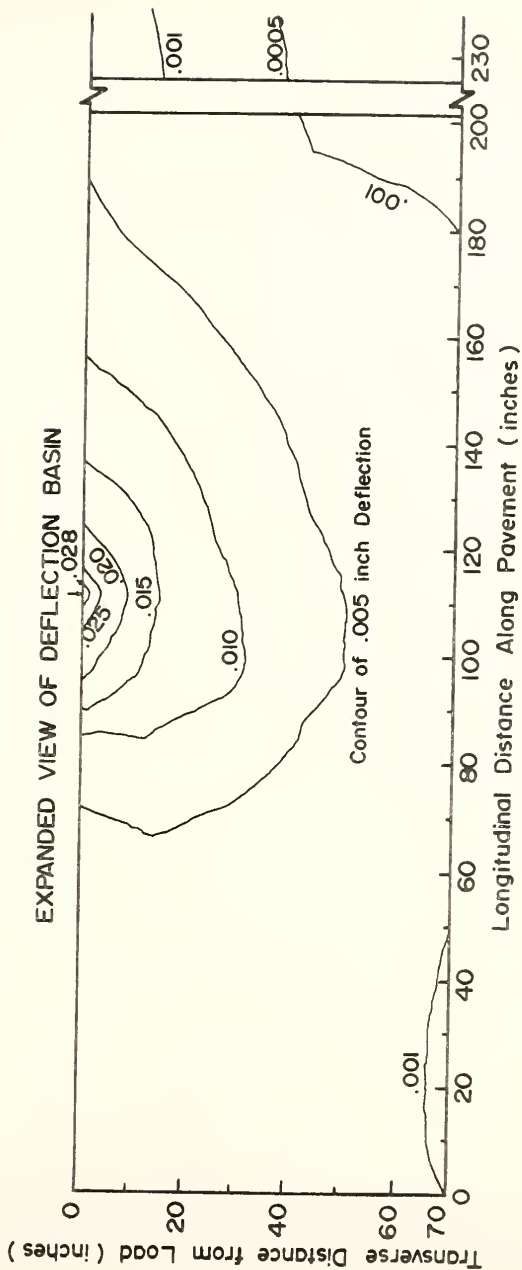
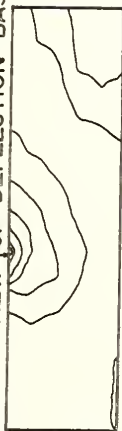
COMPLETE VIEW OF DEFLECTION BASIN



DIRECTION OF TRAVEL WAS RIGHT TO LEFT. PAVEMENT TEMPERATURE WAS 68°F. ARROWS INDICATE POINTS OF LOAD APPLICATION.

FIGURE 33 DEFLECTION BASIN FOR LOAD CART ON TAXIWAY 2. ASPHALT THICKNESS 11.5 INCHES.

COMPLETE VIEW OF DEFLECTION BASIN



DIRECTION OF TRAVEL WAS RIGHT TO LEFT. PAVEMENT TEMPERATURE WAS 72°F. ARROW INDICATE POINT OF LOAD APPLICATION.

FIGURE 34 DEFLECTION BASIN FOR LOAD CART ON TAXIWAY 2. ASPHALT THICKNESS 13.5 INCHES.

Figures 31-34; the contour line 1×10^{-2} inches in the deflection basin would be 1×10^{-4} inches squared in the energy basin. The pavement system reaction coefficient S is defined as

$$S = \frac{\text{Work done in deflecting the pavement}}{\text{Volume of the energy basin}} \quad (14)$$

or

$$S = \frac{\sum_{i=1}^n \frac{W_i \cdot d_i}{\int_{x_1}^{x_2} \int_{y_1}^{y_2} D^2(x,y) \, dx \, dy}} \quad (15)$$

where W_i is the weight supported by the i th wheel of an n wheel prime mover,

d_i is the deflection of the pavement under the i th wheel,

$D^2(x,y)$ is the square of the deflection D at point (x,y) of the deflection basin.

As the deflection will increase as W increases, an examination of equation 15 indicates that the work done to a pavement by a prime mover (vehicle or aircraft) is not only a function of the total weight of the prime mover but also of the manner in which its weight is transferred to the pavement. This emphasizes the fact that the energy imparted to a pavement by an aircraft is a function of its landing gear configuration.

Solving equation 15 dimensionally,

$$S = \frac{FL}{L^4} = FL^{-3} \quad (16)$$

it is seen that S has the same units as the modulus of subgrade reaction, k . S and k are similar parameters except that S takes into account the

surface course of the pavement system as well as subgrade characteristics.

Equation 15 was solved for 3 prime movers, the load cart and the C-130 and C-135 aircraft at the same test site, T-2, and for the load cart on each of the four overlays of T-2. The results are illustrated in Figure 35. It is seen that S increases with decreasing pavement temperature and with increasing asphalt thickness for the same subgrade conditions. If S were independent of magnitude and mode of loading, the C-135, the C-130, and the load cart should have identical values for the same pavement temperature at a given site.

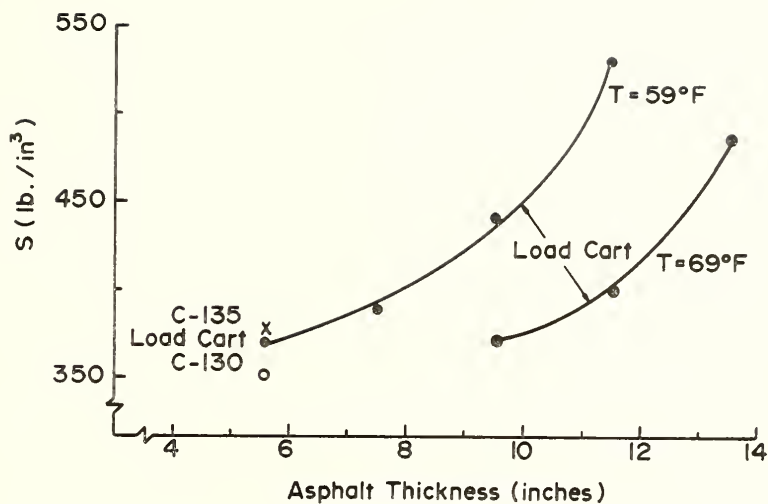


FIGURE 35 PAVEMENT SYSTEM REACTION COEFFICIENT AS A FUNCTION OF ASPHALT THICKNESS AND TEMPERATURE FOR THE SAME SUBGRADE CONDITIONS.

SECTION VIII

A CASE HISTORY AND A CASE FOR THE FUTURE

Introduction

This section has two primary purposes. The first is to synthesize some of the concepts developed in preceeding sections in order to illustrate how the working hypothesis can be applied. A case history is developed in which the service life of a pavement section is estimated based upon the volume of anticipated traffic. Data from the AASHO Road Test are used in the case history because, as was noted previously, the data record is much more complete than for airport pavements. However, there is every reason to believe that the same procedures could be applied to airport pavements once proper and sufficient data become available. The second purpose of this Section is to show how transfer function theory, as advanced by Harr and Boyer (Ref. 4), could be used to quantify a measure of the energy imparted to pavements by aircraft, thereby generating the information needed so that engineers can predict the performance of airport pavements and do so in a non-destructive manner.

Case History-Highway Overlays

Figure 36 indicates that the pavement deflection caused by a given load decreases approximately 10 percent for each additional inch of surface course thickness. Figure 10 shows that the energy level, as measured by cumulative deflections, corresponding to a given pavement

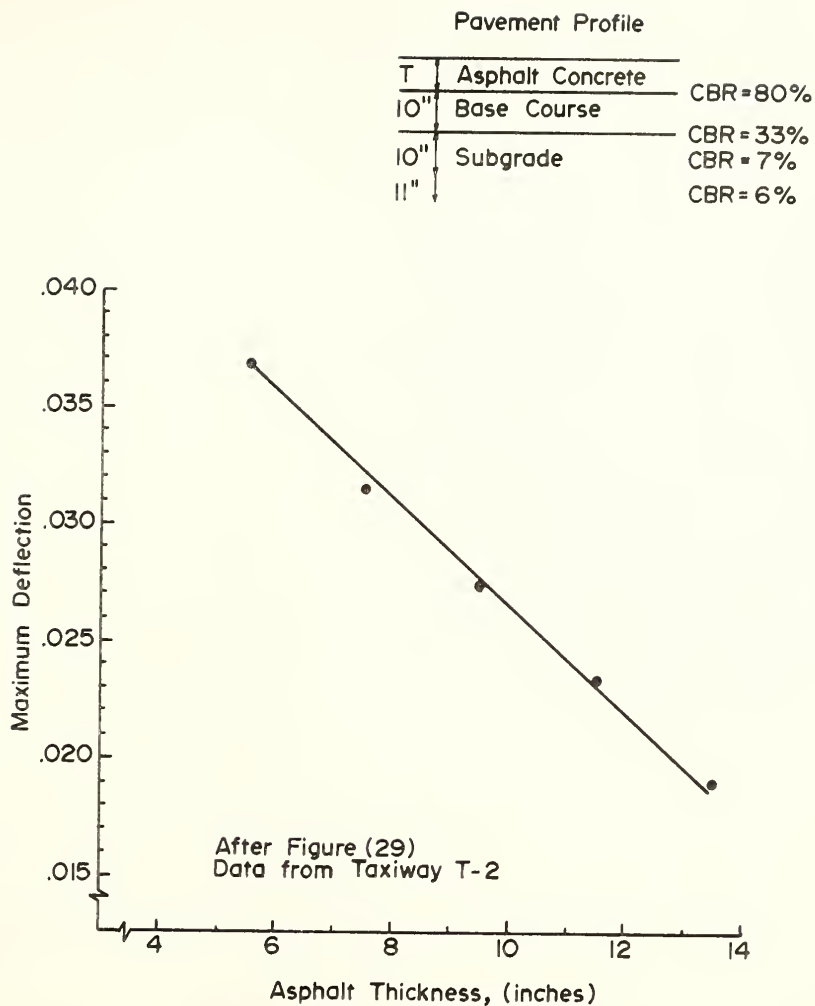


FIGURE 36 THE EFFECT OF SURFACE THICKNESS ON SURFACE DEFLECTION.

condition (PSI) increases as the surface course thickness increases. At a PSI value of 1.5 the pavement section with 4 inches of asphalt concrete has experienced 1200 feet of cumulative deflection, that with 5 inches 1800 feet and the section with 6 inches of surface course was able to accommodate 2700 feet before its condition deteriorated to a present serviceability index of 1.5. Thus the benefits accrued by overlays (thicker surface course) are twofold - more energy can be accommodated before failure occurs and the rate at which the energy is imparted to the pavement decreases as the asphalt thickness increases.

Having an estimate of the anticipated energy (traffic) that a given pavement will be required to accommodate, and having data of the type illustrated by Figures 10 and 36, predictions can be had of the service life of a given pavement design. This capability would provide for the programming of a rational plan for remedial action. For example, if a highway were constructed with 4 inches of asphalt concrete underlain by 9 inches of base and 16 inches of subbase material, which conformed to AASHO Road Test material and construction specifications, and the highway was expected to carry 1000 vehicles per day with each vehicle deflecting the pavement 0.015 inches; then, referring to Figure 10 the service life of the pavement would be:

$$\frac{1200}{\left(\frac{.015}{12}\right) 1000} = 961 \text{ days} = 2.6 \text{ years.}$$

If a 5 inches of surface course were used, the service life would then be:

$$\frac{1800}{\frac{(.015)(.9) 1000}{12}} = 1600 \text{ days} = 4.4 \text{ years.}$$

Figure 37 illustrates the effect of surface course thickness on the service life of the pavement.

When the pavement reaches the end of its service life, remedial measures must be taken if it is to continue to serve a functional purpose. One such remedial measure is to increase the asphalt thickness by the application of an overlay. If it is assumed that when an overlay is applied, the resulting pavement section has no memory of the energy applied to it by previous traffic, then the pavement would be completely rejuvenated and would again be in the infancy of its service life. The pavement engineer would then be able to anticipate impending failure and plan a maintenance program. Figure 38 is a schematic representation of such a schedule. The figure should be thought of as providing an upper bound of the benefits accrued from overlays because it illustrates the maximum performance that overlays could achieve.

It is doubtful that overlays would completely rejuvenate a pavement because after many vehicle passes the original pavement system acts in a nonconservative fashion. Energy is lost to the system and part of this energy loss is manifested by doing work to the pavement such as causing permanent deformations in the structure. It should be expected that even after an overlay is applied the pavement system would have a memory of previous traffic.

It was shown that overlays have a twofold effect - they increase the cumulative deflection at which a given condition occurs and they

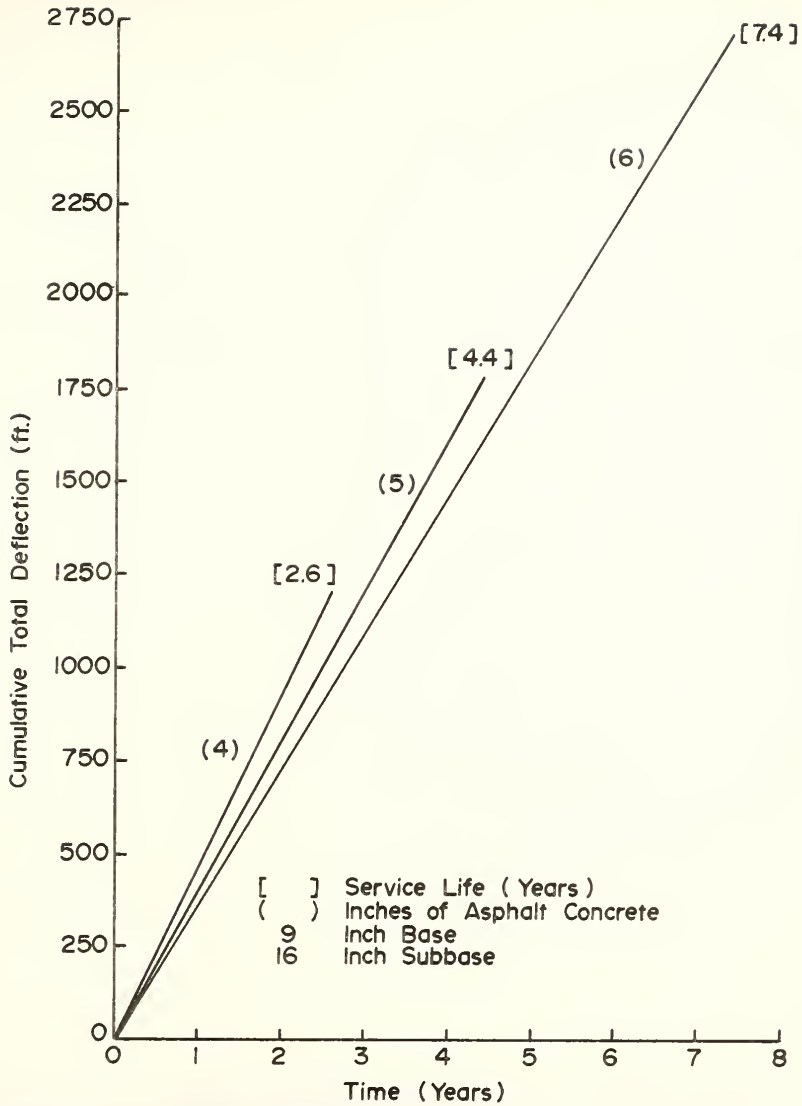


FIGURE 37 THE EFFECT OF SURFACE COURSE THICKNESS ON THE SERVICE LIFE OF A HIGHWAY PAVEMENT .

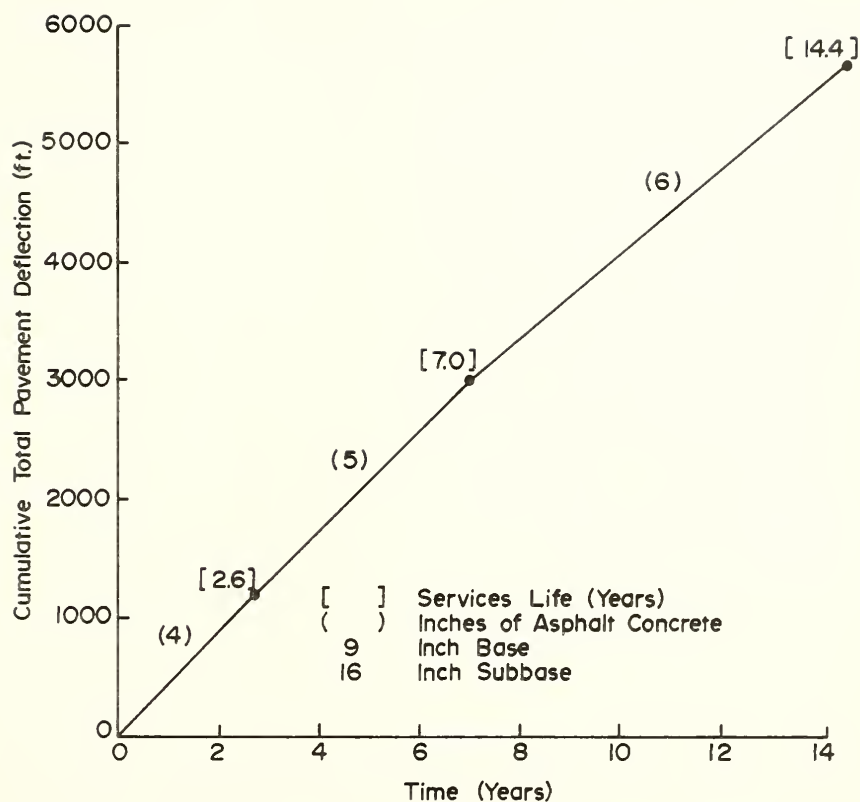


FIGURE 38 THE EFFECT OF OVERLAYS (UPPER BOUND, 100 % REJUVENATION).

decrease the rate at which the critical cumulative deflection is approached. If the first effect is ignored, then a lower bound of the benefit accrued from overlays could be quantified. For example, if an engineer designed a pavement section with 4 inches of asphalt concrete, 9 inches of base, and 16 inches of subbase all conforming to AASHTO Road Test material and construction specifications, he would expect the pavement to be in poor condition after experiencing 1200 feet of cumulative deflection. If he applied overlays when the cumulative deflection reached 800 feet, the extended pavement service life would be as depicted in Figure 39. The figure indicates that each inch of overlay would result in an extended service life of only 0.125 years. This development is believed to represent a lower bound because the assumed effect of the overlays here is only to diminish the rate at which failure (1200 feet of cumulative deflection) is attained.

Figures 38 and 39 illustrate upper and lower bounds, respectively, of the effect of overlays on pavement service life for the given example. Perhaps, a more reasonable approach to the problem of the effectiveness of overlays is to assume that an overlay does increase the cumulative deflection at which failure occurs but not to the extent of complete rejuvenation as was depicted in Figure 38. If 50% rejuvenation is assumed, the original 4 inch asphaltic concrete section will still fail when it experiences 1200 feet of cumulative deflection but an additional inch of overlay will increase the critical cumulative deflection by $1800 \times 50\% = 900$ feet. If another inch of overlay is applied when the critical cumulative deflection reaches 2100 feet, the cumulative deflection at failure for a 6 inch asphaltic

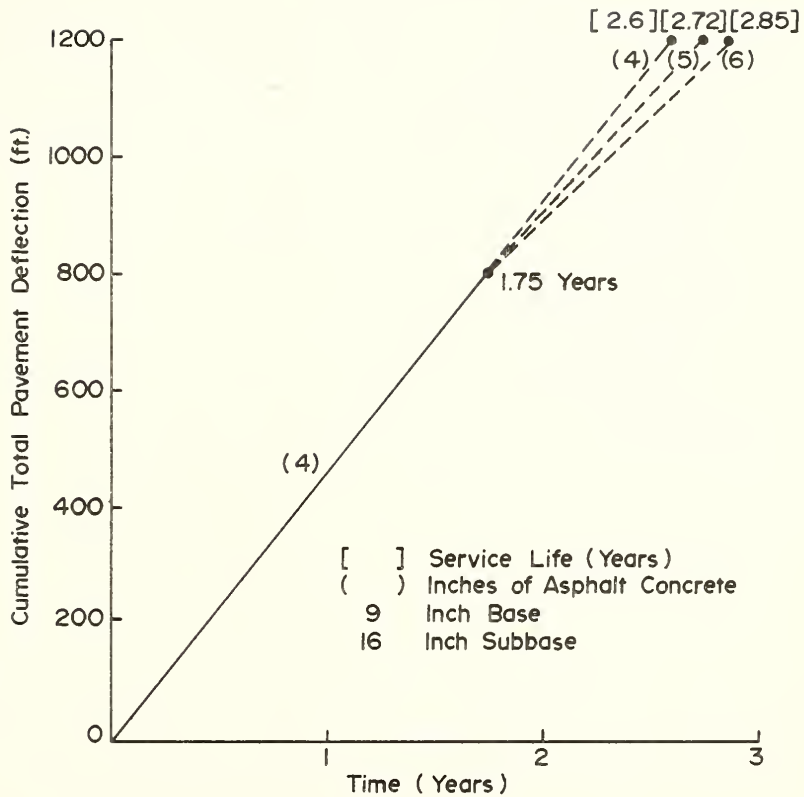


FIGURE 39 THE EFFECT OF OVERLAYS (LOWER BOUND ,
0 % REJUVENATION)

concrete section would be $1200 + 900 + 2700 \times 50\% = 3450$ feet.

Figure 40 illustrates a maintenance schedule for 50% rejuvenation.

Sample calculations for determining the pavement service life of overlays are illustrated in Figure 41. Similar procedures could have been applied to airport pavements had the required data been available. The following subsection describes a method whereby such information could be obtained quickly and in a non-destructive manner.

The Future--Transfer Functions and Energy Concepts

The steady-state energy trough depicted schematically for a symmetrically loaded vehicle in Figure 4 is central to the working hypothesis of the present research. It has been shown that the shape of the trough depends on characteristics of both the prime mover and the pavement. Thus in order to obtain a measure of the energy imparted to pavements by aircraft, it appears that it is necessary to measure the deflections caused by each aircraft in the Air Force inventory everywhere on all Air Force Bases. Moreover, since pavement characteristics which control the magnitude and attenuation of load imposed deflections change with time and environmental conditions it would appear that the deflection measurements would have to be obtained continuously. Since this is an impossible task, there is an obvious need for a procedure that would enable engineers to obtain the required deflection troughs quickly and non-destructively. In concept, such a procedure is available to the Profession today.

Harr and Boyer (Ref. 4) demonstrated that transfer function theory could be used to predict the surface pavement deflections

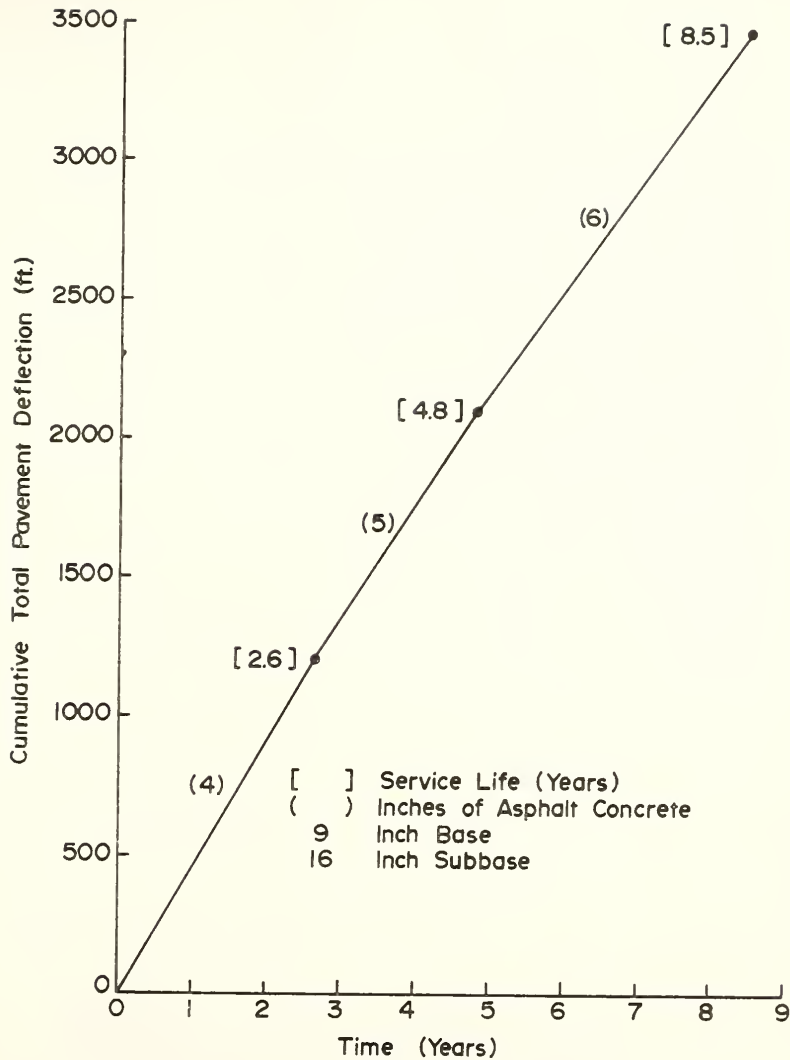


FIGURE 40 THE EFFECT OF OVERLAYS (50 % REJUVENATION).

From Figure 10

Inches of Asphalt	PSI	Cumulative Deflection
4	1.5	1200
5	1.5	1800
6	1.5	2700

Assumed Traffic: 1000 Vehicles/Day. Each Vehicle Deflects the 4 inch Asphalt Pavement 0.015 inches. Figure 36 indicates a 5 inch Asphalt Pavement would then be deflected $(0.015)(.9) = 0.0135$ inches; a 6 inch Asphalt Pavement would be deflected $(0.015)(.8) = 0.012$ inches.

A. Sample Calculation Figure 37

$$\frac{1200}{\frac{(.015)(1000)}{12}} = 961 \text{ days} = 2.6 \text{ years}$$

B. Sample Calculation Figure 39

$$\frac{800}{\frac{(.015)(1000)}{12}} = 640 \text{ days} = 1.75 \text{ years}$$

Additional service life for 1 inch overlay

$$\frac{1200-800}{\frac{(.0135)(1000)}{12}} = 355 \text{ days} = .97 \text{ years}$$

$$.97 + 1.75 = 2.72 \text{ years}$$

C. Sample Calculation Figure 40

$$\frac{1800 \times .5}{\frac{(.0135)(1000)}{12}} = 800 \text{ days} = 2.2 \text{ years}$$

$$2.6 + 2.2 = 4.8 \text{ years}$$

FIGURE 41 SAMPLE CALCULATIONS FOR THE
SERVICE LIFE OF OVERLAYS

operated by moving aircraft. As pointed out previously, a transfer function is a measure of relevant pavement parameters and thus the theory precludes the necessity of assuming a model to characterize the response behavior of a pavement. Furthermore, since pertinent pavement characteristics are included in transfer functions, temperature and trafficking effects will also be taken into account by the functions.

The authors were able to predict deflection basins for aircraft by the following procedure. They established one aircraft and one pavement section as "standard". Then signatures for each aircraft, defined as the maximum pavement deflection, were established at the standard site and at an additional site for the standard aircraft. Transfer functions were also found at the second site and a signature for the second aircraft at the additional site was determined by proportioning the signatures of the standard aircraft and the second aircraft at the standard site and multiplying this ratio by the standard's signature at the second site. This signature was then combined with the transfer functions to predict the deflection basin for the second aircraft at the second site.

The procedure predicted deflections quite well and can be extended so that the entire steady-state energy trough can be determined. This could be accomplished by establishing a standard prime mover with a built-in pavement deflection measuring system. This dynamic system could then travel down a runway or taxiway and continuously compile transfer functions while simultaneously determining its own energy trough. Following the same procedure as outlined above, the standard vehicle's energy trough could be combined with the signature of any

desired aircraft to obtain that aircraft's energy trough. Then, by simply maintaining accurate operational traffic records (such as found in Appendix I) an accurate measure of the load-induced cumulative energy imparted to airport pavements could be maintained. If this were done over a period of time an accurate correspondence between cumulative energy and airport pavement condition could be established. This would enable airport pavement engineers to predict the performance of their structures from an estimate of future traffic as well as to program preventative maintenance.

SECTION IX

SUMMARY

Section II reviewed the methods which are used to predict load induced deflections in pavement systems. Three of the theories used "a priori" models which require the engineer to assume a model that characterizes the behavior of the system and to determine parameters that fit the model. The fourth theory uses an "a posteriori" modelling technique to predict pavement deflections. It was pointed out that an advantage of transfer function theory is that it is capable of accommodating more material descriptors than are normally included in a priori models. Section II also discussed failure criteria applied to pavement systems at the present time and, in addition, presented a brief discussion of energy methods.

Section III modelled a pavement system as an elastic beam supported by a Winkler foundation to illustrate that the peak deflection induced in such a system by external loads is a measure of the energy introduced to the system by the loads. It was pointed out that as the dynamic loads that are imparted to pavements by aircraft are difficult to predict, a method of predicting pavement performance which does not require knowledge of the magnitude of the prime mover loads is urgently needed by the Profession today.

Because the Air Force does not compile deflection data that were needed to test the working hypothesis, Section IV used data gathered at the AASHO Road Test to validate the working hypothesis quantitatively. Regression analysis was used to determine a functional relationship

between the condition of a given pavement system and the cumulative total peak deflection it had experienced. It was found that increasing the asphalt thickness by 2 inches (from 4 to 6 inches) increased the cumulative total deflection at failure by 100 percent.

Airport traffic data and pavement condition information were used in Section V to show that there is a threshold cumulative total peak pavement deflection at which cracking occurs in asphalt concrete airfield pavements. An elastic layer analysis was used to predict deflections from the air base traffic records.

The Kirtland Field Test discussed in Section VII provided the following results:

(1) The deflected shape of a pavement in a direction perpendicular to the direction of travel of a prime mover can be described adequately by the equation

$$D(X) = Ae^{-BX^2}$$

where $D(X)$ is the deflection of the pavement x distance away from the load

- A is the maximum deflection which occurs under the load,
- B is a parameter that reflects characteristics of the pavement system. It was found to be sensitive to changes in pavement temperature and thickness.

(2) The maximum vertical velocity of a deflecting pavement surface occurs directly under the load and is independent of the speed and load characteristics of the prime mover causing the deflection. The maximum vertical velocity seems to be a function of the pavement system only.

(3) The maximum deflection of a pavement system created by a given prime mover increases rapidly when the pavement temperature reaches about 65°F. and seems to begin to stabilize at about 80°F.

(4) For a given pavement section, the maximum pavement deflection decreases about 10 percent for each additional inch of asphalt thickness.

(5) The curvature of a deflected pavement is highest in the vicinity of the load and seems to increase with increasing wheel load.

(6) Limited evidence was developed to show that there may exist a pavement system reaction coefficient defined as the ratio of the work done in deflecting a pavement to the volume of the energy basin. The coefficient was found to be independent of the loads induced by the prime mover. In addition, it seems to be more responsive to temperature changes in the pavement system than the subgrade modulus.

Section VIII presented a "case history" which illustrates how an estimate of anticipated load-induced deflection can be used when planning a highway maintenance program.

Finally, it is recommended that the agencies responsible for monitoring pavement condition begin to compile deflection data for airfield pavements so that the condition or performance trends of pavement can be predicted. It is suggested that the theory advanced by Harr and Boyer (Ref. 4) be applied so that accurate deflection data can be obtained easily and with a minimum of interruption to airfield operations.

SECTION X

CONCLUSIONS

The objective of this research effort was to verify the following working hypothesis:

There is a functional relationship between the cumulative energy as measured by cumulative peak deflections imparted to a given pavement system and the condition of that system.

On the basis of experience and the results of this investigation the hypothesis appears to be valid. In addition, as a result of this research, the following conclusions seem to be warranted:

- (1) The pavement deflections which occur under the wheels of a prime mover are a measure of the work done to the pavement system by the prime mover.
- (2) The condition of a highway pavement can be predicted within reasonable limits from knowledge of the thickness of its constitutive layers and the amount of load induced deflection it has been subjected to.
- (3) There is a threshold cumulative total peak pavement deflection at which cracking occurs in asphaltic concrete airfield pavements. It is not unreasonable to presume that the condition of an airfield pavement can be correlated with the cumulative total peak pavement deflection it has undergone.
- (4) The effects of an increase in asphalt surface thickness - an overlay - are twofold: the pavement deflection caused by a given load decreases (approximately ten percent for the information available for each additional inch of surface

course thickness); and, the cumulative total peak pavement deflection corresponding to a given pavement condition increases with increasing surface course thickness.

- (5) The application of the working hypothesis provides a means for planning programs of pavement maintenance for both airfield and highway systems.

SECTION XI

RECOMMENDATIONS FOR FUTURE RESEARCH

Harr and Boyer (Ref. 4) advanced the state of the art by developing a procedure whereby the surface deflections created by a prime mover can be predicted accurately. The present research showed that such deflections are a measure of the energy imparted to pavement systems by prime movers (ground vehicles and aircraft). These two developments point out the need for a vehicle which can provide a measure of the transfer functions quickly and with a minimum of interruption to operational traffic. Such a vehicle should be one which is common to most air bases (such as a fire truck) or one which can be transported from airfield to airfield easily. The transfer functions obtained by such a vehicle could then be convoluted with known signatures of aircraft. Then, by keeping operational traffic records at airbases, a compilation of the cumulative energy imparted to airfields could be maintained. This procedure should provide

- (1) a rapid and non-destructive airfield pavement evaluation system,
- (2) a rational method for predicting when remedial measures should be carried out at a given airfield,
- (3) insight into the direction to be taken in upgrading existing pavements so as to accommodate new and future aircraft,
- (4) a better understanding of the effects of aircraft gear.

Any efforts undertaken to implement the above steps are recommended for future research.

BIBLIOGRAPHY

BIBLIOGRAPHY

1. Robinson, K. G., Future Generation of Aircraft, The Boeing Company, 1969.
2. "Deteriorating Airport Pavements Spur Efforts to Head Off Crisis," Engineering News Record, 4 November 1971.
3. Parsons, W. E., Economics of Aircraft vs. Cost of Airport Development, Available as Paper 5635, Douglas Aircraft Company, McDonnell Douglas Corporation, 1969.
4. Harr, M. E., Boyer, R. E., Predicting Pavement Performance Using Time-Dependent Transfer Functions, Draft Report submitted to the Air Force Weapons Laboratory, Kirtland Air Force Base, New Mexico, August 1972.
5. Boyer, R. E., Predicting Pavement Performance Using Time-Dependent Transfer Functions, Ph.D. Thesis, Purdue University, August 1972.
6. Winkler, E., Die Lehre von der Elasticitaet and Festigkeit, Dominicus, Prague, 1867.
7. Zimmermann, H., Die Berechnung des Eisenbahnoberbaues, Berlin, 1888.
8. Hayashi, K., Theorie des Tragers auf Elastischer Unterlage, J. Springer, Berlin, 1921.
9. Florin, V. A., Raschety Osnovani Gidrotekhnicheskikh Sooruzhenii, Stroiizdat, 1948.
10. Westergaard, H. M., "Stresses in Concrete Pavements Computed by Theoretical Analysis," Journal of Public Roads, Vol. 7, No. 2, 1926.
11. Westergaard, H. M., "New Formulas for Stresses in Concrete Pavements of Airfields," Proceedings of the American Society of Civil Engineers, Vol. 73, 1947.
12. Yoder, E. J., Principles of Pavement Design, Wiley, New York, 1959.
13. Timoshenko, S., Strength of Materials - Part II, Second Edition, D. Van Nostrand Company, New York, 1941.
14. Hetenyi, M., Beams on Elastic Foundations, The University of Michigan Press, Ann Arbor, 1946.

15. Harr, M. E., Leonards, G. A., "Analysis of Concrete Slabs on Ground," Journal of the Soil Mechanics and Foundations Division, Proceedings of the American Society of Civil Engineers, Vol. 85, No. SM3, June, 1959.
16. Terzaghi, K., "Evaluation of Coefficients of Subgrade Reaction", Geotechnique, Vol. 5, No. 4, December, 1955.
17. Vesic, A. S., Saxena, S. K., Analysis of Structural Behavior of AASHO Road Test Rigid Pavements, National Cooperative Highway Research Program, Report 97, 1970.
18. Finn, F. N., "Asphalt Institute Discussion", Conference on the AASHO Road Test, Highway Research Board, Special Report 73, 1962.
19. The AASHO Road Test, Report 5, Pavement Research, Highway Research Board, Special Report 61E, 1962.
20. Sebastyan, G. Y., "Flexible Airport Pavement Design and Performance", Proceedings of the Second International Conference on the Structural Design of Asphalt Pavements, University of Michigan, Ann Arbor, 1968.
21. Biot, M. A., "Bending of an Infinite Beam on an Elastic Foundation," Journal of Applied Mechanics, Transactions of the American Society of Mechanical Engineers, Vol. 59, 1937.
22. Hogg, A. H. A., "Equilibrium of a Thin Plate, Symmetrically Loaded, Resting on an Elastic Foundation of Infinite Depth," Philosophical Magazine, Vol. 25, 1938.
23. Burmister, D. M., "The Theory of Stresses and Displacements in Layered Systems and Applications to the Design of Airport Runways", Proceedings of the Highway Research Board, Vol. 23, 1943.
24. Burmister, D. M., "The General Theory of Stresses and Displacements in Layered Soil Systems," Journal of Applied Physics, Vol. 16, 1945.
25. Burmister, D. M., "Evaluation of Pavement Systems of the WASHO Road Test by Layered System: Methods," Highway Research Board, Bulletin 177, 1958.
26. Fox, L., "Computation of Traffic Stresses in a Simple Road Structure," Proceedings of the Second International Conference on Soil Mechanics and Foundation Engineering, Vol. 2, Rotterdam, 1948.

27. Acum, W.E.A., Fox, L., "Computation of Load Stresses in a Three Layer Elastic System", *Geotechnique*, Vol. 2, No. 4, 1950.
28. Jones, A., "Tables of Stresses in Three-Layer Elastic Systems", Highway Research Board, Bulletin 342, 1962.
29. Peattie, K. R., "Stress and Strain Factors for Three-Layer Elastic Systems", Highway Research Board, Bulletin 342, 1962.
30. Barksdale, R. D., Leonards, G. A., "Predicting Performance of Bituminous Surfaced Pavements", Proceedings of the Second International Conference on the Structural Design of Asphalt Pavements, University of Michigan, Ann Arbor, 1968.
31. Dehlen, G. L., Monismith, C. L., "Effect of Nonlinear Material Response on the Behavior of Pavements Under Traffic," Highway Research Board, Record No. 310, 1970.
32. Klomp, A. J. G., Niesman, Tn. W., "Observed and Calculated Strains at Various Depths in Asphalt Pavements", Proceedings of the Second International Conference on the Structural Design of Asphalt Pavements, University of Michigan, Ann Arbor, 1968.
33. Nijboer, L. W., Delcour, J., "Testing Flexible Pavements Under Normal Traffic Loadings by Means of Measuring Some Physical Quantities Related to Design Theories," Proceedings of the Second International Conference on the Structural Design of Asphalt Pavements, University of Michigan, Ann Arbor, 1968.
34. Seed, H. B., Chan, C. K., Lee, C. E., "Resilient Characteristics of Subgrade Soils and Their Relation to Fatigue Failures in Asphalt Pavements", Proceedings of the International Conference on the Structural Design of Asphalt Pavements, University of Michigan, Ann Arbor, 1963.
35. Larew, H. G., Leonards, G. A., "A Strength Criterion for Repeated Loads", Proceedings of the Highway Research Board, Vol. 41, 1962.
36. Geldmacher, R. C., Anderson, R. L., Dunkin, J. W., Partridge, G. R., Harr, M. E., Wood, L. E., "Subgrade Support Characteristics as Indicated by Measurements of Deflection and Strain", Proceedings of the Highway Research Board, Vol. 36, 1957.
37. Lee, E. H., "Viscoelastic Stress Analysis," Proceedings of the First Symposium on Naval Structural Mechanics, Pergamon Press, New York, 1960.
38. Biot, M. A., "Dynamics of Viscoelastic Anisotropic Media," Proceedings of the Fourth Midwestern Conference on Solid Mechanics, 1955.

39. Van der Poel, C., "A General System: Describing the Viscoelastic Properties of Bitumens and its Relation to Routine Test Data," Journal of Applied Chemistry, May, 1954.
40. Brown, A. B., Sparks, J. W., "Viscoelastic Properties of a Penetration Grade Paving Asphalt at Winter Temperature," Proceedings of the Association of Asphalt Paving Technologists, Vol. 27, 1958.
41. Kuhn, S. H., Rigden, P. J., "Measurement of Viscoelastic Properties of Bitumens Under Dynamic Loadings," Proceedings of the Highway Research Board, Vol. 38, 1959.
42. Brodnyan, J. G., "Use of Rheological and Other Data in Asphalt Engineering Problems", Highway Research Board, Bulletin No. 192, 1958.
43. Mack, C., "Deformation Mechanisms and Bearing Strength of Bituminous Pavements", Proceedings of the Highway Research Board, Vol. 33, 1954.
44. Mack, C., "Bearing Strength Determination on Bituminous Pavements by the Methods of Constant Rate of Loading or Deformation", Proceedings of the Highway Research Board, Vol. 36, 1957.
45. Wood, L. E., Goetz, W. H., "Rheological Characteristics of a Sand-Asphalt Mixture", Proceedings of the Association of Asphalt Paving Technologists, Vol. 28, 1959.
46. Pister, K. S., Monismith, C. L., "Analysis of Viscoelastic Flexible Pavements", Highway Research Board, Bulletin No. 269, 1960.
47. Harr, M. E., "Influence of Vehicle Speed on Pavement Deflection", Proceedings of the Highway Research Board, Volume 41, 1962.
48. Monismith, C. L., Secor, K. E., "Viscoelastic Behavior of Asphalt Concrete Pavements", Proceedings of the International Conference on the Structural Design of Asphalt Pavements, University of Michigan, Ann Arbor, 1963.
49. Pister, K. S., Westmann, R. A., "Analysis of Viscoelastic Pavements Subjected to Moving Loads," Proceedings of the International Conference on the Structural Design of Asphalt Pavements, University of Michigan, Ann Arbor, 1963.
50. Perloff, W. H., Moavenzadeh, F., "Deflection of Viscoelastic Medium Due to a Moving Load," Proceedings of the Second International Conference on the Structural Design of Asphalt Pavements, University of Michigan, Ann Arbor, 1968.

51. Tsien, H. S., Engineering Cybernetics, McGraw-Hill Book Company Inc., New York, 1954.
52. Crafton, P. A., Shock and Vibration in Linear Systems, Harper and Brothers, Inc., New York, 1961.
53. Raven, F. H., Automatic Control Engineering, McGraw-Hill Book Company, New York, 1968.
54. Senaut, C. J., Jr., Control System Design, McGraw-Hill Book Company Inc., New York, 1968.
55. Swami, S. A., Goetz, W. H., Harr, M. E., "Time and Load Independent Properties of Bituminous Mixtures", Highway Research Board, Record No. 313, 1970.
56. Ali, G. A., A Laboratory Investigation of the Application of Transfer Functions to Flexible Pavements, Ph.D. Thesis, Purdue University, August 1972.
57. Tse, F. S., Morse, I. E., Hinkle, R. T., Mechanical Vibrations, Allyn and Bacon, Boston, 1963.
58. Rogers, G. L., Causey, M. L., Mechanics of Engineering Structures, John Wiley and Sons, 1962.
59. Moore, R. K., Kennedy, T. W., "Tensile Behavior of Asphalt-Treated Materials Under Repetitive Loading," Proceedings of the Third International Conference on the Structural Design of Asphalt Pavements, Grosvenor House, London, University of Michigan, Ann Arbor, 1972.
60. Pell, P. S., Brown, S. F., "The Characteristics of Materials for the Design of Flexible Pavement Structures," Proceedings of The Third International Conference on the Structural Design of Asphalt Pavements, Grosvenor House, London, University of Michigan, Ann Arbor, 1972.
61. Van Dijk, W., Moreaud, H., Quedeveille, A., Uge, P., "The Fatigue of Bitumen and Bituminous Mixes", Proceedings of the Third International Conference on the Structural Design of Asphalt Pavements, Grosvenor House, London, University of Michigan, Ann Arbor, 1972.
62. Chomton, C., Valayer, P. J., "Applied Rheology of Asphalt Mixes- Practical Application," Proceedings of the Third International Conference on the Structural Design of Asphalt Pavements, Grosvenor House, London, University of Michigan, Ann Arbor, 1972.
63. Kasianchuk, D. A., Fatigue Considerations in the Design of Asphalt Concrete Pavements, Ph.D. Thesis, University of California, Berkeley, 1968.

64. Sebastyan, G. Y., "Pavement Deflection and Rebound Measurement and Their Application to Pavement Design and Evaluation", Proceedings of the Association of Asphalt Paving Technologists, Vol. 31, 1962.
65. Bulman, J. N., Strengthening of Flexible Roads in the Tropics: The Use of Deflection Measurements, Transport and Road Research Laboratory Report LR444, 1972.
66. Asphalt Overlays and Pavement Rehabilitation, The Asphalt Institute, Manual Series No. 17 (MS-17), November 1969.
67. Ahlvin, R. G., "Developments in Pavement Design in the U.S.A. - Flexible Pavements", Proceedings of the Aircraft Pavement Design Symposium, The Institution of Civil Engineers, London, 1971.
68. Houbolt, J. C., "Runway Roughness Studies in the Aeronautical Field", Journal of the Air Transport Division, American Society of Civil Engineers, Vol. 87, No. AT1, 1961.
69. Newark Airport Redevelopment: The Pavement Story, The Port of New York Authority, May 1969.
70. Hall, A. W., Kopelson, S., "The Location and Simulated Repair of Rough Areas of a Given Runway by an Analytical Method," NASA Technical Note D-1486, 1962.
71. Foxworth, T. G., Marthinsen, H. F., "Another Look at Accelerate-Stop Criteria", AIAA Paper No. 69-772, July, 1969.
72. Carey, W. N., Jr., Irick, P. E., "The Pavement-Serviceability Performance Concept," Highway Research Board, Bulletin No. 250, 1960.
73. Wignot, J. E., Durup, P. C., Wittlin, G., Scott, R. B., Gamon, M. A., Aircraft Dynamic Wheel Load Effects on Airport Pavements, Federal Aviation Administration Report No. FAA-RD-70-19, 1970.
74. Barksdale, R. D., Elastic and Viscoelastic Analysis of Layered Pavement Systems, Ph.D. Thesis, Purdue University, June 1966.
75. Wiseman, J. F., Harr, M. E., Leonards, G. A., "Warping Stresses and Deflections in Concrete Pavements: Part II," Proceedings of the Highway Research Board, Vol. 39, 1960.
76. Local Climatological Data, Annual Summary with Comparative Data, U. S. Dept. of Commerce, National Oceanic and Atmospheric Administration, Environmental Data Service, 1971.
77. Corps of Engineer, Study of Channelized Traffic, Waterways Experiment Station Technical Memorandum 3-426, February 1956.

78. Horonjeff, R., Jones, J. H., "The Effect of Traffic on the Cross Section of a Runway Pavement", Transactions of the American Society of Civil Engineers, Vol. 122, 1957.
79. Dixon, W. J., Massey, F. J., Jr., Introduction to Statistical Analysis, Third Edition, McGraw-Hill Book Company, 1969.
80. Turner, A. K., The GCARS System Fortran IV Programmers Manual Part C - Programs for Contour Mapping, Joint Highway Research Project Report No. 27, Purdue University, 1969.

APPENDIX 1

THEORY OF THE EARTH AND ITS HISTORY

THEORY OF THE EARTH AND ITS HISTORY

The theory of the earth and its history is a branch of geology which deals with the origin and development of the earth and its various parts.

The theory of the earth and its history is a branch of geology which deals with the origin and development of the earth and its various parts.

The theory of the earth and its history is a branch of geology which deals with the origin and development of the earth and its various parts.

The theory of the earth and its history is a branch of geology which deals with the origin and development of the earth and its various parts.

The theory of the earth and its history is a branch of geology which deals with the origin and development of the earth and its various parts.

The theory of the earth and its history is a branch of geology which deals with the origin and development of the earth and its various parts.

The theory of the earth and its history is a branch of geology which deals with the origin and development of the earth and its various parts.

The theory of the earth and its history is a branch of geology which deals with the origin and development of the earth and its various parts.

The theory of the earth and its history is a branch of geology which deals with the origin and development of the earth and its various parts.

APPENDICES

The theory of the earth and its history is a branch of geology which deals with the origin and development of the earth and its various parts.

The theory of the earth and its history is a branch of geology which deals with the origin and development of the earth and its various parts.

The theory of the earth and its history is a branch of geology which deals with the origin and development of the earth and its various parts.

The theory of the earth and its history is a branch of geology which deals with the origin and development of the earth and its various parts.

APPENDIX I

TRAFFIC AND CONSTRUCTION HISTORIES OF
SELECTED AIR FORCE BASES

The Air Force does not compile traffic data for all its bases. However, for some selected bases, the number of operations (landings and takeoffs) for each type of aircraft have been recorded. Traffic data from four of these bases are presented in this appendix along with abbreviated construction histories and pavement condition information for two of the bases. Construction histories for the two bases having flexible pavements (Pease and Castle) were available; those having rigid pavements (Dyess and Minot) were not. Traffic data for the latter two bases are presented for future references. The data are presented in tabular form by aircraft type where available; otherwise a range of aircraft weights is given. The bases were chosen with two criteria in mind - longevity of the traffic data record and, varied geographic locations within the continental U. S. (see Figure 42).

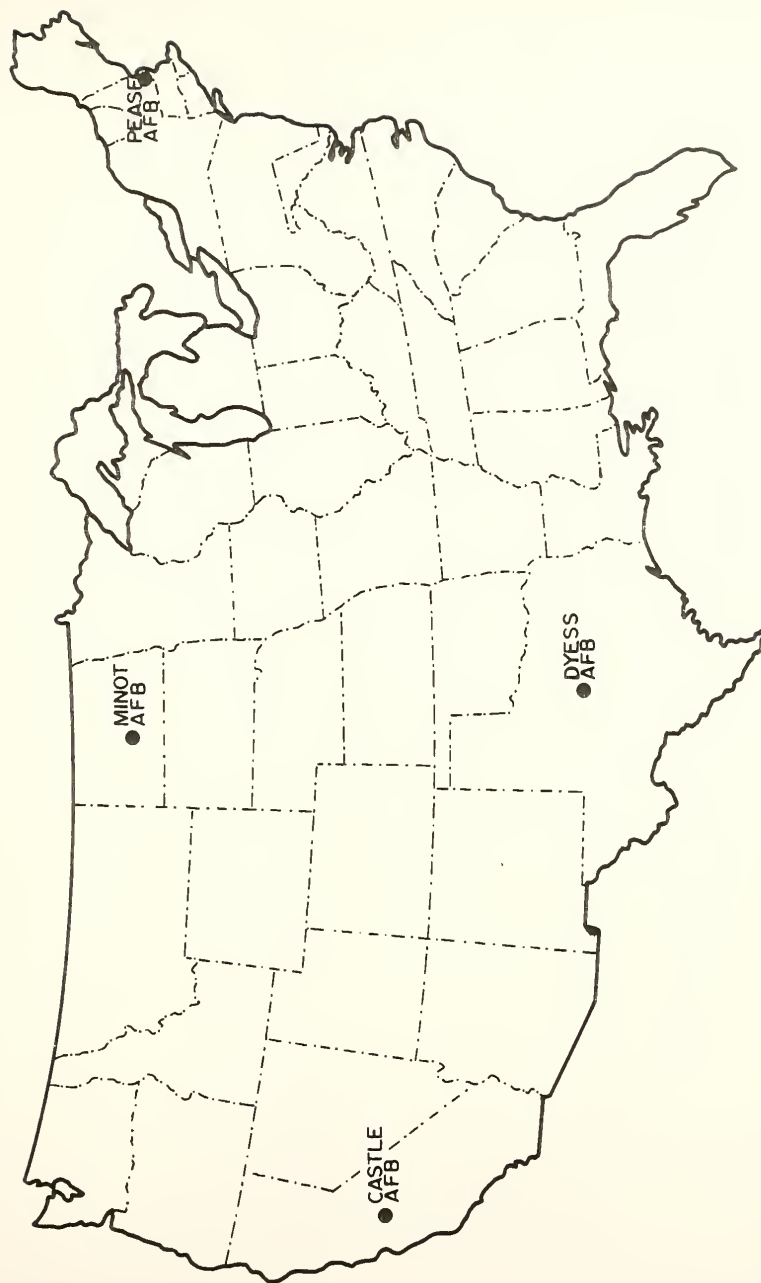


FIGURE 42 LOCATION OF SELECTED AIR FORCE BASES AT WHICH TRAFFIC DATA WERE ANALYZED.

Table VIII

ABBREVIATED CONSTRUCTION HISTORY, PEASE AFB, NEW HAMPSHIRE

Designation	Foundation Material		Pavement		Construction	
	Thickness	Type	Classification	Thickness	Type	Remarks
NW-SE Runway	8	Base	Sand (SW-SM)	4	AC	Original Construction
	26	Subbase	Sand (SP-SM)			
		Subgrade	Sand (SM)			

Comments: (1) The runway was in very good condition in 1964.

(2) A seal coat was applied in 1968.

(3) Cracking had developed and was extensive by 1970.

(4) A 3/4 inch overlay of porous friction coating was applied in 1972 to reduce hydroplaning.

Table IX

ABBREVIATED CONSTRUCTION HISTORY, CASTLE AIR FORCE BASE, CALIFORNIA

Designation	Foundation Material		Pavement		Construction	
	Thickness (inches)	Type	Classification	Thickness (inches)	Type	Remarks Year Agency
Interior NW-SE Runway	7-8	Base Course	Silty Gravelly Sand (SM)	3	AC	Original Construction 1946 Corps of Engineers
NW-SE Runway Sta. 22+00 to 77+00				4	AC	Overlay 1954 Corps of Engineers
NW-SE Runway Sta. 77+00 to 110+00				3	AC	Overlay 1954 Corps of Engineers

Comments: (1) In 1963 that part of the runway having the 4" overlay was in "good" condition; that having the 3" overlay was cracking.

(2) By 1968 the runway had developed irregularities as a result of permanent deformations and was heater planed and capped back with close control.

Table X

TRAFFIC DATA FOR PEASE AIR FORCE BASE, NEW HAMPSHIRE

Aircraft	Number of Operations (1 Operation = 1 Landing + 1 Takeoff)											
	1960	1961	1962	1963	1964	1965	1966	1967	1968	1969	1970	
B-47/B-58	11364	7617	6544	5470	2606							
B-52	23	16	8		4	3	616	715	312	158		
KC-97/KC-135	4035	2998	2701	2404	1173							
C-135/C-133/ C-141/C-124	474	351	238	126	81		2	31	136			
25-75 ^k	4553	4709	3694	2678	2550	2121	2079					
KC-135					211	207	854	1466	906	522		
KC-97					1076	1666	328			58	100	
C-124					36	283	62	12	28	731	906	
B-47						4988	150	3			2	
B-58						2		1	6			
50-180 ^k								1378		2524	2159	
10-45 ^k								1387	2136			
C-130									320			
C-131										54		
C-141										30	44	
KC-135/C-133										491	1574	

Table XII

TRAFFIC DATA FOR DYESS AIR FORCE BASE, TEXAS

Aircraft	Number of Operations (1 Operation = 1 Landing + 1 Takeoff)										
	1960	1961	1962*	1963	1964	1965	1966	1967	1968	1969	1970
B-58/B-47	10772	4868	4200								
KC-97/KC-135	102										
C-135/C-133/ C-141/C-124	1506	821	800	3322							
10-75 ^k	8556	7487	7500								
B-52				7	801	830	930	854	846	690	678
40 ^k				3850	5419						
C-130					2703	1823	2212	2307	1942	2325	2218
KC-135						835	917	860	942	827	782
80 ^k						4634	4931	4822	5466	6150	6616

*Estimated, No Data

APPENDIX II

DESCRIPTION OF THE FIELD TEST INSTALLATION

Description of Deflection Measuring System

The system used to determine the transient deflections is shown schematically in Figure 43. Specifications and descriptions of the equipment are presented in Table XIV.

Tests carried out by Geldmacher et al (Ref. 36) suggest that the depth of the LVDT reference rods should be at least 12 feet. Because of the heavy loads exerted by the aircraft and the load cart, the reference rods used in the present field test were embedded at a depth of approximately 17.5 feet below the pavement surface.

Figure 44 shows the position of the LVDTs for measurements of transient deflections and also the wheels of the load cart with respect to the LVDT installations. The aluminum beam illustrated in the figure allowed greater flexibility in positioning the LVDTs that were located outside the track of the vehicle. Figures 45 and 46 show details of the in-hole LVDT installation and the beam LVDT installation respectively. Figure 47 is a detail of the beam support rods which were also embedded to a depth of 17.5 feet.

Figure 48 illustrates the in-hole LVDT installation with the overlay holder mount extension. The styrofoam ring between the original holder mount and the holder mount extension is to insure that surface deflections are measured. As the second, third, and fourth overlays were applied the holder mounts were extended as

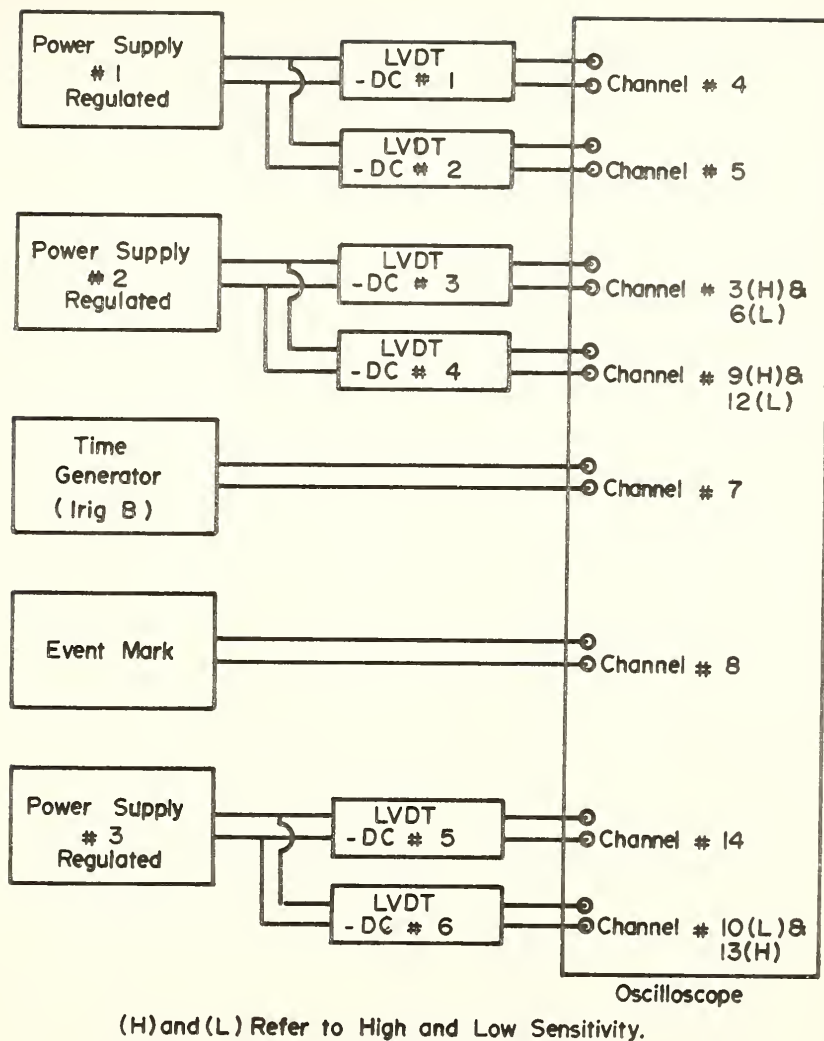


FIGURE 43 SCHEMATIC REPRESENTATION OF THE TRANSIENT DEFLECTION MEASURING SYSTEM.

Table XIV

DESCRIPTION OF INSTRUMENTS USED IN FIELD TEST

I. Linear Variable Differential Transformers (LVDTs')

Location	Manufacturer	Model Number	Range
Hole 1	Hewlett-Packard	24DCDT-100	+ 0.100 inches
Hole 2	Hewlett-Packard	24DCDT-100	+ 0.100 inches
Hole 3	Hewlett-Packard	24DCDT-50	+ 0.050 inches
Hole 4	Hewlett-Packard	24DCDT-50	+ 0.050 inches
Beam 5	Control Components Div.	15-020-DC	+ 0.020 inches
Beam 6	Internal Resistance Co.	15-020-DC	+ 0.020 inches

II. IRIG B Time Generator System

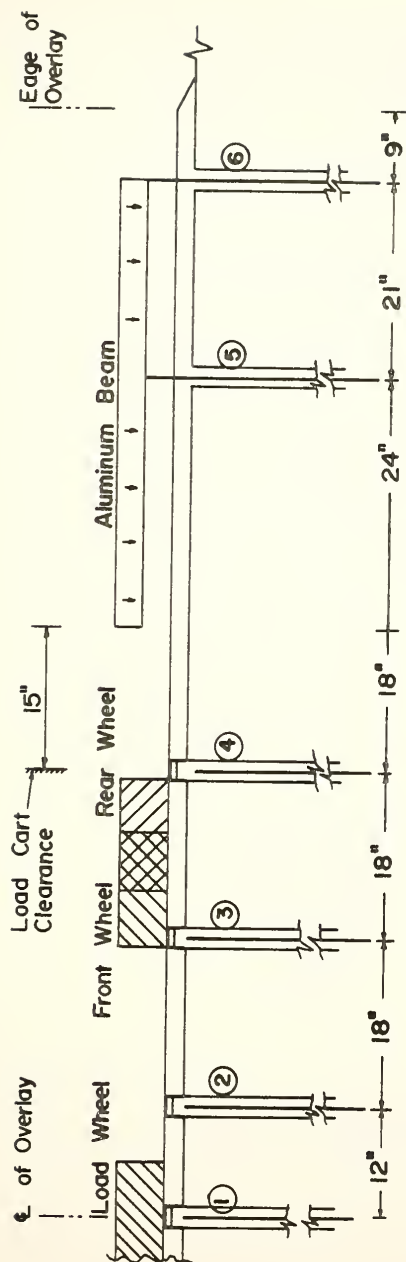
Instrument	Model	Manufacturer
Time Code Reader	DST 820	Gulton Industries
Time Code Generator	DST 830	Albuquerque
Tape Search	DST 850	New Mexico

III. Oscilloscope

Model 502 Two Channel Textronic with Polaroid Camera

IV. Tape Recorder

Ampex Model FR-1300, 14 channels.



1 - See Detail Fig. 45
4 - See Detail Fig. 45

2 - See Detail Fig. 45
5 - See Detail Fig. 47

3 - See Detail Fig. 45
6 - See Detail Fig. 47

LVDT's Installed in Holes 1-4 Plus 2 Selected Locations on Beam.
Arrows Indicate Positions on Beam where LVDT's Can Be Installed

Scale $\frac{1"}{16} = 1"$

FIGURE 4.4 INSTRUMENTATION LAYOUT USING THE LOAD CART AS THE PRIME MOVER.

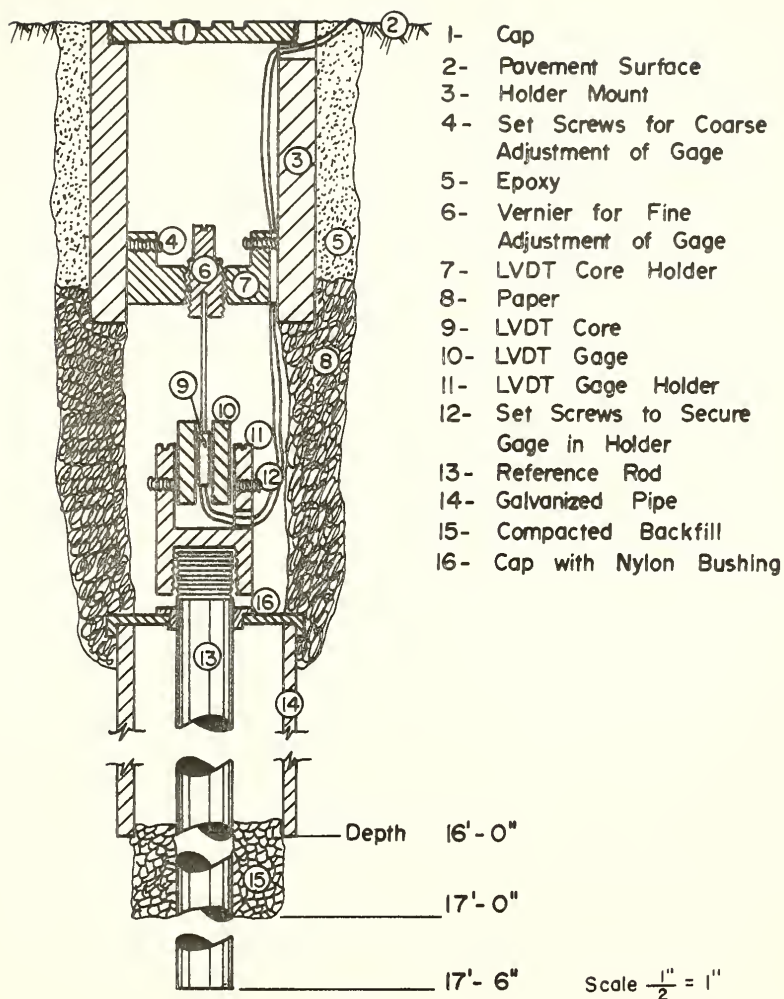


FIGURE 45 IN-HOLE LVDT INSTALLATION, PRIME MOVERS CAN RUN DIRECTLY OVER THIS INSTALLATION.

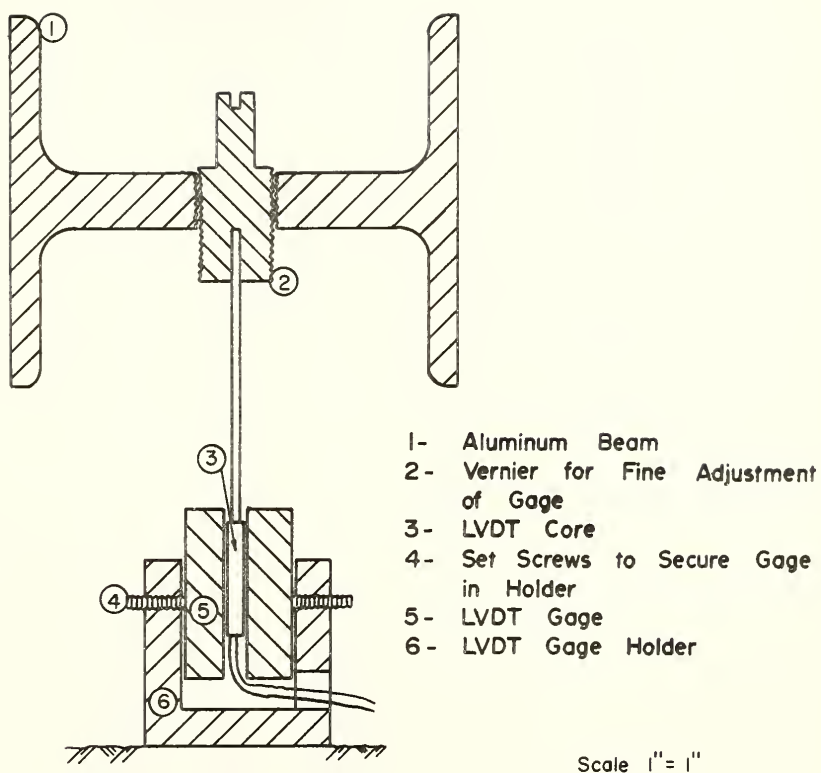


FIGURE 46 LINEAR VARIABLE DIFFERENTIAL TRANSFORMER BEAM INSTALLATION.

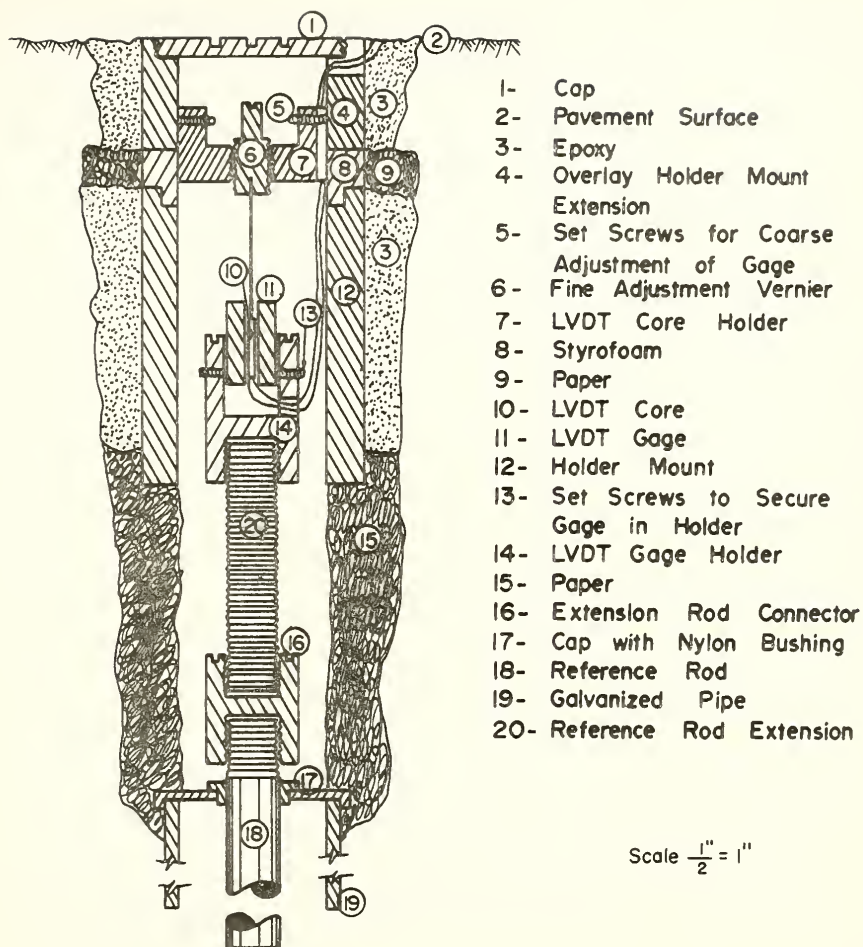


FIGURE 48 IN-HOLE LVDT INSTALLATION WITH OVERLAY HOLDER MOUNT EXTENSION.

indicated in Figure 48.

The preceeding pages are a description of the field test supported by scaled schematic illustrations. The following pages contain a description of the installation of the overlay and test equipment.

Description of the LVDT Installation

Prior to the application of the overlays, holes were drilled for the reference rods and galvanized pipe and the holder mounts were epoxied into place. Harr and Boyer (Ref. 4) describe this in detail. Before the overlay was applied the installation was as depicted schematically in Figure 45.

Figures 49 and 50 show the assembly for epoxying the overlay holder mount extension into place. An extension rod and connector were screwed on to the existing reference rod and supported a bushing which insured that the overlay holder mount extension was aligned with the reference rod. A low modulus styrofoam disc 1/2 inch thick was sandwiched between the holder mount and holder mount extension. The latter was knurled to insure strong adherence to the epoxy. The levelling bar shown in the picture was screwed to the cap in the epoxying process so that the holder mount extension was flush with the asphalt surface.

Figures 51 and 52 show the LVDT assembly with the overlay holder mount extension. The connector and rod extension total 2 inches - the thickness of the overlay.

Figure 53 shows the beam support assembly. It was found that this configuration did not give sufficient lateral support and the system

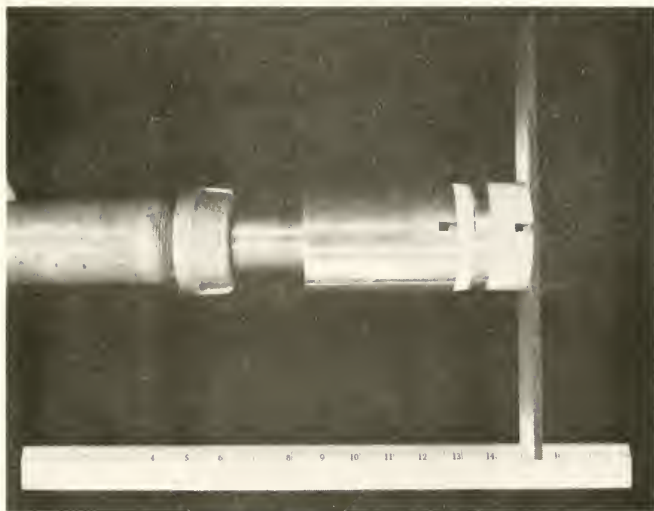


Figure 50 Holder mount extension in position for epoxying. Bar keeps top of mount flush with pavement surface.

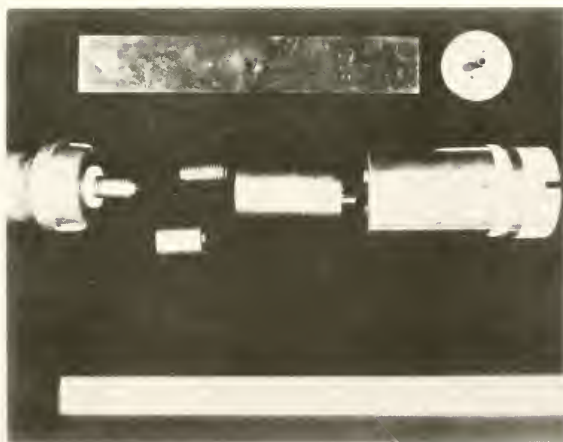


Figure 49 Pre-assembled view of components required to epoxy holder mount extension. Bushing aligns holder mount extension (knurled) with previously epoxied holder mount.

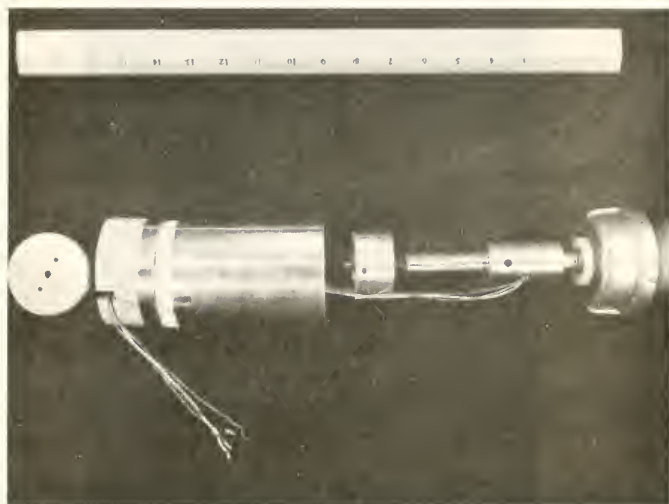


Figure 52 Assembled view of in-hole
LVDT installation.

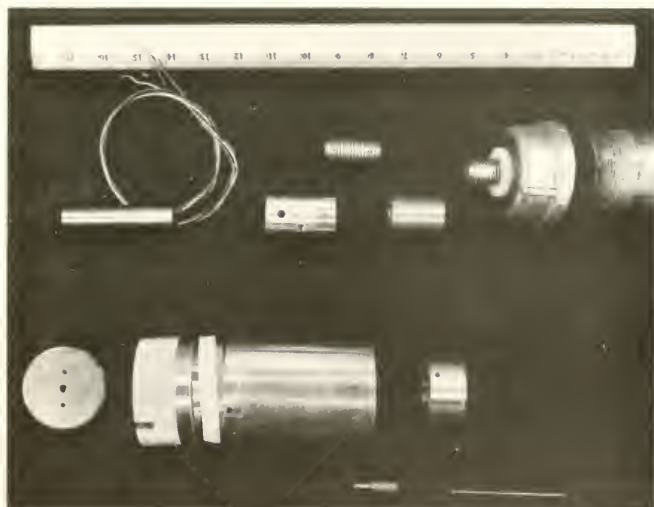


Figure 51 Pre-assembled view of in-hole
LVDT installation.

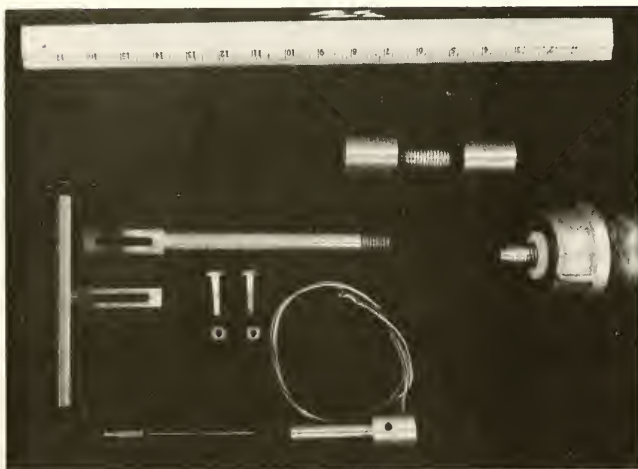


Figure 53 Pre-assembled view of beam support components. This configuration lacked lateral stability.



Figure 54 View of installed beam support. Nylon bushing in cap provides lateral support.

shown in Figures 47 and 54 was adopted. The LVDT vernier and core shown in Figure 53 were fastened to the beam, and the LVDT gage holder was epoxied to the asphalt surface.

The overlay was applied in four 2 inch lifts by personnel from the Base Civil Engineer's Office, Kirtland Air Force Base. The caps on the holder mount extension were covered with a double layer of aluminum foil in order to keep the cap spanner holes clean and then the asphalt was dumped from a truck, raked to the desired depth, and rolled by a steel wheel roller. The operations are illustrated in Figures 55 and 56. Cores taken from outside the traffic lanes indicate the average rolled density of the overlays was 135 pounds per cubic feet. The maximum aggregate size of the mix was 3/4 inches.

When the surface of the asphalt had hardened to the point where it could be walked on without leaving a footprint, the reference rod holes were located (Figure 57), and two inches of asphalt were removed (Figures 58 and 59) exposing the cap which was level with the top of the previous overlay (Figure 60). Next the caps were removed with a spanner wrench exposing the reference rods and LVDT holder mounts used in previous overlays.

All loose particles were removed from the holes, the styrofoam disc, the bushing aligner, the overlay holder mount extension and cap, and the holder mount levelling bar were placed in position as shown in Figure 50. For the first overlay, paper was packed loosely around the styrofoam disc but epoxy leaked through the disc - mount interface and cemented the aligner to the holder mount. Thereafter butyl caulk was used; it performed satisfactorily throughout the testing process.



Figure 55 Placing asphalt before hand spreading.



Figure 56 Raking and rolling two inch asphalt lift.



Figure 57 Locating reference rod holes after overlay has been compacted.



Figure 58 A cylinder of asphalt about one inch greater in diameter than the holder cap is ready for removal.



Figure 59 Removing asphalt to expose cap.



Figure 60 Loose asphalt was removed and holder mount cap from previous overlay is exposed.

The use of a soft material around the disc allowed the disc to deform under load and the deflections measured were those of the top of the overlay. After the caulking had been applied, the holes were heated for a few minutes to hasten the reaction time of the epoxy.

The epoxy used was purchased from the Hysol Division of the Dexter Corporation of Olean, N. Y. 14760. The mixture used was 3 parts resin (Hysol R8-2038) to 1 part hardener (Hysol H2-3475). The epoxy was mixed with paint stirrers and blended to an even consistency. It was then poured into the holes until the level of epoxy was even with the slot in the holder mount extension. Heat was applied as before and the epoxy was allowed to cure (Figure 61). As soon as the epoxy had hardened to the point where it could support the weight of the holder, the levelling bars and caps were removed and the aligning bushings were gently pulled from the hole with a twisting motion. The slot in the holder was then filled with butyl caulk, the caps were replaced and taped so that no epoxy could penetrate the threads. Enough epoxy was added to bring its level to that of the asphalt surface.

Two statements of warning about epoxy should be made - epoxy is such a strong adhering material that a few drops in the threads of the cap made the cap very difficult to remove. When epoxy was spilled, wiping it away while it was still in its liquid stage eliminated this problem. Secondly, heat is generated by the epoxy as it hardens and a serious burn can result upon touching it. The heat was intense enough to cause occasional slumping of the asphalt immediately adjacent and in contact with the epoxy. The result was



Figure 61 Heating epoxy and asphalt to accelerate curing.

the appearance of very small cracks in the asphalt but these cracks were filled with epoxy about 1/4 inch below the surface and were found to have no effect on the deflections of the pavement.

After all six holder mounts had been epoxied into place, a shallow trench was chiseled into the asphalt surface so that the wires leading from the LVDTs would not be pinched and possibly be severed by the wheels of the load cart.

Figure 62 shows the holder mount extensions with the styrofoam discs sandwiched between them. A connector and extension rod (Figure 63) were screwed on top of the existing reference rod to bring it 2 inches closer (the thickness of the overlay) to the surface (Figure 64). The LVDT gage holder was then screwed to the reference rod extension (Figure 65). The gage holder, being fastened to the reference rod, did not move as the surface deflected. The LVDT lead wires emerged from the hole through a slot in the overlay holder mount extension (Figure 66). An LVDT core holder was then placed in the hole and fastened to the holder mount extension with 3 set screws (Figure 67). An LVDT core was screwed into the vernier (Figure 67) and this assembly was screwed down through the core holder so that the core entered the hole in the LVDT gage (see Figure 66). The complete assembly, without the cap, is shown in Figure 68.

The LVDT beam installation is best described by referring to Figure 47. The beam was attached to the reference rods and thus was fixed. The LVDT gage holders were epoxied to the pavement surface and moved as the surface deflected. The vernier and LVDT core were fixed to the beam and did not move. The field installation of the beam



Figure 62 Styrofoam disc is visible between holder mount extensions.



Figure 63 Reference rod extension and connector are first screwed on to 17.5 foot reference rod.



Figure 64 Reference rod extension in place. Note spanner wrench holes in connector.



Figure 65 The LVDT is then fastened to the reference rod extension.



Figure 66 LVDT wires extend through slot in holder mount.



Figure 67 Installing the LVDT core holder. LVDT core is visible in the foreground.

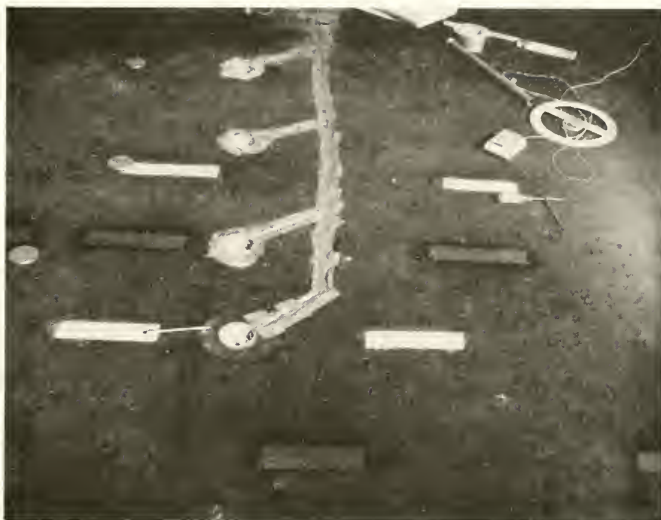


Figure 68 LVDT lead wires are protected by a shallow trench cut into the pavement.



Figure 69 Installing LVDT's on the aluminum beam.

LVDT # is shown in Figure 69.

When all six instruments had been installed, they were nulled or zeroed. This was accomplished by turning the vernier with a screwdriver thus raising or lowering the LVDT core in the LVDT gage. An intercom system (Figure 70) was used for communication between the man doing the nulling and the instrumentation man in the van. By watching the oscilloscope the null position could be ascertained. When all instruments had been nulled the tape deck was started, IRIG B time and each instrument reading was recorded for 90 seconds. The tape was then stopped and calibration began.

Calibration was accomplished by turning the verniers down a prescribed amount. Increased accuracy was obtained by fixing a pointer to a screwdriver and inserting it into the center of a 360° 10 inch protractor which was machined to fit snugly on the shoulder of the holder mount extension (Figure 70). Figure 71 shows a close up of the calibration tools. With practice 0.5° turns were possible. Each vernier had 20 thread per inch which made a 360° turn 0.050 inches. When all six instruments had been calibrated the tape was started and run for 90 seconds. The verniers were then turned back to their null positions, the caps were screwed into place with a spanner wrench and the site was ready for deflection measurements. It was found that the instruments were linear beyond the deflection ranges encountered; one calibration per day for each instrument was deemed sufficient.

Figure 72 shows the load cart trafficking an overlay. The center of the load wheel was lined up with the tape line by painting the center grooves of the load tire. It was found that the lateral



Figure 70 Calibrating an LVDT. Note intercom for communicating with instrumentation van.

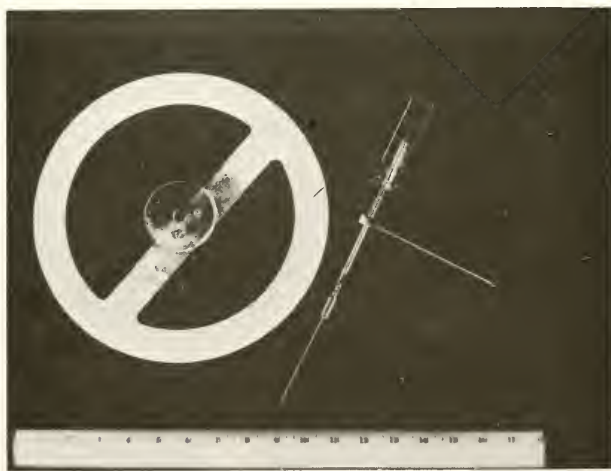


Figure 71 The calibration apparatus allowed an accuracy of 0.5° .



Figure 72 Load wheel passing directly over LVDT installation.

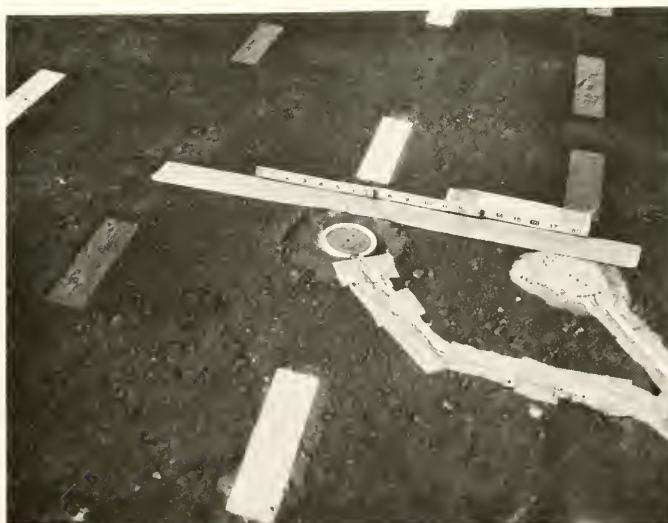


Figure 73 Tread markings of load wheel can be seen on the tape.

position of the wheel could be controlled within about 2 inches. Tape was placed parallel to the axis of the instruments in order that the reference distance from the first (outside) instrument could be determined (Figure 73). Figures 74 and 75 show other views of the load cart trafficking the overlay.

Data were taken at periodic intervals. Two runs were made for each data set; this allowed four instruments to be monitored on the oscilloscope. All instrument were nulled after each pair of data runs.

In order to find the average velocity of the load cart as it traversed the overlay, pressure switches similar to these found at a service station were set a known distance apart (Figure 76). As the vehicle traversed the "on" switch, a jump in voltage was recorded on Channel 8 of the tape deck. This continued until the vehicle ran over the "off" switch. Dividing the distance between switches by the time interval of the voltage jump yielded the average velocity of the vehicle.

Figure 77 shows the interior of the instrumentation van. The IRIG B time generator, the tape deck, the oscilloscope, and trigger switches are identified on the photograph.

Fire Truck Velocity Tests

In order to investigate the possible effects of horizontal vehicle velocity on the vertical velocity of a deflecting pavement, speed tests were run with a standard Air Force P-2 type fire truck (see Figure 21) on Taxiway 6. The velocity fo the fire truck was determined by the



Figure 74 The center grooves of the load wheel were painted so that its lateral position could be controlled.

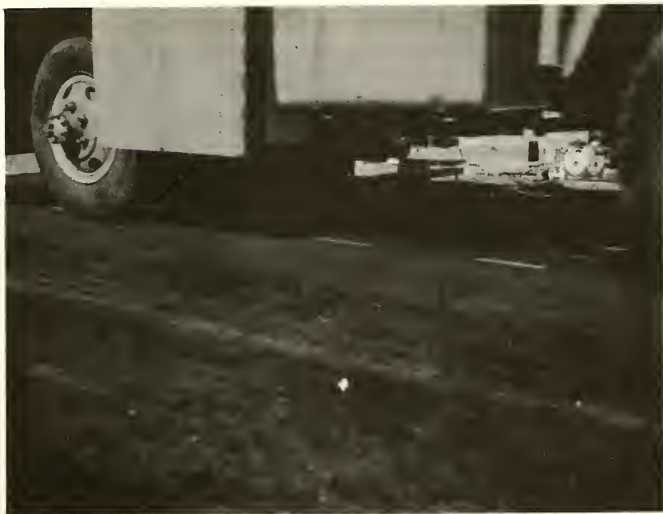


Figure 75 Another view of the load cart showing the beam LVDT installation.



Figure 76 View of the overlay showing pressure switches used to measure the velocity of the load cart.



Figure 77 The interior of the instrumentation van.

use of the trigger switches as described above.

Previous tests with the fire truck indicated that the deflection basin did not extend to instrument No. 5 so the beam used for the overlay tests was not installed.

VITA

VITA

William H. Highter was born in Claremont, New Hampshire on May 5, 1944 and is a U. S. citizen. He enrolled at the University of Notre Dame in 1962 and in 1967 was awarded Bachelor of Science degrees in Civil Engineering and Geology.

In September 1967, he entered graduate school at Purdue University and received a Master of Science degree in Civil Engineering in 1969. During this time he was employed on a half-time basis as a graduate research assistant. His thesis advisors were Professors A. G. Altschaeffl and C. W. Lovell, Jr. From June, 1969 to September, 1969 he was employed as a highway engineer at the Indiana State Highway Commission Research and Training Center.

For the next three years he worked on his Ph.D. at Purdue. Until June 1971 he held an appointment as a graduate instructor; for his remaining tenure at Purdue he was employed as a full-time graduate research assistant. He is presently an Assistant Professor of Civil and Environmental Engineering at Clarkson College of Technology.

Mr. Highter is an associate member of the American Society of Civil Engineers, a supporting member of the Highway Research Board, an associate member of Sigma Xi, and a member of Chi Epsilon. He is a Registered Professional Engineer in Indiana.

He is married and has two children.

